

**DOKUZ EYLÜL UNIVERSITY
GRADUATE SCHOOL OF NATURAL AND APPLIED
SCIENCES**

**EFFECT OF WIND TURBINES ON POWER
SYSTEM OPERATION**

by
Özgür Salih MUTLU

February, 2009

İZMİR

EFFECT OF WIND TURBINES ON POWER SYSTEM OPERATION

**A Thesis Submitted to the
Graduate School of Natural and Applied Sciences of Dokuz Eylül University
In Partial Fulfillment of the Requirements for the Degree of Doctor of
Philosophy in Electrical and Electronics Engineering, Electrical and Electronics
Program**

**by
Özgür Salih MUTLU**

February, 2009

İZMİR

Ph.D. THESIS EXAMINATION RESULT FORM

We have read the thesis entitled “**EFFECT OF WIND TURBINES ON POWER SYSTEM OPERATION**” completed by **ÖZGÜR SALİH MUTLU** under supervision of **PROF. DR. EYÜP AKPINAR** and we certify that in our opinion it is fully adequate, in scope and in quality, as a thesis for the degree of Doctor of Philosophy.

.....
Prof. Dr. Eyüp AKPINAR

Supervisor

.....
Prof.Dr.Coşkun SARI

Thesis Committee Member

.....
Assist.Prof.Dr.H. Ş. ÖZTURA

Thesis Committee Member

.....
Assist.Prof.Dr.H. Ş. ÖZTURA

Examining Committee Member

.....
Associate Prof.Dr.Taner Oğuzer

Examining Committee Member

Prof.Dr. Cahit HELVACI
Director
Graduate School of Natural and Applied Sciences

ACKNOWLEDGEMENTS

The research in the scope of this thesis has been conducted at the Department of Electrical and Electronics Engineering of Dokuz Eylül University under the supervision of Prof. Dr. Eyüp AKPINAR. First, I would like to express my gratitude to him for his guidance and support during this work. I would also like to thank the members of the Electrical Machines and Power Electronics Laboratory Group and other staff of the Department for their assistance.

Site measurement of this thesis was carried out as a part of project, “Power Quality National Projects- Mobile Power Quality Measurements” sponsored by Turkish Scientific and Research Council and Turkish Electrical Power Transmission Co. (TEİAŞ) under contract 106G012. I would like to thank them for their support.

I would like to thank Prof. Dr. Coşkun SARI and Assist. Prof. Dr. Hacer ŞEKERCİ ÖZTURA for their comments and support to this work during their presence in my Ph.D. Thesis Committee. I would also like to thank Assist. Prof. Dr. Tolga SÜRGEVİL and Abdül BALIKCI for their help during simulation study and Özgür TAMER for his support.

Last, but not the least, I feel deeply indebted to my wife Başak MUTLU who above all else deserves respect and gratitude, for her patience and support.

Özgür Salih MUTLU

EFFECT OF WIND TURBINES ON POWER SYSTEM OPERATION

ABSTRACT

In this thesis, effects of wind energy conversion systems on power system operation and vice versa is investigated by a case study of the wind farm. The electrical model of 12 wind energy conversion systems equipped with wound rotor induction machine is developed. After model verification on one machine, whole model of wind farm and power system, including point of common coupling, is used for simulation for power quality analysis.

Site measurement was carried out at the point of common coupling as a part of project, “Power Quality National Projects- Mobile Power Quality Measurements”. The measured results are used for model verification. Wind speed measurement result, which is used as input data in simulation, is obtained from wind farm operators. Effects of wind farm on power system operation is evaluated by the help of simulation results and site measurement results.

Like in other countries, which have particular wind energy conversion system in their power system, in Turkey transmission system operator needs grid codes for wind energy conversion systems. Contribution have been done in thesis for developing grid codes by the help of results obtained, and developing an aggregated model for wind energy conversion system having wound rotor induction machine and its drive.

Keywords: Wind Energy Conversion System, Wound Rotor Induction Machine, Power system, Power Quality.

RÜZGAR TURBİNLERİNİN GÜÇ SİSTEMİ ÜZERİNE ETKİSİ

ÖZ

Bu tezde rüzgar enerjisi dönüşüm sistemlerinin güç sistemi üzerine etki ve karşı etkileri bir rüzgar çiftliği örneği kullanılarak incelenmiştir. Rüzgar çiftliğinde bulunan yuvarlak rotorlu asenkron makine ile donatılmış 12 adet rüzgar enerjisi dönüşüm sisteminin elektriksel modeli oluşturulmuştur. Tek makine modeli üzerinde yapılan çalışmalara daha sonra tüm rüzgar çiftliği ve bağlı olduğu ortak kuplaj noktası itibariyle elektrik güç sistemi dahil edilerek analizler yapılmıştır.

Tez kapsamında “Güç Kalitesi Milli Projesi” mobil ölçüm ekiplerince rüzgar çiftliğinin bağlı olduğu trafo merkezinde elektriksel ölçümler yaptırılmış ve kullanılmıştır. Rüzgar çiftliği işletmecileri tarafından yapılan rüzgar hızı ölçüm sonuçları bilgisayar modeli doğrulama simülasyonlarında girdi olarak kullanılmıştır. Simülasyon sonuçları ve ölçüm sonuçları kullanılarak örnek rüzgar enerjisi dönüşüm sistemi topluluğunun elektrik güç sistemi ile karşılıklı etkileşimi incelenmiştir.

Rüzgar enerjisi dönüşüm sistemlerini elektrik güç sistemi bünyesine katan diğer ülkelerde olduğu gibi ülkemizde de; enerji iletim ve dağıtım sistemini çalıştıranlar tarafından ihtiyaç duyulan; “Rüzgar Çiftlikleri Şebeke Bağlantı Kuralları” için tez kapsamında elde edilen sonuçlar vasıtası ile katkı sağlanmış ve yuvarlak rotorlu asenkron makine ve sürücü devresi ile donatılan rüzgar enerjisi dönüşüm sisteminin birleştirilmiş modeli geliştirilmiştir.

Anahtar Kelimeler: Rüzgar Enerjisi Dönüşüm Sistemi, Yuvarlak Rotorlu Asenkron Makine, Elektrik Güç Sistemi, Güç Kalitesi.

CONTENTS

	Page
Ph.D. THESIS EXAMINATION RESULT FORM.....	iii
ACKNOWLEDGEMENTS.....	iv
ABSTRACT.....	v
ÖZ.....	vi
CHAPTER ONE - INTRODUCTION.....	1
CHAPTER TWO - POWER SYSTEM, DISTRIBUTED GENERATION, WECS CONNECTION ISSUES AND GRID CODES.....	8
2.1 The Structure of the Power System.....	8
2.1.1 Generation System.....	9
2.1.2 Transmission System.....	10
2.1.3 Distribution System.....	10
2.2 Power System Connection Issues of Wind Energy Conversion Systems.....	10
2.2.1 Location of the Wind Farm in the Electric Power System.....	11
2.2.2 Impacts of Wind Farms on Power Quality.....	14
2.2.2.1 Steady-State Voltage.....	16
2.2.2.2 Voltage Fluctuations.....	17
2.2.2.2.1 Continuous Operation.....	18
2.2.2.2.2 Switching Operation.....	19
2.2.2.3 Harmonics.....	20
2.2.2.4 Revision of International Standart: IEC 61400-21.....	21
2.2.3 System Stability.....	22
2.3 Grid Codes for Wind Energy Conversion Systems	24
2.3.1 Low Voltage Ride Through(LVRT) Capability	25
2.3.2 Reactive Power and Voltage Variations.....	28
2.3.3 Frequency Range, Control of Frequency and Active Power	31
2.3.4 Signals, Control and Communications.....	33

**CHAPTER THREE - WIND ENERGY CONVERSION SYSTEMS:
PROPERTIES, CLASSIFICATION AND CHARACTERISTICS.....35**

3.1 Components of Grid Connected Wind Energy Conversion System.....35

3.2 Classification of Wind Energy Conversion Systems.....37

 3.2.1 Fixed Speed Wind Turbines.....37

 3.2.2 Variable Speed Wind Turbines.....38

 3.2.3 Typical Wind Turbine Configurations.....39

 3.2.3.1 Type A.....39

 3.2.3.2 Type B.....40

 3.2.3.3 Type C.....41

 3.2.3.4 Type D.....41

3.3 Technical Features of Wind Power Plants.....42

CHAPTER FOUR - ALAÇATI WIND FARM.....46

4.1 Alaçati Wind Farm46

 4.1.1 Wind Turbine Generators49

 4.1.2 Control System.....50

 4.1.3 Power Factor Correction51

4.2 MATLAB/Simulink Simulation of the Wind Energy Conversion System.....52

**CHAPTER FIVE - WOUND ROTOR INDUCTION GENERATOR AND
SPEED CONTROL.....56**

5.1 Wound Rotor Induction Machine Rotor Circuits for Speed Control.....56

 5.1.1 Speed control with rotor circuit chopper (One resistance).....59

 5.1.2 Speed control with rotor circuit chopper (Three resistances).....61

**CHAPTER SIX - MODELLING AND SIMULATION OF WIND FARM FOR
POWER SYSTEM STUDY.....73**

6.1 Simulations and Modelling73

 6.1.1 Steady-state Voltage Level Influence.....74

6.1.2 Flicker.....	75
6.1.3 Grid Disturbances.....	76
6.2 Aggregated Modeling.....	77
6.3 Validation Procedure of Wind Farm Models.....	79
6.4 Simulation Tool:PSCAD/EMTDC.....	80
6.5 Models for the Wind Farm.....	81
6.5.1 Generator Modelling.....	81
6.5.2 Control Sytem Model.....	82
6.5.3 Turbine Model.....	85
6.5.4 Model of Wind.....	86
6.5.5 Alaçatı Substation.....	87
6.5.6 Power System(Grid).....	88
6.6 Wind Farm Simulation Results with PSCAD/EMTDC.....	88
6.7 Aggregated Model of the Wind Farm.....	92
6.7.1 Aggregated Model PSCAD/EMTDC Simulation Results.....	95
6.7.2 Effect of Power System Components.....	95
6.7.3 Effect of Rotor Resistance Control.....	96
6.7.4 Effect of Substation Voltage Level.....	98
6.8 Comparison of Aggregated Model PSCAD/EMTDC Simulation Results with Complete Model PSCAD/EMTDC Simulation Results.....	99
6.9 Power Quality Project.....	103
6.9.1 Results of Power Quality.....	105
CHAPTER SEVEN – CONCLUSIONS.....	112
REFERENCES.....	114
Appendices.....	122

CHAPTER ONE

INTRODUCTION

Sources of energy for the production of electricity are many and varied. Wind power is being used as a clean and safe energy resource for electricity generation for nearly a hundred years. The early established wind farms had relatively smaller power rated generators with respect to conventional power stations. But nowadays, large power rated offshore wind farms are being installed to control power system data instead of conventional ones.

The wind farms have different impacts and functions on the performance of the grid than conventional power plants, because of variation of wind speed in time. Doubly fed and squirrel cage induction generators are widely used in wind energy conversion systems. These generators are usually grid-coupled via power electronic converters in order to control the voltage, frequency and power flow during the variation of wind speed. As a consequence, wind turbines affect the dynamic behaviour of the power system in a way that might be different from hydrolic or steam turbines(Mutlu, Akpınar & Balıkcı, 2009).

The increasing percentage of wind energy conversion systems in electrical power production has amplified the need to address grid integration concerns. Power system operators or transmission system operators(TSO) need simulation tools and scientific practices before wind power-power system integration to guarantee reliable operation of the system with wind power. Power system reliability consists of system security and adequacy.

At the end of the 1980s, distribution network companies in Europe started to develop their own interconnection rules or standards. In the beginning, each network company that faced an increasing amount of interconnection asks the wind farms to follow its own rules. During the 1990s, these interconnection rules were harmonised on a national level, like in Germany and Spain.

In order to assure reliable operation, TSO demanded high short-circuit power capability at wind farm connection buses, like at least 20 times greater than the wind farm nominal power. These regularities impede further penetration of wind power because of power system operational precautions.

Researchs on technologies, tools and practices for integrating large amounts of wind power into electric power systems are attempting to increase knowledge and resources. Interconnection rules need to be continuously reformulated because of the increasing wind power penetration and the rapid development of wind turbine technology (i.e. wind turbine ratings increased rapidly, from around 200kW in the early 1990s to 3–4MW turbines in early 2004 and ≥ 5 MW nowadays)(Matevosyan, Ackermann & Bolik, 2005).

There are guidelines, recommendations and requirements which deal with the technical data needed to assess the impact of wind turbines on power system and discuss the requirements to be met by networks to which wind turbines are to be connected. Research groups are founded by goverments, universities, manufacturers, wind farm owners and power system operators to develop grid codes for wind farm-grid integration.

European TSO launched an european wide grid study on the integration of wind power, focusing on measures needed to be taken by legislators, regulators, TSO and grid users, aiming at establishing a harmonised set of rules for the integration of wind power. This set of rules is vital for the secure and reliable operation of the electricity networks in presence of variable generation.(ETSO, 2007). There are also different study groups founded for different countries with the same goal.

In the last years the trend has moved from installations including few wind turbines to planning of large wind farms with capacity over hundreds of MW. A model to investigate the power quality impacts of the wind farm during normal operation on power system is given in (Hansen, Sorensen , Janosi & Bech, 2001).

The measured and simulated power quality performances of wind turbines during normal operation is presented.

Chen (2005a) presented the grid connection issues of wind power systems. Also the impacts of wind power on power quality, the grid requirements for integration of wind turbines and potential operation and control methods to meet the challenges are stated. Chen (2005b) simulated the system with wound rotor induction generators having rotor resistance controls and voltage stability and dynamic performance are discussed with possible methods of improving the system performance.

The effects of short-circuit power capacity at the point of common coupling and the reactive power compensation on the system stability were determined in (Ledesma, Usaola, & Rodríguez, 2003). Flicker and switching operations, dynamic stability, harmonic pollution, and voltage variations are the concerning issues about the grid connection capacity of wind farms. The various power factor correction strategies affects the voltage rise problems for fixed-speed wind turbine generators. Because of these backdraws the connection capacity of wind farms is limited to 20% of the short circuit capacity at the point of common coupling(Dinic, Fox, Flynn, Xu & Kennedy, 2006).

Holttinen et al.(2006) outlined impacts of wind power on the power system, the national studies published/on-going and described the goals of the international collaboration. Figure 1.1 shows impacts of wind power on power systems, divided in different time scales and width of area relevant for the studies.

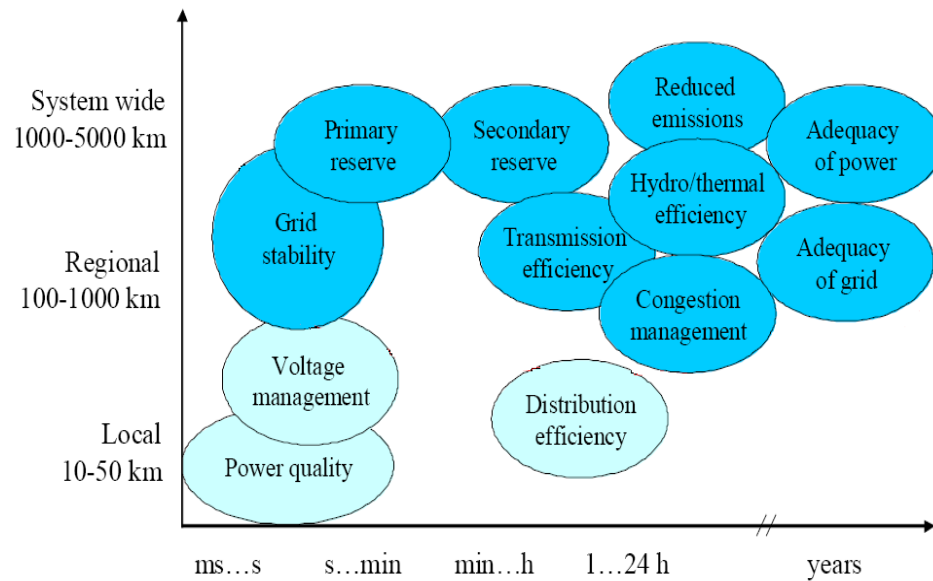


Figure 1.1 Impacts of wind power on power systems, divided in different time scales and width of area relevant for the studies.

At the time of developing the standard IEC 61400-21:“Measurement and assessment of power quality characteristics of grid connected wind turbines-2001”, the wind turbines were mainly connected to the distribution grid, and the basic concern was their possible impact on the voltage quality and not on power system operation. This has changed with the development of large power rated wind farms that may form a significant part of the power system. In consequence, today’s wind turbines are able to control the power (active and reactive) delivered both in transient and steady state, they can cope with power ramp requirements and they have low voltage ride through(LVRT) capability. They may even contribute to the primary frequency control, but then on the cost of dissipating energy. To this, IEC 61400-21 is also currently under revision to provide procedures for assessing these new wind turbine characteristics (Estanqueiro, Tande & Peças Lopes, 2007).

Wind farm projects in Turkey; built wind farms, wind projects waiting decision of State Planning Organization, wind projects under contract discussion, wind projects whose feasibility reports are being assessed, wind projects that awaits revision feasibility reports, and wind projects that await feasibility are presented by

(Kenisarin, Karlı & Çağlar, 2006). Actual status of wind power projects in Turkey can be found in http://www.epdk.gov.tr/lisans/elektrik/lisansdatabase/verilentesis_tipi.asp. Additional total “97 MW” wind power installed and integrated to grid in Turkey, in 2007.

The purpose of this thesis is to analyze the counter effects of a selected wind farm on power system and vice versa by appropriate modeling. The efforts and studies that have been done for these goals can be listed as follows:

Firstly, model of a single wind turbine in the wind farm was implemented in MATLAB/Simulink for transient tests and analysis. The simulation results for the transient process in external short-circuit fault situations were obtained and the impacts of the short circuit on wind turbine were analyzed. The MATLAB/Simulink simulation results of the wind farm were presented in (Mutlu & Akpınar, 2005).

After getting results for a single wind turbine, it was necessary to form the complete model of wind farm. PSCAD/EMTDC was used for this purpose; a detailed model of the wind farm connected to Alaçati Substation was implemented in PSCAD/EMTDC to simulate its impact on power system and vice versa. All wind turbines and their interconnections are modelled separately in PSCAD/EMTDC simulation. Since all wind turbines are equipped with wound rotor induction machine, special attention was given for rotor circuit modelling and speed control.

While studies about simulation were going on, measurements in the wind farm had been carried out in the substation during 7 days in a week by power quality monitoring set-up. The power quality impact of the wind farm has been investigated through the comparison of the computed power quality characteristics from PSCAD/EMTDC simulations with measured power quality characteristics.

Finally, aggregated modelling of the wind farm was investigated. An accurate aggregated model eliminates the need to develop a detailed model of a wind farm with tens or hundreds of wind turbines and their interconnections, and to specify the

wind speed at each individual wind turbine within the farm. Aggregated model for wound rotor induction machine was newly developed and aggregated model of the wind farm in PSCAD/EMTDC was used to evaluate the effects of main parameters on steady-state stability margin. PSCAD/EMTDC simulation results of the developed aggregated model of the wind farm are compared with the PSCAD/EMTDC simulation results of complete wind farm model for both standart operation and grid disturbance.

The rest of the chapters are organized as follows; in Chapter 2, the structure of the power system and power system connection issues of wind energy conversion systems will be given in detail. Grid code studies about wind farms within the “Power Quality National Project” and outcomes are analyzed and discussed for further developmets in “Grid Codes for Wind Farm Grid Connections”.

The properties, classification and characteristics of Wind Energy Conversion Systems will be given in Chapter 3.

In Chapter 4, the wind farm connected to Alaçatı Substation will be analyzed. The simulated and measured system in this thesis is given for this wind farm. Wind turbine generators, control system and power factor correction system of wind farm will be presented. Details about the MATLAB/Simulink simulation of the wind energy conversion system, which was used for energy conversion in the wind farm, will be given.

In Chapter 5, the mathematical model of rotor circuit for wound rotor induction generators is presented. The wind farm consists of twelve wind turbines equipped with wound rotor induction generators. Two different rotor circuit designs were evaluated for appropriate and accurate modelling.

Modeling issues of wind farms connected to grid will be discussed in Chapter 6. PSCAD/EMTDC simulation tool, which was used to simulate the whole wind farm and the grid, is introduced. The system data, priorities, simplifications that have been

done and other important fundamental information are given. Complete and aggregated modeling results of the whole wind farm in PSCAD/EMTDC simulation and site measurement results will also be presented in Chapter 6.

Conclusions will be given in Chapter 7. List of tables, list of figures, list of abbreviations and conference/journal publications are given in Appendices.

CHAPTER TWO
POWER SYSTEM, DISTRIBUTED GENERATION, WECS
CONNECTION ISSUES AND GRID CODES

The interconnected power system is often referred to as the largest and most complex machine ever built by humankind. This may be hyperbole, but it does emphasize an inherent truth: there is a complex interdependency between different parts of the system. The aim of this complex machine is to produce and deliver to the consumers electric energy of defined parameters, where the main quantities describing the electric energy are the voltage and frequency. It has to be operated to ensure a continuous supply at the consumers terminals. The voltage should be a sinusoidal wave with nominal amplitude and a frequency (Venkatasubramanian, & Tomsovic, 2004), (Lubosny, 2003).

2.1 The Structure of the Power System

The power system can be separated into three major subsystems:

- Generation System,
- Transmission System,
- Distribution System.

Generation system includes generators, transmission system consists of transmission lines, power transformers, capacitors, reactors, and distribution system consists of subtransmission lines, distribution transformers, distribution lines and loads. One line diagram of a typical power system, consisting only main parts, shown in Figure 2.1.

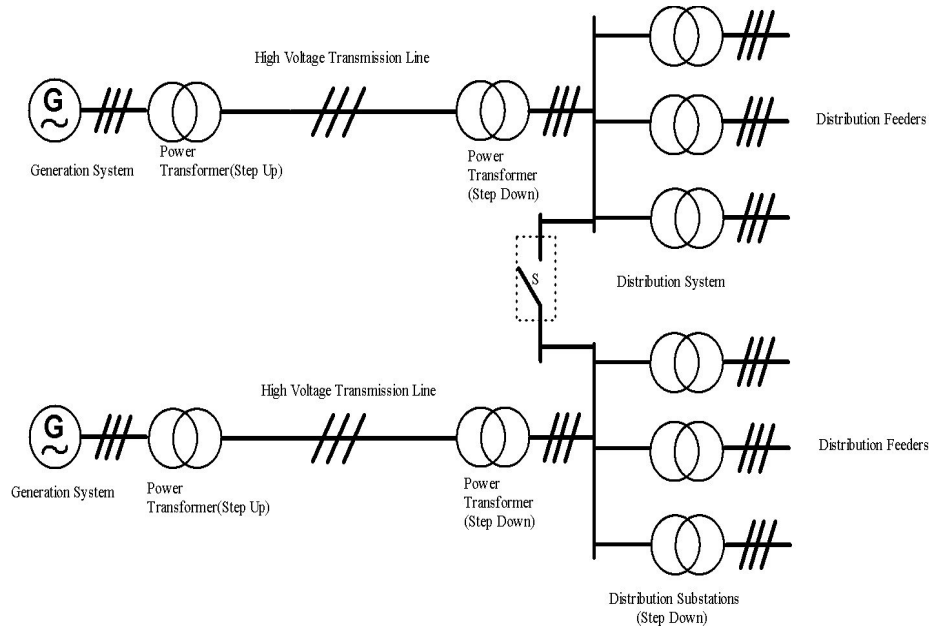


Figure 2.1 The main parts of typical AC 3 phase power system

2.1.1 Generation System

The vast majority of generation is carried out by synchronous generators. A generator is an electromechanical machine composed of a static part (the stator) and a rotating part (the rotor) whose relative position is changed periodically by rotating angle ωt . In other words, a generator is a three-phase electromagnetic machine composed of time varying inductance $l(t)$ and resistance r of stator and rotor windings (Hase, 2007).

The source of the mechanical power, commonly known as the prime mover, are hydraulic turbines, steam turbines or alternate sources. Hydraulic turbines operate with low speed and their generators have salient type rotor with many poles. Steam turbines operate relatively high speeds and coupled with cylindrical rotors. Alternate sources can be listed as wind power, solar power, geothermal power, tidal power and biomass (El-Hawary, 2000). The wind energy conversion systems connected to the power system will be analyzed here.

2.1.2 Transmission System

The purpose of the electric transmission system is the optimal high voltage interconnection of the electric energy producing power plants or generating stations with the loads. A three-phase AC system is used for most transmission lines. The transmission systems usually contain loops to assure that each load substation is supplied by at least two lines. This assures that the outage of a single line does not cause loss of power to any customer. The system voltage is defined as the rms voltage between two phases, also called line-to-line voltage(Karady, 2001).

2.1.3 Distribution System

The distribution system is the part of electric power system between the bulk power source and the consumers' service switches. It operates in low and medium voltage levels and includes subtransmission systems; distribution substations; distribution lines; and appropriate protective and control equipment(Gönen, 2004).

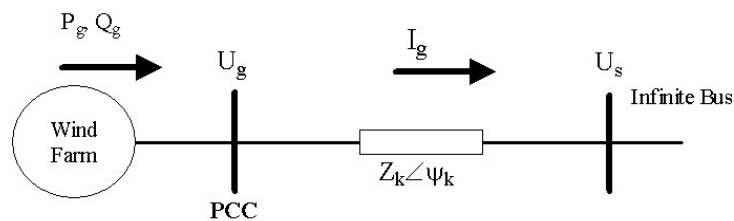
2.2 Power System Connection Issues of Wind Energy Conversion Systems

The wind farms have different impacts and functions on the performance of the grid than conventional power plants, because of variation of wind speed in time. Many studies have been performed on grid connected wind farms and related power system issues. Different techniques and models have been used for determining problems; the impacts of wind farms on technical and operational characteristics of power systems and technical requirements for wind farm-grid connections were analyzed. The doubly fed and squirrel cage induction generators are widely used in wind energy conversion systems. These generators are usually grid-coupled via power electronic converters in order to control the voltage, frequency and power flow during the variation of wind speed. As a consequence, wind turbines affect the dynamic behaviour of the power system in a way that might be different from hydrolic or steam turbines. The factors that cause these affects will be analyzed in this section.

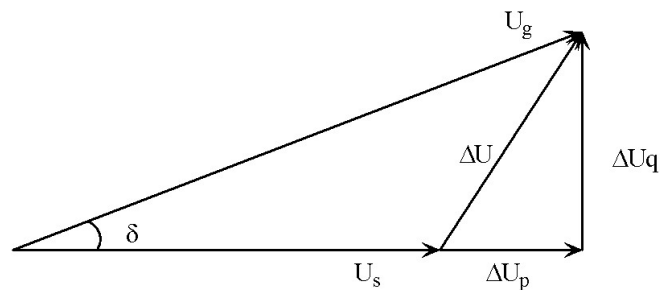
2.2.1 Location of the Wind Farm in the Electric Power System

The point of common coupling (PCC) of wind farms and the power system, including the parameters of the power system, the parameters of wind farm and the structure of the grid are of essential significance in further operation of the wind farm in the power system and their influence on each other. The size and the location of the considered wind farm and the parameters of the grid in that region highly influences the appropriate PCC.

Wind farms must be located in the regions that have favourable wind conditions. These regions can be shorelines and islands where the power network in these regions can be named as “weakly developed”. A part of power grid can be named as “weak” when it is electrically far away from the infinite bus of the interconnected power system. The weak grids have lower short circuit power than strong grids relatively. The short circuit power level in a given point in the electrical network represents the system strength. Figure 2.2(a) illustrates an example of one line diagram of wind farm connection to a grid and (b) shows phasor diagram.



(a)



(b)

Figure 2.2 (a) One line diagram of wind farm connection to a grid,
(b) Phasor diagram

Wind farm is connected to the network with equivalent short circuit impedance, Z_k . The network voltage at the assumed infinite busbar and the voltage at the PCC are U_s and U_g , respectively. The output power and reactive power of the wind farm are P_g and Q_g , which corresponds to a current I_g .

$$I_g = \left(\frac{S_g}{U_g} \right)^* = \frac{P_g - jQ_g}{U_g} \quad (2.1)$$

The voltage difference, ΔU , between the infinite system and the PCC is given by

$$U_g - U_s = \Delta U = Z_k \cdot I_g = (R_k + jX_k) \left(\frac{P_g - jQ_g}{U_g} \right) \quad (2.2)$$

$$\Delta U = \frac{R_k P_g + X_k Q_g}{U_g} + j \frac{P_g X_k - Q_g R_k}{U_g} = \Delta U_p + j\Delta U_q \quad (2.3)$$

The short circuit impedance, the real and reactive power output of the wind farm determines the voltage difference. The variations of the generated power will result in the variations of the voltage at PCC. When the impedance Z_k is small, then the grid can be named as strong and when Z_k is large, then the grid can be named as weak. Since strong or weak are relative concepts, for a given electrical wind power capacity P , the ratio,

$$R_{sc} = \frac{S_{sc}}{P} = \frac{U_s^2}{Z_k \cdot P} \quad (2.4)$$

stated as the measure of the strength, where S_{sc} is short circuit power. The grid may be considered as strong with respect to the wind farm installation if R_{sc} is above 20. It is obvious from (2.4) that for large wind farm-grid connections, the PCC voltage level have to be as high as possible to limit voltage variations(Chen, 2005a).

As the amount of power system incorporated wind power continues rapidly to increase; a distinction have been made between local wind turbines and large wind farms. Large wind farms that are connected to transmission system are subject to grid codes of TSO and must react like conventional power plants. Unlike local wind farms that are connected to distribution system, these wind farms can be named as a member of generation systems(Akhmatov, 2006).

Local wind farms are the most typical forms of distributed generation. Although distribution systems are planned for unidirectional power flow from transmission system to the consumers, the amount of distributed generation located at the distribution level of electrical networks is showing rapid growth worldwide. Issues such as new energy sources, efficiency of local energy production and modularity of small production units are promoting this growth. On the other hand, large power rated wind farms connected directly to the transmission level do not actually meet the definition of distributed generation since those are named as the members of generation system(Mäki, Repo, & Järventausta, 2006).

In case of wind farm installations on islands and offshore platforms the underwater transmission of power to the mainland power system has to be performed by cable. For long distance transmission, the transmission capacity of cables may be mainly occupied by the produced reactive power, therefore ac transmission will meet difficulties. In this situation high voltage direct current (HVDC) transmission techniques may be used. The voltage source converter based HVDC system, provides possibilities for performing voltage regulation and improving dynamic stability of the wind farm as it will be possible to control the reactive power of the wind farm and keep the voltage during the faults clearance and fast reclosures in the onshore transmission system(Chen, 2005a). Figure 2.3 shows different wind farm connections to grid.

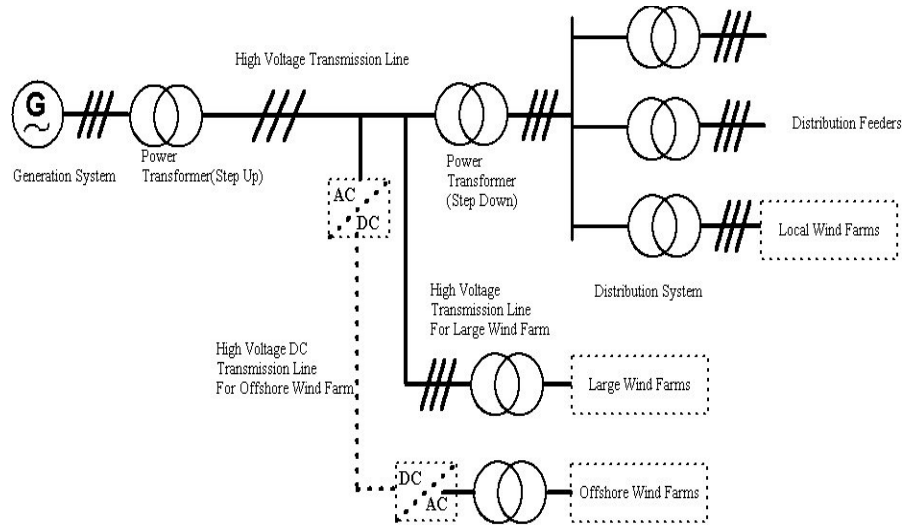


Figure 2.3 Different wind farm connections to a grid.

2.2.2 Impacts of Wind Farms on Power Quality

The currently existing power quality standard for wind turbines, issued by the International Electrotechnical Commission (IEC), IEC 61400-21: “Measurement and assessment of power quality characteristics of grid connected wind turbines”, Ed.1, 2001 defined the parameters that are characteristic of the wind turbine behavior in terms of the quality of power, and also provides recommendations to carry out measurements and assess the power quality characteristics of grid connected wind turbines. Although the standard mainly describes measurement methods for characterizing single wind turbines, there are methodologies and models developed that enable, for well pre-defined conditions, to extrapolate the single turbine unit parameters to the typical quality characteristics of wind farms.

Until the development of IEC 61400-21 there were no standard procedures for determining the power quality characteristics of a wind turbine, and simplified rules like; requiring a minimum short-circuit ratio of 25 or that the wind farm should not cause a voltage increment of more than 1%, were often applied for dimensioning the grid connection of wind turbines. This approach has proved generally to ensure acceptable voltage quality; however, it has been costly by imposing grid

reinforcements not needed and has greatly limited the development of wind farms in distribution grids.

Table 2.1 gives the list of the factors and characteristics identified [Estanqueiro et.al., 2007] with highest influence on the power quality of wind turbines and the parameters more adapted to their quantification, to act as normalized quality indicators by the help of the outcomes of some European funded research projects and IEC 61400-21(Estanqueiro, Tande, & Peças Lopes, 2007).

Table 2.1 Factors and characteristics with impact on the power quality of wind farms.

Wind Turbine Technology	Grid Conditions at the PCC
Type of Electrical Generator	Short Circuit Power and X/R ratio
Gearbox or Gearless Transmission	Interconnection Voltage Level and Regulation
Direct/Controlled Connection to the Grid	Type of Interconnecting Transformers
	Coordination of the Protections
Wind Farm Design and Control	Wind Flow Local Characteristics
Number and Nominal Power of the Wind Turbines	Turbulence Intensity
Wind Farm Internal Power Collecting System Characteristics (X/R)	Turbine Operation Under Wake Flow
Possible Capacity Effects from the Wind Farm Internal Cabling System	Spectrum of the Wind 3D Components
Added Power/Voltage Control and Regulation	Spatial Variability of the Wind

Since voltage variation and flicker are caused by power flow changes in the grid, operation of wind farms may affect the voltage in the connected network. On the local level, voltage variations are the main problem associated with wind power. This can be the limiting factor on the amount of wind power which can be installed. If necessary, the appropriate methods should be taken to ensure that the wind turbine installation does not bring the magnitude of the voltage at PCC outside the required limits.

In normal operational condition, the voltage quality of a wind turbine or a group of wind turbines may be assessed in terms of the following parameters: Steady state voltage under continuous production of power, voltage fluctuations as flicker during normal operation and flicker due to switching(Chen, Blaabjerg, & Sun, 2004).

2.2.2.1 Steady-State Voltage

The equation for the voltage difference at PCC of a wind farm is given by (2.2). The voltage difference can be calculated with load flow methods as well as other simulation techniques. The voltage at PCC should be maintained within the grid codes of the TSO. The voltage in the connected network may be affected by operation of wind turbines. The appropriate methods should be taken to ensure that the wind turbine installation does not bring the magnitude of the voltage outside the required limits. Modelling, simulation and load flow studies must be conducted to assess this effect to ensure that the wind farm installation does not bring the magnitude of the voltage outside the required limits of the TSO.

A wind turbine installation may be assumed as a PQ node, which may use ten minutes average data as; P_{mc} and Q_{mc} , or 60 s average data as; P_{60} and Q_{60} , or 0.2 s average data as; $P_{0.2}$ and $Q_{0.2}$. A wind farm with multiple wind turbines may be represented with its output power at the PCC. Ten minutes average data and 60 s average data can be calculated by simple summation of the output from each wind turbine, whereas 0.2 s average data may be calculated according to (2.5) and (2.6);

$$P_{0.2\Sigma} = \sum_{i=1}^{N_{wt}} P_{n,i} + \sqrt{\sum_{i=1}^{N_{wt}} (P_{0.2i} - P_{n,i})^2} \quad (2.5)$$

$$Q_{0.2\Sigma} = \sum_{i=1}^{N_{wt}} Q_{n,i} + \sqrt{\sum_{i=1}^{N_{wt}} (Q_{0.2i} - Q_{n,i})^2} \quad (2.6)$$

where $P_{n,i}$, $Q_{n,i}$ are the rated real and reactive power of the individual wind turbine; $P_{0.2i}$ is the highest valid 0.2 second average real power data of the individual wind

turbine recorded during the measurement period specified in the standart, $Q_{0.2i}$ is the 0.2 average reactive power data at $P_{0.2i}$ of the individual wind turbine, N_{wt} is the number of wind turbines in the wind farm(IEC61400-21, 2001).

2.2.2.2 Voltage Fluctuations

Flicker is defined as an impression of unsteadiness of visual sensation induced by a light stimulus, whose luminance or spectral distribution fluctuates with time, which can cause consumer annoyance and complaint. Flicker can become a limiting factor for integrating wind turbines into weak grids, and even into relatively strong grids where the wind power penetration levels are high. The allowable flicker limits for Turkish National Transmission System is given in Table 2.2.

There are two types of flicker emissions associated with wind turbines, the flicker emission during continuous operation and the flicker emission due to switchings(IEC, 2001). Often, one or the other will be predominant. In order to prevent flicker emission from impairing the voltage quality, the operation of the generation units should not cause excessive voltage flicker. IEC 61000-4-15 specifies a flickermeter which can be used to measure flicker directly (IEC, 1997). The flicker measurement is based on the measurements of three instantaneous phase voltages and currents followed by using a “flicker algorithm” to calculate the P_{st} and P_{lt} , where P_{st} is the short term flicker disturbance factor and measured over 10 minutes, and the long term flicker disturbance factor P_{lt} is defined for two hour periods. Disturbances just visible are said to have a flicker disturbance factor of $P_{st} = 1$.

Table 2.2 Short-term and Long-term flicker disturbance factor limits for Turkish National Transmission System

Voltage Level (kV)	P _{st}	P _{lt}
V > 154 kV	0.85	0.63
34.5 kV < V < 154 kV	0.97	0.72
1 kV < V < 34.5 kV	1.15	0.85
V < 1 kV	1.15	0.85

The flicker emissions from a wind farm installation should be limited to comply with the flicker emission limits. Different utilities may have different flicker emission limits. The assessments of the flicker emissions are described below.

2.2.2.2.1 Continuous Operation. The flicker emission produced by grid connected wind turbines during continuous operation is mainly caused by fluctuations in the output power due to wind speed variations, the wind gradient and the tower shadow effect; blocking of the air flow by the tower results in regions of reduced wind speed both upwind and downwind of the tower. As a consequence of the combination of wind speed variations, the wind gradient and the tower shadow effect, an output power drop will appear three times per revolution for a threebladed wind turbine. This frequency is normally referred to as the $3p$ frequency. For fixed speed wind turbines with induction generators, power pulsations up to 20% of the average power at the frequency of $3p$ will be generated.

Wind characteristics as mean wind speed and turbulence intensity and also grid conditions as short circuit capacity, grid impedance angle and load type are the factors that affect flicker emission of grid-connected wind turbines during continuous operation. Flicker emission is also related to the type of wind turbine. Better performance of variable speed wind turbines have been reported, related to flicker emission in comparison with fixed speed wind turbines. Variable speed operation of the rotor has the advantage that the faster power variations are not transmitted to the grid but are smoothed by the flywheel action of the rotor(Sun, Chen & Blaabjerg, 2005).

The flicker emission from a single wind turbine during continuous operation may be estimated by:

$$P_{st} = c_f(\psi_k, v_a) \frac{S_n}{S_{sc}} \quad (2.7)$$

where $c_f(\psi_k, v_a)$ is the flicker coefficient of the wind turbine for the given network impedance phase angle, ψ_k , at the PCC, and for the given annual average wind speed, v_a , at hub-height of the wind turbine, S_n is the rated apparent power of the wind turbine. A table of data is needed, that is produced from the measurements at a number of specified impedance angles and wind speeds. From the table, the flicker coefficient of the wind turbine for the actual ψ_k and v_a at the site, may be found by applying linear interpolation. The flicker emission from a group of wind turbines connected to the PCC is estimated using equation (2.8)

$$P_{st\Sigma} = \frac{1}{S_{sc}} \sqrt{\sum_{i=1}^{N_{wt}} (c_{f,i}(\psi_k, v_a) S_{n,i})^2} \quad (2.8)$$

where $c_{f,i}(\psi_k, v_a)$ is the flicker coefficient of the individual wind turbine; $S_{n,i}$ is the rated apparent power of the individual wind turbine; N_{wt} is the number of wind turbines connected to the PCC. If the limits of the flicker emission are known, the maximum allowable number of wind turbines for connection can be determined.

2.2.2.2.2 Switching Operation. Switching operations will produce flicker. Typical switching operations are the start and stop of wind turbines. Start, stop and switching between generators or generator windings will cause a change in the power production. The change in the power production will cause voltage changes at the PCC. These voltage changes will, in turn, cause flicker. Hence, switching operations must be considered in wind turbine grid interconnections. The flicker emission due to switching operations of a single wind turbine can be calculated as

$$P_{st} = 18 \cdot N_{10}^{0.31} \cdot k_f(\psi_k) \frac{S_n}{S_{sc}} \quad (2.9)$$

where $k_f(\psi_k)$ is the flicker step factor of the wind turbine for the given ψ_k at the PCC. The flicker step factor of the wind turbine for the actual ψ_k at the site may be found by applying linear interpolation to the table of data produced from

measurements. Flicker step factor is a normalised measure of the flicker emission due to a single worst-case switching operation. The worst case switching operation is commonly a start-up, although IEC 61400-21 also requires the assessment of switching operations between generators, if applicable to the wind turbine in question.

The flicker emission from a group of wind turbines connected to the PCC can be estimated from:

$$P_{st\Sigma} = \frac{18}{S_{sc}} \cdot \left\{ \sum_{i=1}^{N_{wt}} N_{10,i} \cdot (k_{f,i}(\psi_k) S_{n,i})^{3.2} \right\}^{0.31} \quad (2.10)$$

where $k_{f,i}(\psi_k)$ is the flicker step factor of the individual wind turbine; $N_{10,i}$ is the number of switching operations of the individual wind turbine within 10 minute period. $S_{n,i}$ is the rated apparent power of the individual wind turbine; if the limits of the flicker emission are given, the maximum allowable number of switching operations in a specified period, or the maximum permissible flicker emission factor, or the required short circuit capacity at the PCC may be determined.

2.2.2.3 Harmonics

Harmonic disturbances are a phenomenon associated with the distortion of the fundamental sine wave and are produced by non-linearity of electrical equipment. Harmonics cause increased currents, power losses, possible destructive overheating in equipment, resonance and problems in communication circuits. Harmonic standards are specified to set up the limits on the total harmonic distortion (THD) as well as on the individual harmonics.

The emissions of harmonic currents during continuous operation of a wind turbine with a power electronic converter has to be stated according to IEC 61400-21 and in accordance with IEC 61000-4-7. The individual harmonic currents will be given as 10-minute average data for each harmonic order up to the 50th at the output

power giving the maximum individual harmonic current and further the maximum THD also has to be stated.

Harmonic emissions had been reported from a few installations of wind turbines with induction generators but without power electronic converters before IEC 61400-21 was developed. Since there was no known instance of customer annoyance or damage to equipment as a result of harmonic emissions from such wind turbines, IEC 61400-21 does not require measurements of harmonic emissions from them. Harmonic emissions of wind turbine installations has been measured and reported in the literature. A common conclusion in these observations is that the harmonic current emission is below the recommended values. In general harmonic standards can be met by modern wind turbines(Chen, 2005a), (Tande, 2005), (Thiringer, Petru, & Lundberg, 2004).

2.2.2.4 Revision of International Standard: IEC 61400-21

It is stated that IEC 61400-21 is currently under revision to provide procedures for assessing the newly developed wind turbine characteristics(Estanqueiro, Tande, & Peças Lopes, 2007). When the IEC 61400-21 standard was developed as published, the assessment of the wind turbine's power quality was, in its essence, the assessment of the turbines voltage quality. The reason for this was that at the time of developing the standard, the wind turbines were mainly connected to the distribution grid, and the basic concern was their possible impact on the voltage quality and not on power system operation. This has changed with the development of large wind farms that may form a significant part of the power system. In consequence, today's wind turbines are able to control the power delivered both in transient and steady state, they can cope with power ramp requirements and they have LVRT capabilities. They may even contribute to the primary frequency control, but then on the cost of dissipating energy.

2.2.3 System Stability

Stability analysis of the power system is a large area that covers many different topics. A formal definition of power system stability is provided by “IEEE/CIGRE Joint Task Force on Stability Terms and Definitions” as the ability of an electric power system, for a given initial operating condition, to regain a state of operating equilibrium after being subjected to a physical disturbance, with most system variables bounded so that practically the entire system remains intact. Figure 2.4 shows the overall picture of the power system stability problem, identifying its categories and subcategories(Kundur et.al., 2004).

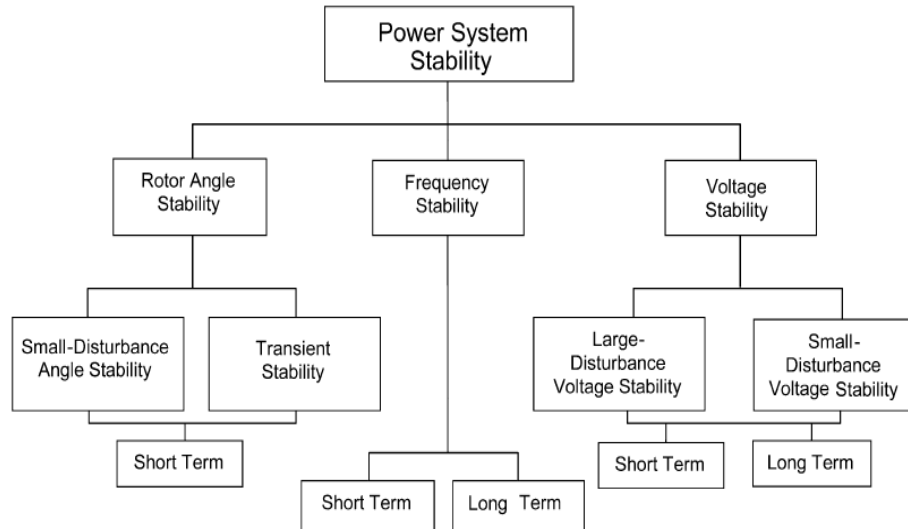


Figure 2.4 Classification of power system stability.

When an induction machine is used as a grid connected energy conversion unit, severe voltage sags due to faults in the connecting network cause significant speed increase of the turbine and generator rotor. After voltage recovery, the rotor speed of the induction generator may be so high that it does not return to the prefault value. Listed stability concepts used in power system analysis and shown in Figure 2.4 do not include this phenomenon. Samuelsson and Lindahl provided a tentative definition for this phenomenon and named it as rotor speed stability. Rotor speed stability refers to the ability of an induction machine to remain connected to the

electric power system and running at a mechanical speed close to the speed corresponding to the actual system frequency after being subjected to a disturbance (Samuelsson & Lindahl, 2005).

Tripping of transmission lines, loss of production capacity and short circuits are named as power system faults which are related to system stability. These failures affect the balance of both real and reactive power and change the power flow. Though the capacity of the operating generators may be adequate, large voltage drops may occur suddenly. The unbalance and re-distribution of real and reactive power in the network may force the voltage to vary beyond the boundary of stability. A period of low voltage may occur and possibly be followed by a complete loss of power. Many of power system faults are cleared by the relay protection of the transmission system either by disconnection or by disconnection and fast reclosure. In all the situations the result is a short period with low or no voltage followed by a period when the voltage returns. A wind farm nearby will see this event. In early days of the development of wind energy only a few wind turbines, named earlier as local wind turbines, were connected to the grid. In this situation, when a fault somewhere in the lines caused the voltage at the PCC of local wind turbines to drop, local wind turbines were simply disconnected from the grid and were reconnected when the fault was cleared and the voltage returned to normal.

Because the penetration of wind power in the early days was low, the sudden disconnection of a wind turbine or even a wind farm from the grid did not cause a significant impact on the stability of the power system. With the increasing penetration of wind energy, the contribution of power generated by a wind farm can be significant. If a large power rated wind farm is suddenly disconnected at full generation, the system will lose further production capability. Unless the remaining operating power plants have enough “spinning reserve”, to replace the loss within very short time, a large frequency and voltage drop will occur and possibly followed by a blackout. Therefore, the new generation of wind turbines is required to be able to LVRT during disturbances and faults to avoid total disconnection from the grid. In order to keep system stability, it is necessary to ensure that the wind turbine restores

normal operation in an appropriate way and within appropriate time. This could have different focuses in different types of wind turbine technologies, and may include supporting the system voltage with reactive power compensation devices, such as interface power electronics, SVC, STATCOM and keeping the generator at appropriate speed by regulating the power etc.(Chen, 2005a)

2.3 Grid Codes for Wind Energy Conversion Systems

Modern MW wind turbines currently replace a large number of small wind turbines and there is a significant attention to offshore wind farms, mainly because of higher average wind speed and no space limitations. Large power rated wind farms are started to operate in superior power systems and more large power rated wind farms are in construction or in the planning stage all over the world.

However, in order to achieve objectives as continuity and security of the supply, a high level of wind power into electrical network poses new challenges as well as new approaches in operation of the power system. Therefore countries started to issue dedicated “grid codes” for connecting the wind turbines/farms to the electrical network addressed to transmission and/or distributed system.

These requirements have focus on power controllability, power quality, LVRT capability and grid support during network disturbances. Grid code regulations often contain costly and demanding requirements for wind farm operators due to the increase in share of wind farms in power production. Large wind farms connected at the transmission level have to act as a conventional power plant and participate in primary (local) and secondary(system level) frequency/power control.

Since these demanding requirements can limit the penetration of the wind power in a given area, it was stated that grid codes and other technical requirements should reflect the true technical needs for system operation and should be developed in cooperation between TSO, the wind energy sector, government bodies, universities and research institutes(Iov, Hansen, Sørensen, & Cutululis, 2007), (EWEA, 2005).

Study and research groups are founded in different countries to investigate about further development of wind power utilization in power systems and the consequences on system stability, operation and grid extensions. With the experiences and results acquired from these studies, existing grid codes are evaluated and improved in all aspects.

In Turkey, the currently existing regulations for grid connected wind farms and other kind of renewable energy power plants are given in “Elektrik İletim Sistemi Arz Güvenilirliği ve Kalitesi Yönetmeliği” and “Elektrik Piyasası Şebeke Yönetmeliği”. Since, the share of wind power in power system continuously increases, issuing a dedicated grid code for grid connected wind farms in Turkey becomes a necessity.

Studies and investigations about Turkish transmission system grid codes for wind farms are being still continued by Turkish TSO(TEİAŞ). Since TEİAŞ and Dokuz Eylül University are participants of “Power Quality National Project, the further developmets in draft version of “Rüzgar Santralleri Şebeke Bağlantı Kriterleri - Grid Codes for Wind Farm Grid Connections” has been considered in this thesis. After getting the results of simulations and scientific researches, that have been carried out during this study, the proposals and suggestions were transfered to TEİAŞ about the new grid codes. The outlines of the new grid code are given below with relevant information.

2.3.1 Low Voltage Ride Through(LVRT) Capability

Conventional synchronous generators are equipped with exciter and voltage control. Besides, energy is also stored in the magnetic fields within the machine, particularly in the rotor circuits. Therefore, synchronous generators are able to supply high short-circuit currents to the fault location during considerable time intervals. High generator short-circuit currents keep the voltage within the grid relatively high

and thus the low voltage area caused by the fault is reduced. In consequence, less consumer, wind turbines or other distributed generator units are affected.

However, many conventional power plants will be replaced by large power rated wind farms in the future. In the past, local wind turbines were allowed to disconnect from the system in case of a fault. As wind turbines begin to replace conventional generation, there is an increasing requirement that they should remain connected to the power system during faults. Due to this requirement, power system operators in many countries have recently established transmission and distribution system grid codes that specify the range of voltage conditions for which wind turbine generators must remain connected to the power system. These are commonly referred to as the LVRT specifications and achieving these requirements is a significant technical issue on which turbine manufacturers are still working.

In terms of wind farms, LVRT capability indicates that a wind farm should stay connected to the network following voltage dips caused by short-circuit or lightning on any or all phases, where the voltage measured at the high voltage terminals of the grid connected transformer remains above the solid line of Figure 2.5. The vertical axis shows the percentage of voltage change and horizontal axis shows the time in milliseconds. The given limits of Figure 2.5 are changed for new wind farms, which will be integrated to the transmission system after 01.01.2009, as seen in Figure 2.6.

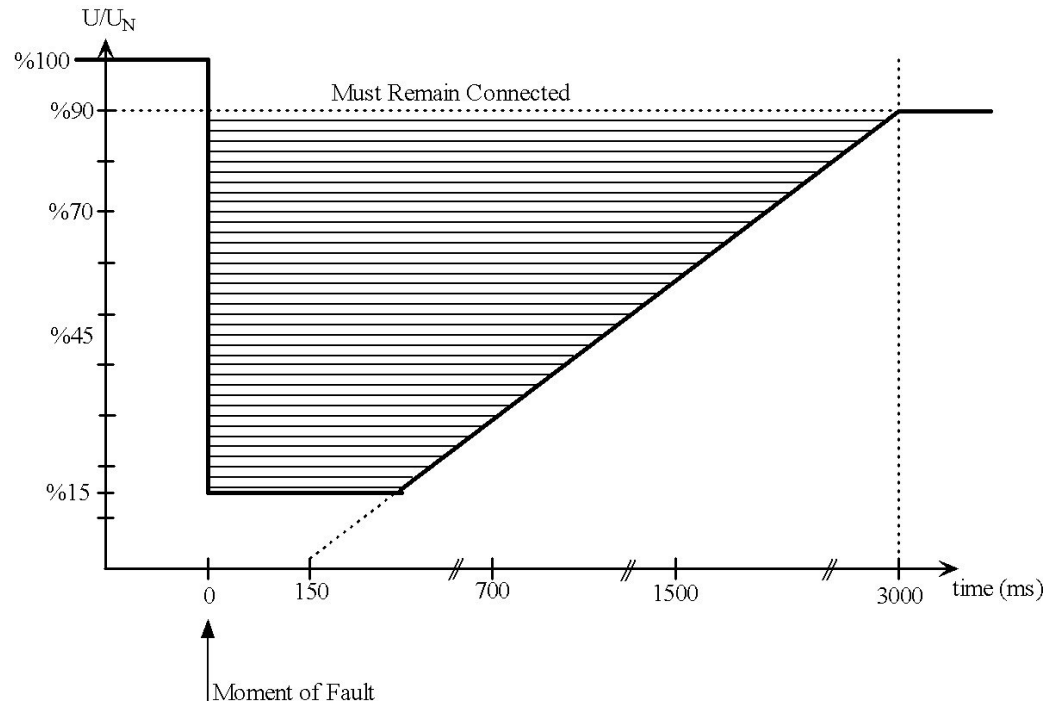


Figure 2.5 LVRT capability limits for wind turbines connected before 01.01.2009 to transmission system of Turkey.

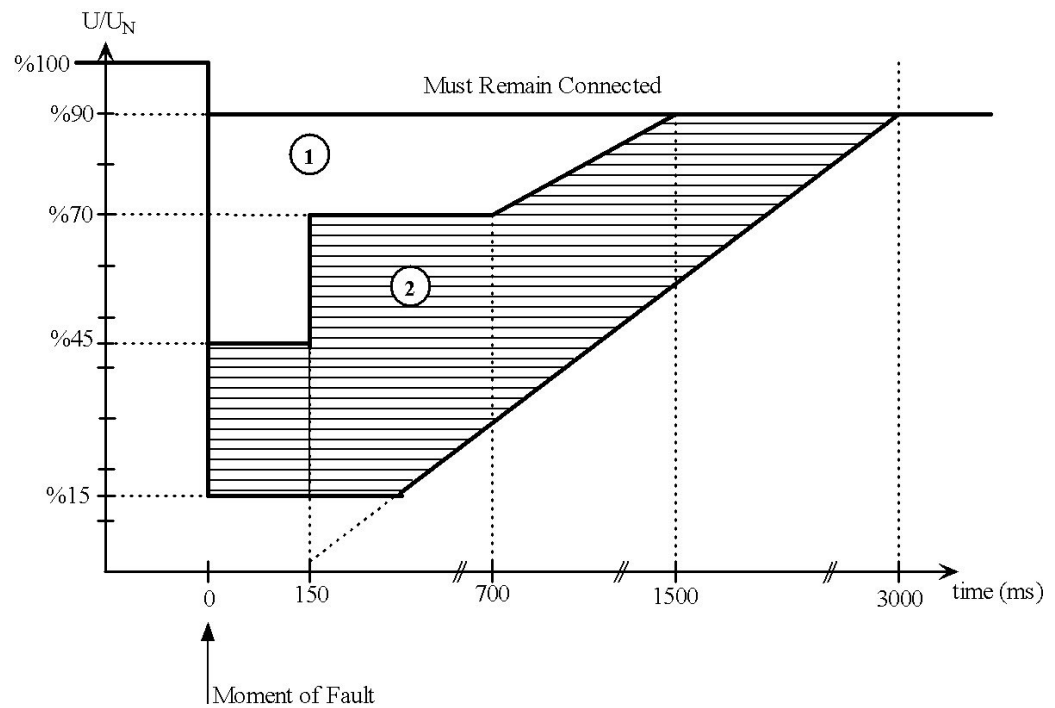


Figure 2.6 LVRT capability limits for wind turbines connected after 01.01.2009 to transmission system of Turkey

Zone 1, zone 2, and all above solid line specifies the range of voltage conditions for which wind turbine generators must remain connected to the power system. When the system voltage gets in zone 1 just after the fault, the wind turbine have to increase active power production in %20 of rated power for each second, and have to reach its maximum active power production. When the system voltage gets in zone 2 just after the fault, the wind turbine have to increase active power production in %5 of rated power for every second, and have to reach its maximum active power production.

LVRT capability limits are based on a time voltage diagram and are important subjects of grid codes that affect the appropriate wind turbine technology for wind farm installations. If wind farms disconnect from the grid in case of a voltage dip; depending on the output of wind generation connected at that time, system reserve might be insufficient to make up the shortfall and under-frequency load shedding might be necessary. A voltage dip that causes the loss of a conventional generator, in addition to the widespread loss of wind generation, is an even more severe scenario.

According to the grid codes, wind farm operators have to provide evidence of the fulfilment of LVRT capability requirements for their particular case. For single wind turbines it may be sufficient to present a certificate for LVRT capability, but large power rated wind farms need to be investigated by simulations which include steady state as well as dynamic studies. Besides, fulfilling grid requirements must be monitored continuously after installation(Erlich, Winter, & Dittrich, 2006).

2.3.2 Reactive Power and Voltage Variations

Equation (2.4) shows that the voltage variation at PCC are related to the reactive power output of wind farms. The fundamental requirement is that the steady state voltage variation in the grid, after the integration of a wind farm, must be maintained within a certain range. This requires a dynamic control of reactive power in wind farm due to the variation of active power generation.

Analysis of the impact of fluctuating wind generation output on the voltage performance of different parts of power grids showed that a fixed power factor would lead to unacceptable voltage variation as wind generator output varies. A power factor range of 0.95 leading to 0.95 lagging was found to limit voltage variation to an acceptable level. As grid codes are updated, reactive power requirements are also can be changed for secure power system operation with large power rated wind farms.

The power factor range shown in Figure 2.7, was adopted by TEİAŞ as many other countries. Wind farm that will be connected to transmission system must be operated in this power factor range, and this will be suitable for a wide range of system conditions. The range is not too dissimilar to grid code requirements for conventional generation and does not impose unreasonable costs on wind energy conversion system developers.

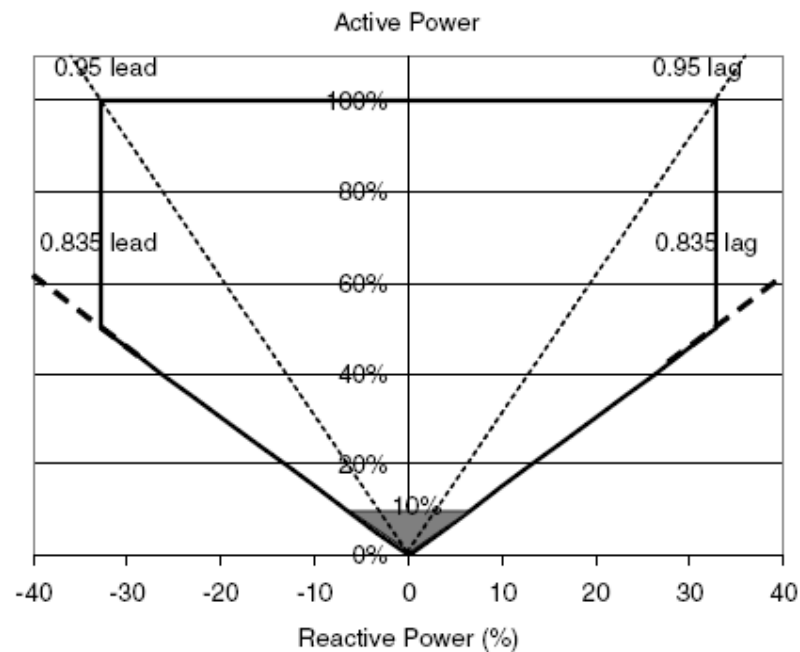


Figure 2.7 Reactive power requirements for wind farms in Turkey.

Wind farms have to provide voltage support during faults and, to some extent, also during normal operation. According to new grid codes of TEİAŞ; voltage support is required when the terminal voltage exits the dead band of $\pm 10\%$ around

the operating point which is shown in Figure 2.8. The wind farm's reactive power output should be regulated within its reactive power range to achieve the set-points. As seen from the slope of control characteristic, the minimum reactive current/voltage gain required is 2.0 pu. According to this, a reactive current of 1.0 pu will be supplied when the voltage level is 0.5 pu or 1.5 pu. Furthermore, the rise time required for this control is less than 20 ms and the reactive current support must continue at least 3 s. $I_{reactive}$ is the reactive current and I_n is the rated current of the wind farm.

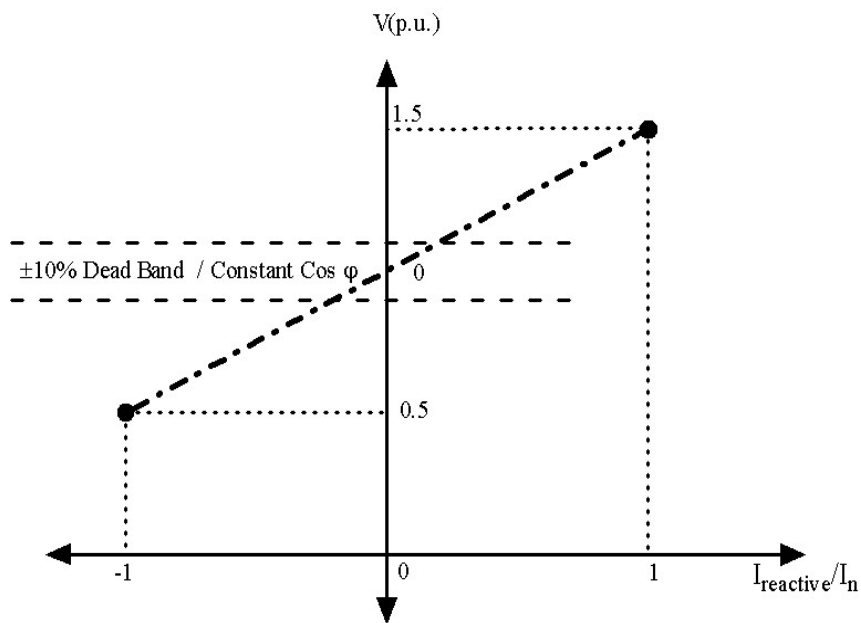


Figure 2.8 Voltage support characteristic of wind farms in Turkey.

To ensure variable voltage support during normal operation utilities can require continuous voltage control too, as practised by conventional synchronous generators. Fast continuous voltage control guarantees also maximum available reactive current in-feed during faults and some smoothening of voltage flicker may be caused by the fluctuating wind power. Large power rated offshore wind farms are candidates for continuous voltage control. Besides, wind farms have to provide a contribution to stabilizing power system electromechanical oscillations that require the design of voltage controller taking power system stability aspects into account (Erlich, Winter,

& Dittrich, 2006), (Fagan, Grimes, McArdle, Smith, & Stronge, 2005), (TEİAŞ, 2008).

2.3.3 Frequency Range, Control of Frequency and Active Power

In the power system, the frequency is an indicator of the balance between production and consumption. The issues affecting the power system frequency that are important for wind farms can be listed as; frequency range, provision of frequency control, provision of active power and ramp rates.

The frequency ranges that are required for conventional generators, will be required for wind generators which will be integrated to transmission system after 01.01.2009 in Turkey. Power system frequency usually remains within the normal operating range, but there are occurrences where the frequency deviates outside the range and TSO must ensure that all generators connected to the system can tolerate these frequency excursions. Generators are required to operate within the normal operating range continuously at normal rated output. All generators must be capable of staying “synchronised”, in the case of conventional plant, and “connected”, in the case of wind generators, to the transmission system at frequencies and periods given in Figure 2.9 below.

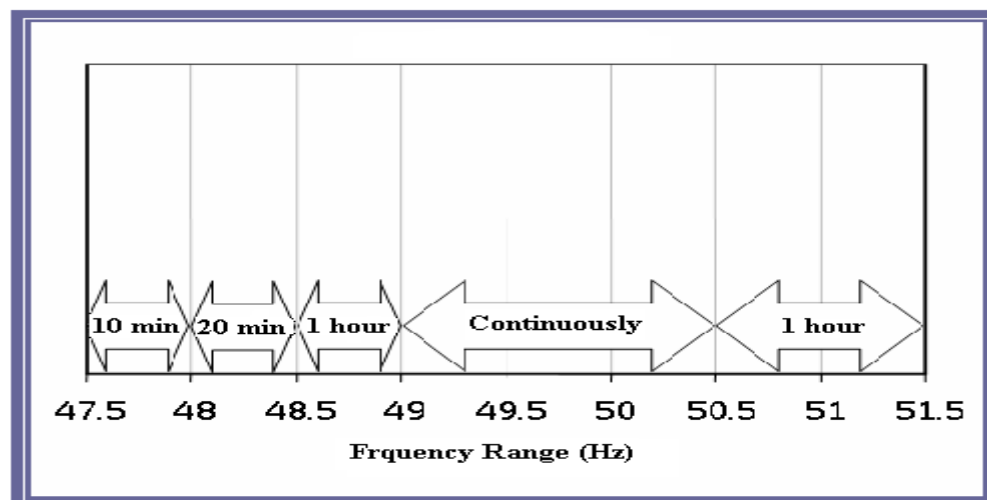


Figure 2.9 Frequency range for wind farms in Turkey.

Frequency control has been traditionally provided by conventional thermal plants through the use of on-load governors. However, as more wind generation replaces conventional plant, wind generators must also provide this service. The requirements for the provision of frequency control are set out in power-frequency control curves, which are shown in Figure 2.10.

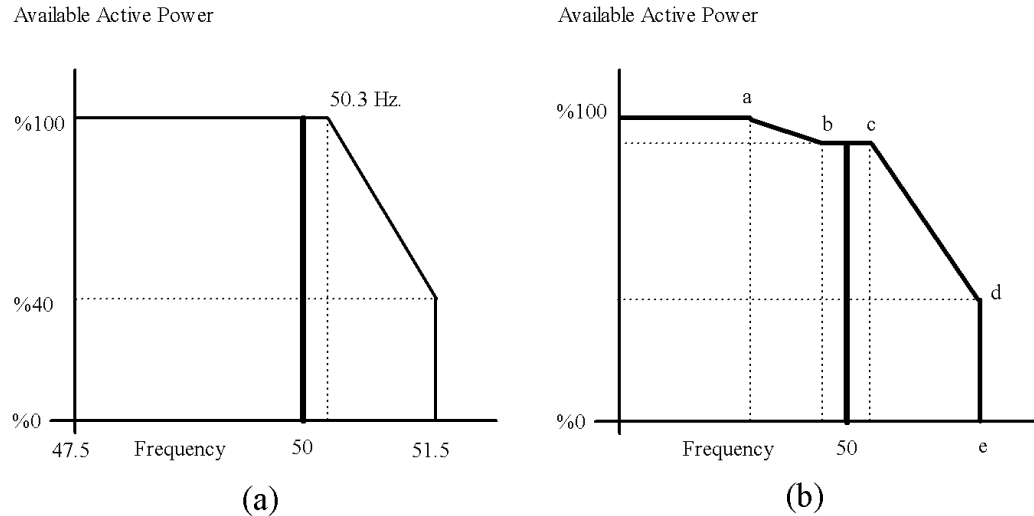


Figure 2.10 Power-frequency control curves: (a) Without underfrequency control, (b) With underfrequency control

Two different power-frequency control curves are shown in Figure 2.10; power-frequency control curve without underfrequency control in Figure 2.10(a) and power-frequency control curve with underfrequency control in Figure 2.10(b).

According to the given curve in Figure 2.10(a), which is adopted by TEİAŞ; wind farms have to participate in frequency control only in case of overfrequencies (above 50.3 Hz. for this curve) by decreasing production. During normal power system operation, wind farm can produce 100% of its possible active power.

Wind farms have to keep their production lower than possible above the frequency “a (for example 49.3 Hz.)” in order to participate in frequency control in case of underfrequencies according to the given curve in Figure 2.10(b). The reduced active power output at frequencies in the normal range; between b (for example 49.7 Hz.) and c (for example 50.3 Hz.), allows for an increase in output when the

frequency falls below the defined limit b(49.7), and thus assisting in increasing the frequency. The limits “a, b, c, d, e” can be adjusted according to the system characteristics by the TSO.

In order to avoid long-term unbalanced conditions in the power system, the power demand is predicted and power plants adjust their power production. The requirements regarding active power control of wind farms aim to ensure; a stable frequency in the system as detailed above, to prevent overloading of transmission lines, to ensure compliance with power quality standards and to avoid large voltage steps and in-rush currents during startup and shutdown of wind turbines.

According to the new grid codes; each wind farm connected to Turkish transmission system must be capable of accepting an active power set-point signal from TEİAŞ and implementing the necessary changes. If necessary; the output power of wind farms will be controlled in the range of %20-%100 of rated powers by TEİAŞ.

Ramp rates refer to the change in active power output over time. The maximum ramp rates of wind farms complies with the conventional plants’ ramp rates to prevent adverse effects with the new grid code:

- (a) Ramp rate for wind farms under 100 MW rated power :
%5 of Rated Power in a minute.
- (b) Ramp rate for wind farms over 100 MW rated power :
%4 of Rated Power in a minute.

2.3.4 Signals, Control and Communications

In most regulations, the wind farm operator is required to provide the signals necessary for the operation of the power system. The signals, control and communications requirements specified in the grid codes are originally written with conventional generation in mind. There are also a number of new signals and control

commands that are required due to the implementation of the various requirements as detailed above.

As the source for wind generation is the wind, the TSO must receive meteorological data from each wind farm site. This is essential for the TSO to run its own wind forecasting programs. The meteorological signals that are required are wind speed and direction, air temperature and air pressure. The meteorological data signals can be provided by a dedicated on-site meteorological mast, or, if the wind farm can prove that the signals would be as accurate or more accurate taken elsewhere then this can be allowed.

The TSO also needs to be able to control each wind farm. The control signals that each wind farm must be capable of accepting are active power curtailment signal; a signal to change the mode of the frequency controller and a signal to set the kV setpoint for voltage regulation purposes. In the case of a total or partial system blackout, the TSO shall send the wind farm a trip and inhibit signal which shall prevent the wind farm from reconnecting. The TSO must be able to communicate with a responsible operator for the wind farm, who must also be on site within one hour. Large power rated wind farms must provide power output forecasts to the TSO (Fagan, Grimes, McArdle, Smith, & Stronge, 2005), (Matevosyan, Ackermann, & Bolik, 2005).

CHAPTER THREE
WIND ENERGY CONVERSION SYSTEMS
PROPERTIES, CLASSIFICATION AND CHARACTERISTICS

Grid connected wind energy conversion systems are designed and build for converting wind energy into electrical energy, which is fed into grid. A group of wind energy conversion systems, which are connected to the same PCC, consists a “wind farm - wind power plant” as shown in Figure 3.1.

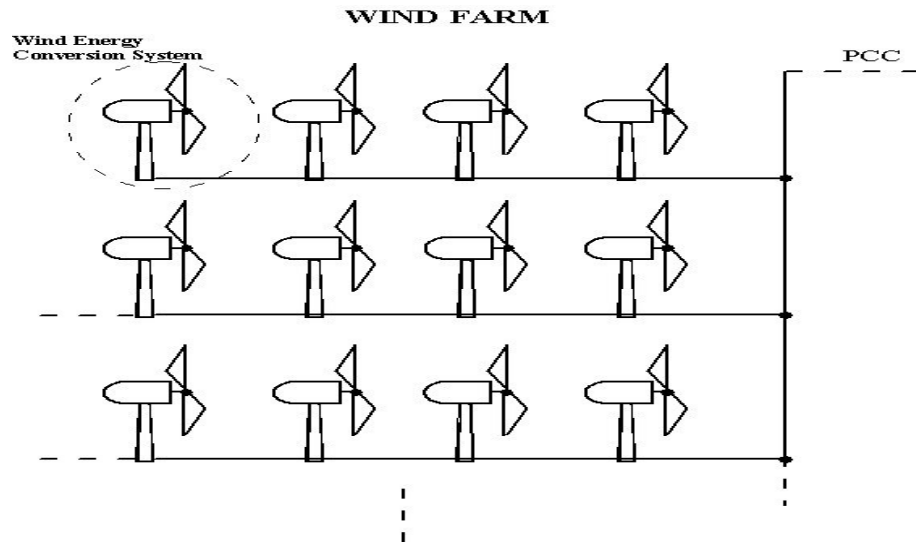


Figure 3.1 Wind farm configuration

Wind power has quite distinctive generation characteristics compared to conventional generation. Typical technical features of wind farms and performance indicators which make them different from conventional power generators will be discussed in this chapter.

3.1 Components of Grid Connected Wind Energy Conversion System

Grid connected wind energy conversion systems are composed of; wind turbine, control system and grid integration system.

Table 3.1 . Components of Grid Connected WECS

Wind turbine	Nacelle, Generator, Rotor(Blades&Hub), Shafts(Low Speed-High Speed), Gearbox, , Brakes, Tower, Yaw: Shown in Figure 3.2.
Control System	Control and communication devices, Wind Sensors.
Grid Integration System	Step-up Transformers, Cables, Substation(PCC), Companzation Equipments, Protection devices.

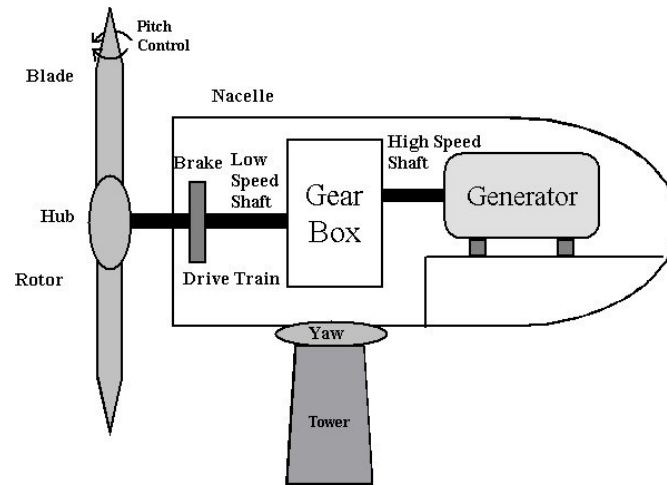


Figure 3.2 Major components of a wind turbine.

The blades and the hub together are called the rotor, which converts wind energy to mechanical energy. The efficiency of this conversion depends on several factors such as blade profiles, pitch angle, tip speed ratio and air density. The pitch angle, β is the angle of the blades towards the rotational plane. If the pitch angle is low, the blades are almost perpendicular to the wind and if the pitch angle is high (near 90 degrees) the blades are almost in parallel with the hub direction.

A wind turbine can be equipped with any type of three-phase generator. Several generic types of generators may be used in wind turbines; squirrel cage induction generators, wound rotor induction generators, doubly fed induction generators, wound rotor synchronous generators, and permanent magnet synchronous generators. Also high voltage generators, switch reluctance generators and transverse flux generators are reported as other types of potential interest(Hansen, 2005).

3.2 Classification of Wind Energy Conversion Systems

The most commonly applied wind turbine configurations are classified; by their ability to control turbine speed, by the type of power control used, by the type of grid connection, and by the type of the generator used. Wind turbines have to be designed with some sort of power control in order to limit the power in very high winds and avoid damage to the wind turbine. Stall control, pitch control and active stall control are the methods for power control in wind turbines. Active stall control means that the pitch angle is adjusted slightly at higher wind speeds in order to obtain appropriate power level. Wind turbines can be connected to the grid directly, by one power electronic converter or by two power electronic converters; one for stator and one for rotor, (doubly fed).

3.2.1 Fixed Speed Wind Turbines

The wind turbines of early installations operate at near constant speed. This means that regardless of the wind speed, the angular speed of the rotor is fixed and determined by the frequency of the grid, the gear ratio, and the generator layout. They are designed to achieve maximum efficiency at one particular wind speed. Induction generators and the wound rotor synchronous generators have been applied, where the majority have been based on the induction generator.

Fixed speed wind turbines generally use squirrel cage induction generators with direct grid connection so as to maintain a fixed speed that matches the electrical frequency of the grid. The reasons for this popularity are mainly due to its simplicity, high efficiency, and low maintenance requirements, which generally are restricted to bearing lubrication only. When the induction generator is coupled directly to the supply grid, the wind turbine will have a very high impact on the supply grid because of the necessity to obtain the excitation current from the supply grid. Also, because of the steep torque speed characteristic of an induction generator, the fluctuations in the wind power will to some extent be transferred directly to the supply grid. These transients become especially critical during connection of the wind turbine to the

grid. To overcome these two problems, wind turbines based on a squirrel cage induction generator are usually equipped with a soft-starter mechanism and an installation for reactive power compensation. Fixed speed wind turbines have a certain impact on the supply grid, especially in the areas with weak supply grids and a high penetration of wind energy(Helle & Blaabjerg, 2002).

In order to operate the fixed speed systems at low and high wind speeds efficiently, pole changing is generally employed. Smaller number of pole pairs is used at high wind speeds and higher number at lower wind speeds. This allows the generator to operate at a different mechanical speed without affecting its electrical frequency. The advantage is that a cost-effective aerodynamic control like stall control can be used. The drawbacks of fixed speed systems can be listed as follows(Chowdhury & Chellapilla, 2006);

- a) Available wind power cannot be optimally used due to constant speed operation.
- b) Since there is no inherent reactive power control method in this configuration, compensation equipment must be used for not to draw the reactive power from the grid.
- c) Since the generator is made to run at a constant speed in spite of fluctuations in wind speed, it will result in fluctuation of generated voltage as well as output power.

3.2.2 Variable Speed Wind Turbines

Variable speed wind turbines with power electronic converters has become more common than traditional fixed speed wind turbines. Modern wind farms are mostly equipped with variable speed wind turbines that are usually operated to maintain the maximum aerodynamic efficiency condition, so the maximum power can be obtained from the actual wind at every instant and delivered to the power system. This operation strategy is generally denominated maximum power tracking. Fast control of active and reactive power can be achieved from these types of turbines. Variable

speed operation yields more energy than the fixed speed operation, providing benefits in reducing power fluctuations and improving var supply. Also, better performance of variable speed wind turbines, related to flicker emission in comparison with fixed speed wind turbines have been reported(Larsson, 2002).

In variable speed systems, the turbine rotor absorbs the mechanical power fluctuations by changing its speed. So the output power curve is smoother which greatly enhances the quality of power. The reason is that variable speed operation of the rotor has the advantage that the faster power variations are not transmitted to the grid but are smoothed by the flywheel action of the rotor. However, since variable speed operation produces a variable frequency voltage, a power electronic converter must be used to connect to the constant frequency grid. Economical power electronic devices have made the variable speed technology more preferred and common.

3.2.3 Typical Wind Turbine Configurations

Studies have been performed and reported about different wind turbine configurations in the literature, to adapt the designs to the requirement of improved grid compatibility with increasing wind power penetration. As a result, there are four typical wind turbine configurations accepted on common literature. Brief information will be given about these configurations in this section.

3.2.3.1 Type A

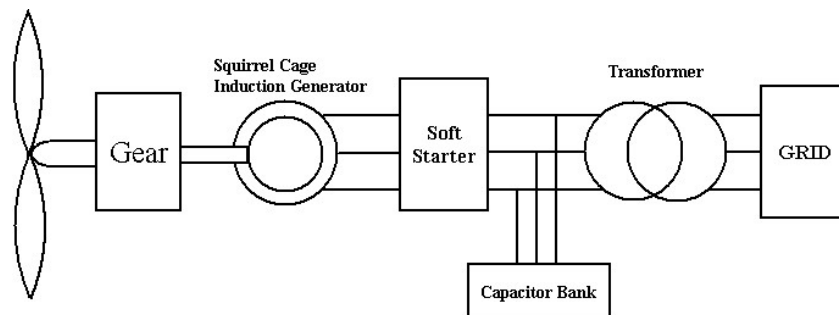


Figure 3.3 Type A configuration.

This configuration denotes the fixed speed wind turbine with squirrel cage induction generator directly connected to the grid via a transformer as shown in Figure 3.3. Since squirrel cage induction generator always draws reactive power from the grid, this configuration uses a capacitor bank for reactive power compensation. A smoother grid connection is achieved by using a soft-starter.

Nearly all configurations need a gearbox mechanism to increase the turbine shaft speed to rotational speed of the generator, since the rotational speed of wind turbine is considerably low in comparison with that of the conventional electrical machines.

3.2.3.2 Type B

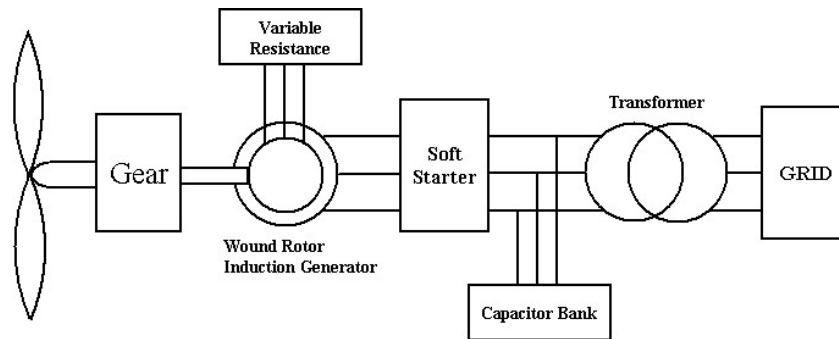


Figure 3.4 Type B configuration.

This configuration corresponds to the limited variable speed wind turbine with variable generator rotor resistance. The generator is directly connected to the grid. A capacitor bank performs the the reactive power compensation. The unique feature of this concept is that it has a variable additional rotor resistance, which can be changed by a controlled converter mounted on the rotor shaft. The wind turbines of type B are equipped with an active blade pitch control system.

3.2.3.3 Type C

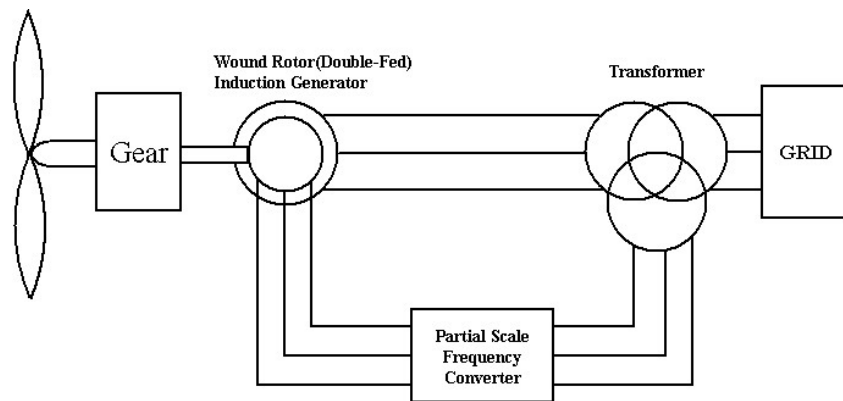


Figure 3.5 Type C configuration.

This configuration, known as the doubly fed induction generator (DFIG) concept, corresponds to the limited variable speed wind turbine with a wound rotor induction generator and partial scale frequency converter (rated at approximately 30% of nominal generator power) on the rotor circuit. The partial scale frequency converter performs the reactive power compensation and the smoother grid connection.

3.2.3.4 Type D

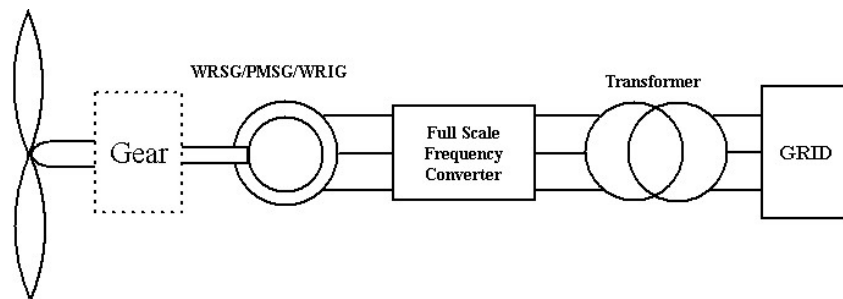


Figure 3.6 Type D configuration.

This configuration corresponds to the full variable speed wind turbine with generator connected to the grid through a full-scale frequency converter. The frequency converter performs the reactive power compensation and the smoother grid connection. The generator can be excited electrically or by a permanent magnet.

Some full variable speed systems have no gearbox. In these cases, a direct driven multipole generator with a large diameter is used.

3.3 Technical Features of Wind Power Plants

The wind turbine generator system operation is permanently determined by the speed and variations of the wind. The following four basic operating states can be distinguished:

- a) Standstill of the turbine – as a result of the wind speed value falling below the cut-in wind speed $v < v_{cut-in}$
- b) Partial load – operation with maximum energy extraction from the wind, when the wind speed v is within the range $v_{cut-in} \leq v \leq v_n$, where v_n is the rated wind speed. Wind turbine generator generates the rated power at the rated wind speed.
- c) Full load – operation with constant and rated load when the wind speed is higher than the rated wind speed $v_n < v \leq v_{cut-out}$ and simultaneously lower than the maximum one. The cut-out wind speed is usually $v_{cut-out} = 25$ m/s.
- d) Standstill of the turbine – because of too high wind speed $v > v_{cut-out}$.

These operating states of the wind turbine are usually presented in the form of the power versus wind speed characteristics of the wind turbine. An example of such a characteristic is shown in Figure 3.7(Lubosny, 2003). The dashed line shows the power in the wind and the continuous line shows the power that the wind turbine can convert to the grid. The vertical axis is the ratio of power generated P_G , to the rated power of the wind turbine P_n , and the horizontal axis is the wind speed.

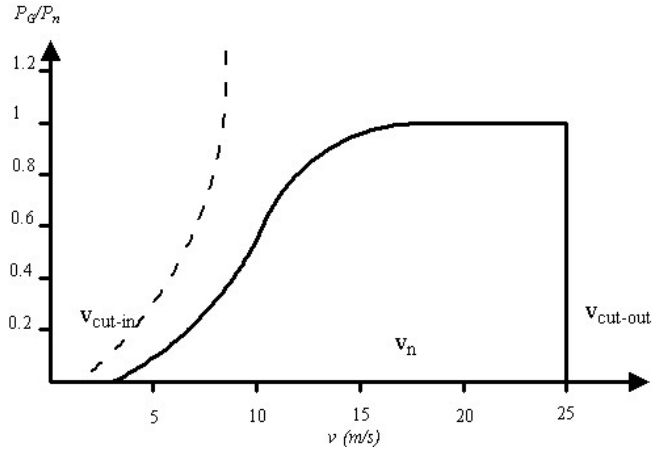


Figure 3.7 Power versus wind speed characteristics of a wind turbine.

The power of an air mass that flows at speed $v(m/s)$ through an area A can be calculated as follows;

$$\text{Power in wind(watts)} = \frac{1}{2} \rho A v^3 \quad (3.1)$$

where, ρ is air density (kg/m^3). As seen from (3.1) the *power in wind* is proportional to the air density, the intercepting area(the area of the wind turbine rotor), and the speed to the third power.

The *power in wind* is the total available energy per unit of time. The power in the wind is converted into mechanical-rotational energy of the wind turbine rotor, which results in a reduced speed in the air mass.

The tip speed ratio, λ , is the ratio between the tip speed of the blades and the wind speed. The mechanical characteristics of wind turbines are formulated by power and torque equations;

$$P_t = C_p(\beta, \lambda) \frac{1}{2} \rho (\pi R^2) v^3 \quad (3.2)$$

$$T_w = \frac{C_p(\beta, \lambda)}{\lambda} \frac{1}{2} \rho \pi R^3 v^2 \quad (3.3)$$

Here, R is the turbine radius, β is the blade pitch angle, and λ is the tip-speed ratio which is defined as

$$\lambda = \frac{\omega_t R}{v} \quad (3.4)$$

where ω_t is the rotational speed of the turbine in rad/s. In equation (3.2) and (3.3), the term $C_p(\beta, \lambda)$ is the power coefficient of the rotor, which is dependent on the pitch blade angle and tip-speed ratio, determines the characteristics of power versus rotational speed. The ratio of the power coefficient to tip-speed ratio is the torque coefficient $C_T(\beta, \lambda)$ of the turbine and given by (Sürgevil, 2004)

$$C_T(\beta, \lambda) = \frac{C_p(\beta, \lambda)}{\lambda} \quad (3.5)$$

The Betz limit, $C_{pmax} = 16/27$, is the maximum theoretically possible rotor power coefficient. In practice three effects lead to a decrease in the maximum achievable power coefficient: rotation of the wake behind the rotor, finite number of blades and associated tip losses, non-zero aerodynamic drag. The overall turbine efficiency is a function of both the rotor power coefficient and the mechanical/electrical efficiency of the wind turbine:

$$\eta_{overall} = \frac{P_{out}}{\frac{1}{2} \rho A v^3} \quad (3.6)$$

Capacity factor, given in (3.7), of a wind farm is relatively lower; 0,25 for low wind speed locations and 0,40 for high wind speed locations, than conventional power plants. This implies that in order to obtain the same energy production from a conventional power plant and a wind farm, the installed wind farm capacity must be

significantly larger than the capacity of the conventional power plant(Manwell, McGovan & Rogers, 2002).

$$Cap.Fac. = \frac{W(Annual)}{P_{rated} \cdot 8760} \quad (3.7)$$

where $W(Annual)$ is the sum of the energy produced by the wind farm for a year in (kW/h).

CHAPTER FOUR

ALAÇATI WIND FARM

4.1 Alaçatı Wind Farm

Alaçatı wind farm was built in 1997 and started to operated in 1998. It is located in Alaçatı-İzmir, which is placed on west region of Turkey with 65-90 meters altitude.



Figure 4.1 Wind farm.

There are twelve 600 kW wind turbines of VESTAS equipped with three phase wound rotor induction generator. Control unit of each turbine is placed at the bottom of turbine tower and named as ground controller.



Figure 4.2 Wind turbine 0.69/34.5 kV star-delta connected transformer in wind farm.

Each wind turbine generator has its own 0.69/34.5 kV star-delta connected transformer. The neutral point of the transformer is grounded to diminish the 3rd harmonic voltages.

Wind turbine transformers are connected to the 34.5 kV bus of wind farm substation. Two loops are formed for connection and each loop has six transformers as seen from Figure 4.3. Wind farm substation is connected to the 34.5 kV distribution feeder of TEİAŞ-Alaçatı Substation, which forms the PCC for the wind farm.

There are various types of loads; mostly residential and commercial, fed from 34.5 kV common bus of Alaçatı Substation, as shown in Figure 4.4. Alaçatı Substation 34,5 kV bus is connected to interconnected 154 kV power lines via 154/34.5 kV, 50 MVA transformer.

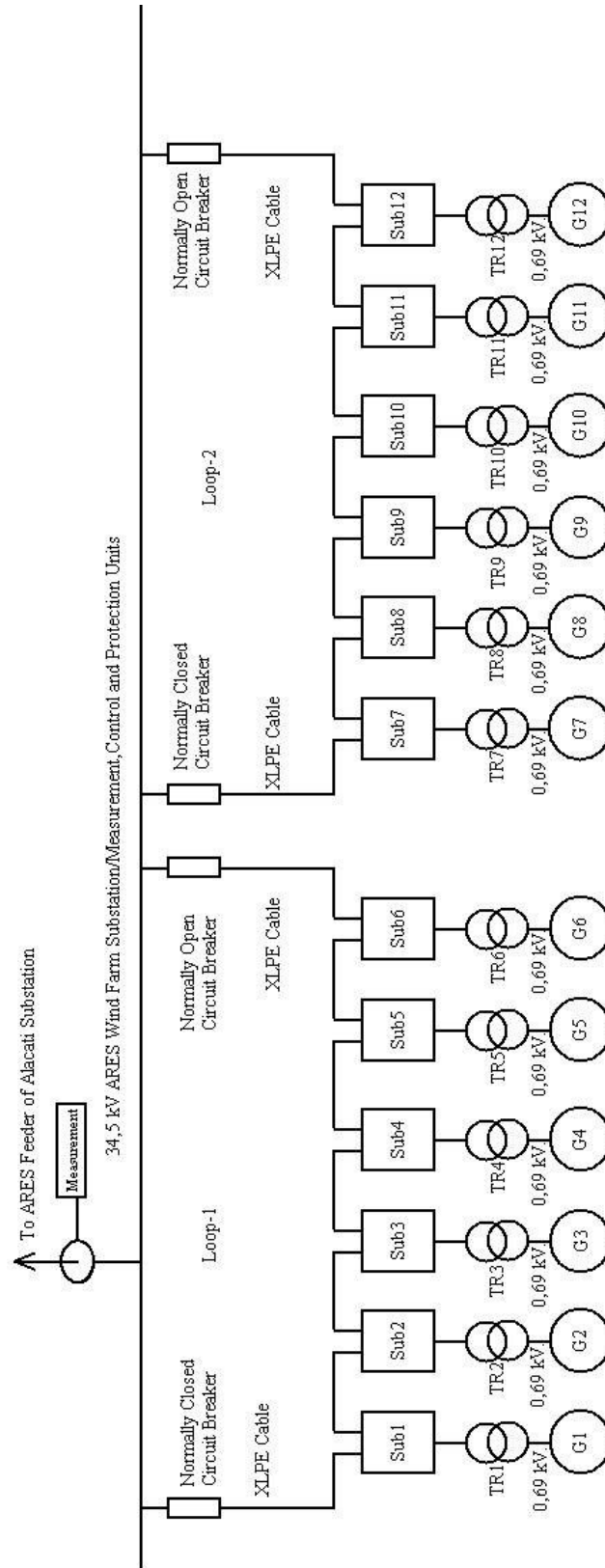


Figure 4.3 Wind farm one line diagram.

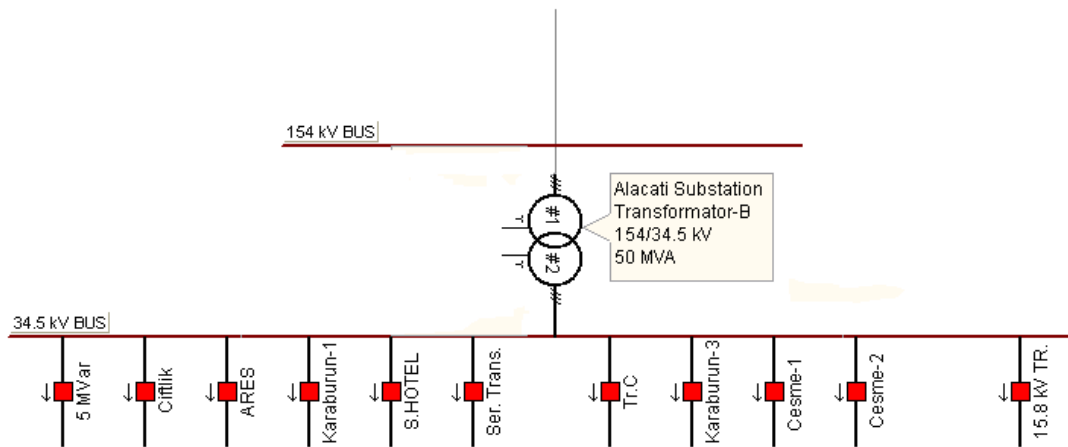


Figure 4.4 : TEİAŞ-Alaçati Substation one line diagram.

4.1.1 Wind Turbine Generators

Wind turbines are equipped with wound rotor induction generators, with a three phase uncontrolled rectifier, IGBT chopping unit, three phase resistor and control unit as shown in Figure 4.5 and Figure 4.6. The equivalent resistance at rotor terminals are adjusted by the electronic control system.

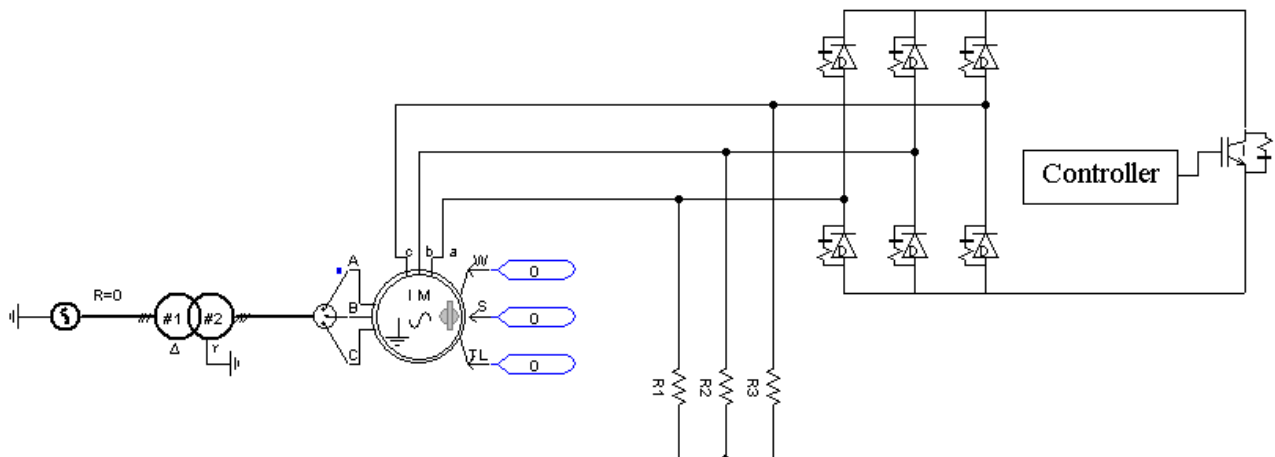


Figure 4.5 WRIG with rotor circuit.

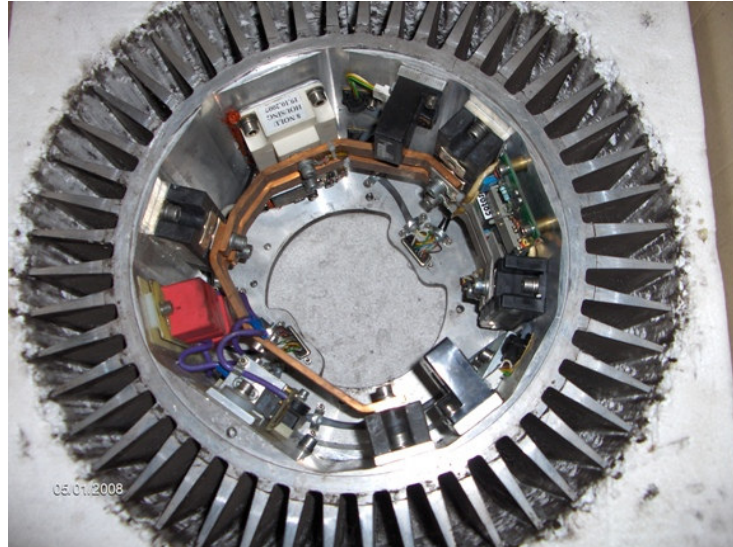


Figure 4.6 A photo of rotor circuit.

The control unit calculates the necessary resistance using the current reference (related to extracted power) and the measured rotor current. This resistance is controlled by chopping the rectifier output current. The IGBT is switched on and off with a 3 kHz switching frequency for this purpose. This control technique keeps the slip between approximately 0.6% and 10% by adjusting the resistance between 0 and the maximum value.

A snubber is used to limit the voltage peak each time the IGBT is switched-off. A thyristor is used for over-voltage protection of the power electronics by short-circuiting the IGBT in case of a short interruption or a short-circuiting on the grid.

4.1.2 Control System

Control unit of each turbine is placed at the bottom of turbine tower and named as ground controller. Overall control system diagram is shown in Figure 4.7. Ground controller collects the data of; wind speed, external rotor resistance, direction of the nacelle, pitch angle of blades, currents, voltages, output power and capacitors. After the calculations are done, the unit makes the necessary changes of; external rotor resistance, direction of the nacelle, pitch angle of blades, and capacitors for maximum efficiency.

The mechanical input power is controlled using the blade pitch angle. The wind turbines are equipped with an active blade pitch control system connected to the ground controller. Basically, the functionality of a pitch-controlled wind turbine consists in its ability to change the power performance coefficient $C_p(\beta, \lambda)$ by turning the rotor blades around their longitudinal axis. Control unit checks the output power of the wind turbine and whenever the output power becomes too high, the rotor blades are pitched slightly out of the wind. Conversely, the blades are turned back into the wind whenever the wind drops again. During normal operation the blades will pitch a fraction of a degree at a time and the rotor will be turning at the same time. Also a yaw system, located in the junction of the nacelle and the tower; is used to make the yaw angle and wind direction equal.

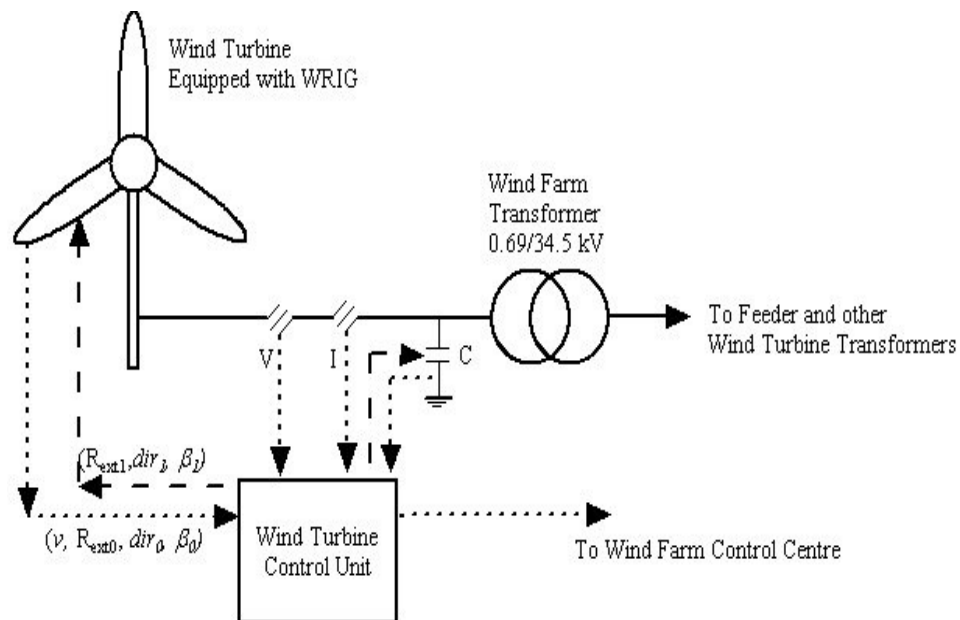


Figure 4.7 : Wind Turbine Control System.

4.1.3 Power Factor Correction

Each wind turbine in the wind farm is equipped with compensation capacitors which are divided into four steps 75 kVAR, 50 kVAR, 50 kVAR, 50 kVAR (totally 225 kVAR) for power factor correction. After the generator starts up, the capacitor banks are switched on with the delay of one second. Once a capacitor bank is

switched off, then it can be connected to bus again due to the reactive power demand after minimum time of 60 seconds in order to ensure that the capacitors are discharged. Just before the generator is cut out all capacitors are switched off simultaneously. In case of a fault in power system operation, the capacitors are cut out temporarily by the controller.

4.2 MATLAB/Simulink Simulation of the Wind Energy Conversion System

At the beginning of the thesis study; a simulation model of wind turbine equipped with wound rotor induction machine developed in MATLAB/Simulink for transient tests and analysis. The aim of the simulation was to get results of a single wind turbine model, especially rotor circuit, in case of a power system fault. Because it is known that wind farm operator had problems about relatively quick IGBT breakdowns in the rotor circuit.

The simulation results for the transient process in an external 100 ms. short-circuit fault situation are given and the impacts of the short circuit on wind energy conversion system are analyzed. Wound rotor induction machine data of Alaçatı wind farm which is given in Table 4.1 is used in simulation. Wind speed is assumed to be constant at 10 m/s which is the first input for the simulink wind turbine model and second input is the rotor speed as rpm.

Table 4.1 Wind farm generator parameters

Parameter	Value	Units
Rated Power	600	kW
Rated Voltage	690	V
Rated Slip	5	%
Slip Regulation Interval	1-10	%
Rated Speed	1575	RPM
Stator Resistance	0.00357	ohm
Stator Leakage Inductance	0.055	ohm
Mutual Inductance	2.39	ohm
Rotor Resistance´	0.0055	ohm
Rotor Leakage Inductance´	0.0662	ohm
External Resistance	1 (per phase)	ohm
Rotor Inertia	29	kgm ²

Simulation circuit is given in Figure 4.8. At first, induction machine starts to operate and reaches rated speed with zero torque input in motor mode. After $t = 1.75$ s, wind turbine starts to operate as a generator with constant wind speed. Power switch(IGBT) current waveform during the simulation is given in Figure 4.9. As seen from Figure 4.9, the current within rotor circuit and IGBT is around 500 A. Three phase-ground short-circuit fault for 100 milliseconds at transmission line which connects wind turbine to grid, is demonstrated by the help of circuit breaker between $t = 2.5 - 2.6$ s. The current within IGBT after the grid fault reaches 8000 A. which will cause thermal breakdown.

Simulation results show LVRT capability and stability limits of the generator depends on the rotor circuit current capability. The present protection system in the Alaçatı wind farm cuts out the wind turbine to protect IGBT, since IGBT can not withstand those high current values in this wind turbine configuration. A time lag in the protection system causes IGBT thermal breakdown.

The wind farm operator will need new precautions in case of new grid code obligations for present wind farms. Additional protection system like crowbar, can be implemented on present generators of the wind farm in order to prevent unnecessary cut outs and excessive IGBT breakdowns.

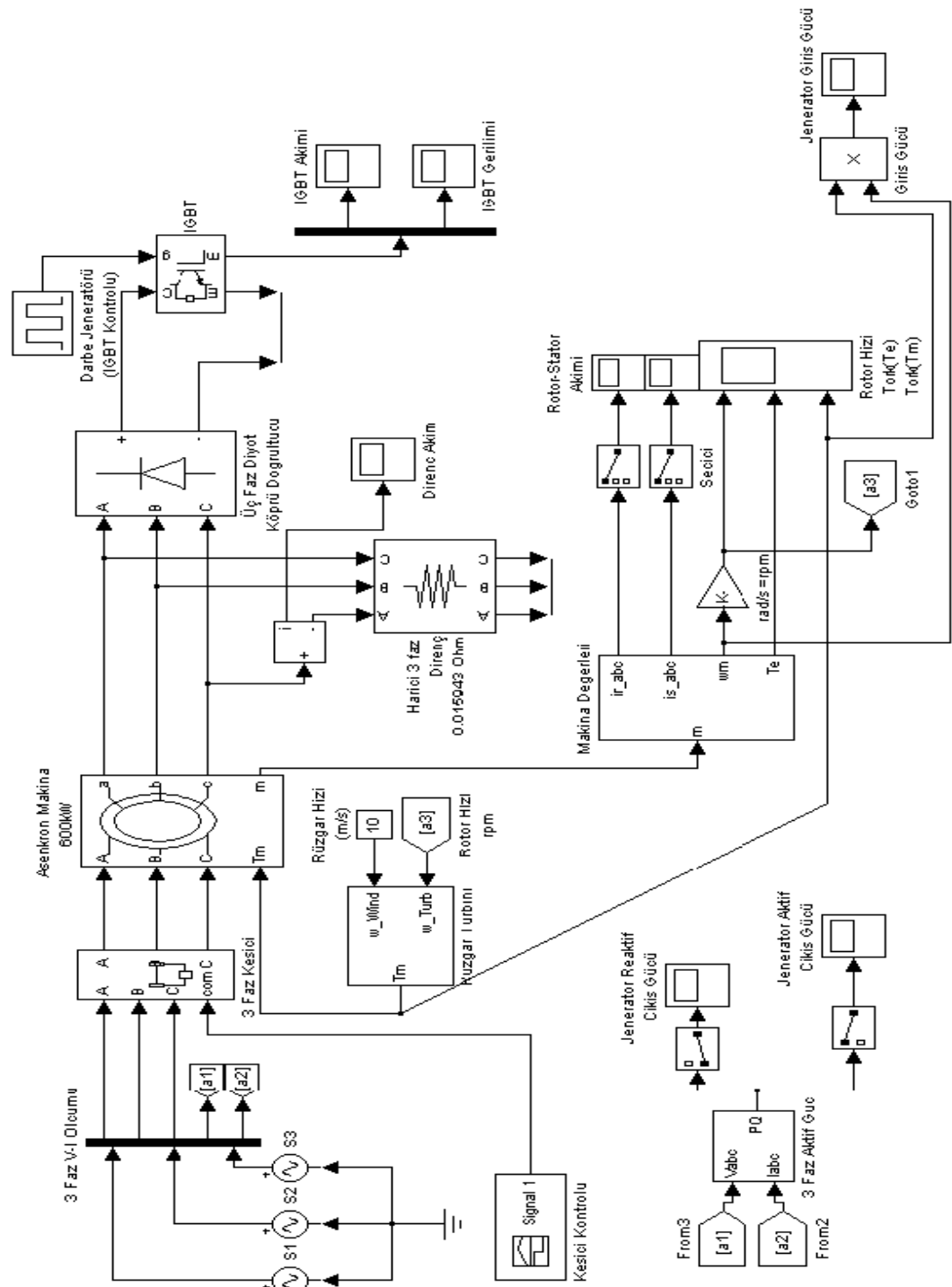


Figure 4.8 Overview of MATLAB/Simulink simulation circuit.

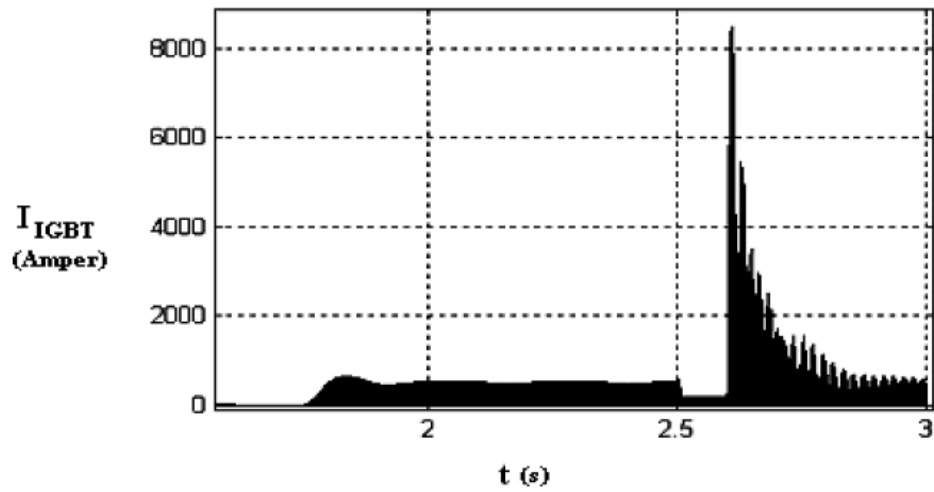


Figure 4.9 IGBT current waveform for MATLAB/Simulink simulation.

After getting results and experiences from MATLAB/Simulink simulations for a single wind turbine, it was necessary to form the complete model of wind farm. Since MATLAB/Simulink is not a tool especially developed for power system analysis, PSCAD/EMTDC was used to develop a detailed model of the wind farm connected to Alaçati Substation. While developing models of wind farm for PSCAD/EMTDC simulation, special attention was given for rotor circuit modelling and speed control.

CHAPTER FIVE

WOUND ROTOR INDUCTION GENERATOR and SPEED CONTROL

Two controllers are designed to operate in a coordinated manner in wind turbine controller units of the wind farm; a pitch controller for turbine and a rotor resistance controller for wound rotor induction generator. This design guarantees that the active power output is equal to the maximum power at wind speeds below and equal to rated power above nominal wind speeds (Divya, & Rao, 2006). Controller data connections of a wind turbine control unit of the wind farm is shown in Figure 4.7.

5.1 Wound Rotor Induction Machine Rotor Circuits for Speed Control

The simplest and oldest method of ac motor speed control is a wound rotor induction machine with a mechanically varying rotor circuit rheostat. Changing the rotor resistance changes the operating speed of the machine; the higher resistance of the rotor windings gives the higher slip. However inserting extra resistance into the rotor circuit of an induction machine reduces the efficiency of the machine.

Main feature of this machine is that the slip power easily becomes available from the slip rings, which can be electronically controlled to control speed of the machine, instead of mechanically varying the resistance. This gives stepless and smooth control, fast response, less maintenance, longer life, compact size, assured balance between rotor phase currents, simple closed loop control and so on. For limited-range speed control applications, like fans, pumps and wind energy conversion systems, the KVA ratings and hence cost of the converter is substantially reduced compared to the full-power converter on the stator side (Akpınar & Pillay, 1990), (Bose, 2002).

The method relies on the dynamics of the systems such that

$$T_a = J \frac{d\omega}{dt} = T_w - T_e \quad (5.1)$$

where T_a is the accelerating torque (Nm), T_w is the torque available from the wind turbine (Nm), T_e is the torque developed by the induction generator (Nm), J is the combined moment of inertia of the rotating system (kg.m^2), ω is the angular velocity (rad/s). T_w depends on wind speed and rotational speed while T_e depends on rotor resistance and rotational speed. The torque developed by the induction generator decreases as the rotor resistance increases and vice versa (ensuring that the rotor speed is maintained constant). Under varying wind conditions, the turbine will be accelerating ($T_a > 0$) or decelerating ($T_a < 0$). The adjustment criteria is to minimize T_a such that, the rotor resistance is decreased while the turbine is accelerating and the rotor resistance is increased while the turbine is decelerating (Sürgevil, 2004).

Two different rotor circuit choppers are shown in Figure 5.1 and Figure 5.2. Wound rotor induction generators of the Alaçatı wind farm are equipped with the rotor circuit chopper that is shown in Figure 5.2. Models of these different circuit designs are developed individually to determine the specific distincts between each of them. Effective resistance value for different duty ratio values of each design has been evaluated. Thus steady-state equations of wound rotor induction machines of the Alaçatı wind farm will be obtained, to make comparisons with simulation results.

A six pulse diode rectifier is connected to the rotor circuit and at the dc side of the rectifier a controllable semiconductor switch, such as an insulated gate bipolar transistor (IGBT), is connected. Controlling the switching duty ratio of the semiconductor switch, the equivalent resistance connected to the rotor circuit can be changed, from fully connected in the circuit (IGBT is off) to totally disconnected resistance (IGBT is on). Consequently, the torque and reactive power characteristics of the machine are changed. The effective resistance seen at the rotor terminals is changed as a parameter of duty cycle hence the rotor speed control is performed in both systems. A snubber must be used to limit the voltage peak each time the switch is switched off and also an overvoltage circuit is needed to short-circuit the switch in case of an grid error.

Wind turbine control unit adjusts the appropriate average resistance of the rotor circuit by switching the semiconductor switch on and off at several kHz. When rotor speed accelerates due to high wind speed, external rotor resistance is increased by decreasing the switch duty ratio, δ . In case of low wind speeds the rotor speed decelerates and rotor resistance can be totally disconnected by the wind turbine control unit to keep the operation of the system near to the maximum power point. A detailed comparison results of these two systems has been given in (Balıkcı, 2008). The ripple in phase current is neglected and waveforms of current and voltage through the switch assumed linear with time during analysis.

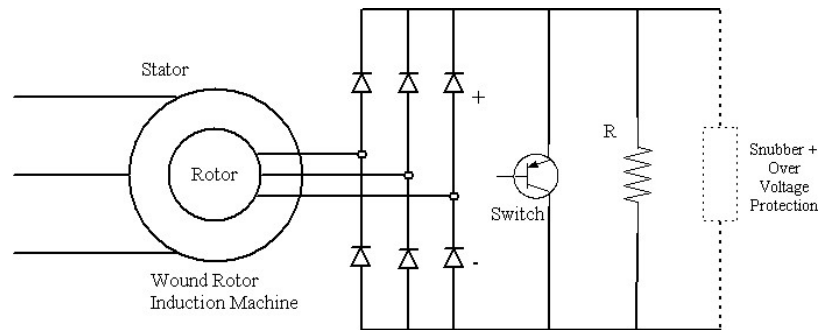


Figure 5.1 Speed control with rotor circuit chopper (One resistance)

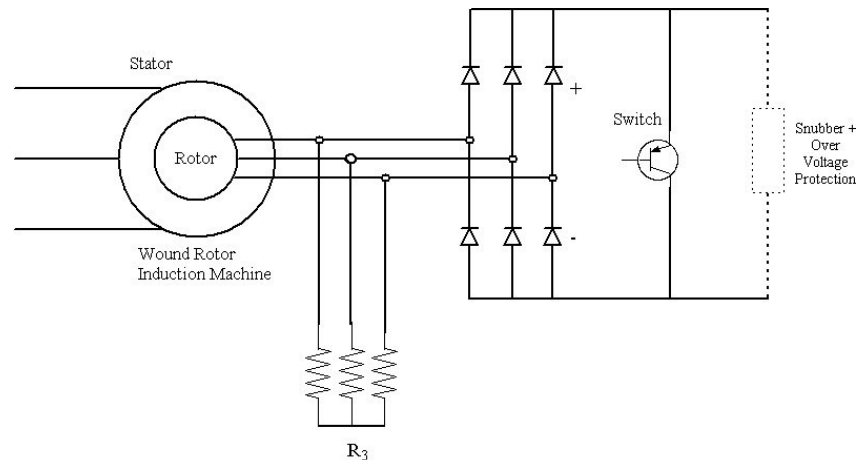


Figure 5.2 Speed control with rotor circuit chopper (Three resistances)

5.1.1 Speed control with rotor circuit chopper (One resistance)

The system given in Figure 5.1 has a wound rotor induction machine, a six pulse diode rectifier and boost converter circuit. There is an inductor in a boost converter between rectifier and IGBT device in a conventional circuit, however, the rotor leakage inductance shows the effect in such a way that normal inductor in a boost converter does. Therefore, this external inductor that would be normally used in boost converter is taken out of circuit. In order to control rotor speed of the machine, the IGBT is driven by PWM signal.

The duty ratio of the power electronic switch δ is defined in the same way as for a chopper;

$$\delta = \frac{t_{on}}{T} \quad (5.2)$$

When the ripple in current I_d is neglected, the energy absorbed by resistance R during a period T of switching is given by

$$W_R = I_d^2 R(T - t_{on}) \quad (5.3)$$

where I_d is the current of diode, t_{on} is the on time period of the power electronic switch. The average power absorbed by resistance R during a period is

$$P_r = \frac{1}{T} [I_d^2 R(T - t_{on})] = [I_d^2 R(1 - \delta)] \quad (5.4)$$

Hence effective resistance R^* can be defined as;

$$R^* = (1 - \delta)R \quad (5.5)$$

From Figure 5.3, the rms value of the rotor phase current is

$$I_{rms} = \left[\frac{1}{\pi} \int_0^{2\pi/3} I_d^2 d(\omega t) \right]^{1/2} = \frac{\sqrt{2}}{\sqrt{3}} I_d \quad (5.6)$$

$$a_1 = \frac{4}{\pi} \int_{\pi/6}^{\pi/2} I_d \sin \omega t d(\omega t) = \frac{2\sqrt{3}}{\pi} I_d \quad (5.7)$$

$$I_r = \frac{a_1}{\sqrt{2}} = \frac{\sqrt{6}}{\pi} I_d = \frac{\sqrt{6}}{\pi} \left(\frac{\sqrt{3}}{\sqrt{2}} \right) I_{rms} \quad (5.8)$$

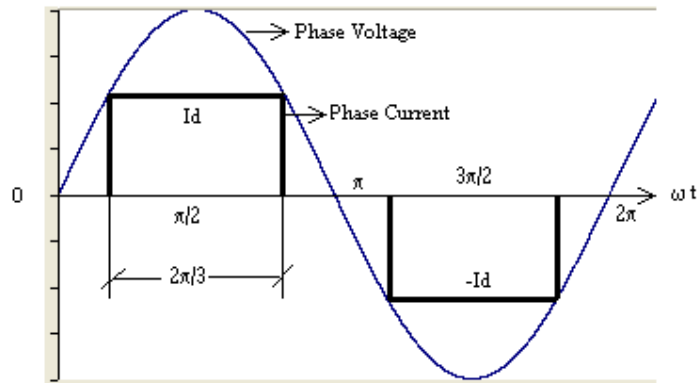


Figure 5.3 Rotor phase voltage and phase current

Hence the fundamental rotor current is

$$I_r = \frac{3}{\pi} I_{rms} \quad (5.9)$$

The per-phase power consumed by resistance R_e is

$$P_e = \frac{1}{3} I_d^2 [(1 - \delta)R] \quad (5.10)$$

Substitute (5.6) into (5.10)

$$P_e = \frac{1}{2} \cdot [(1 - \delta)R] I_{rms}^2 \quad (5.11)$$

This is equivalent to the power dissipation in a resistance of “ $\frac{1}{2} \cdot [(1 - \delta)R]$ ” Ω caused by the rms rotor current I_{rms} . Hence, the effective per-phase value of resistance R_e is given by;

$$R_e^* = \frac{1}{2} \cdot [(1 - \delta)R] \quad (5.12)$$

By controlling the switching duty ratio of the semiconductor switch, the effective per-phase value of R_e (R_e^*) is controlled and the torque and reactive power characteristics of the machine are changed. Also R_e^* can be used for further analysis to get equivalent circuit of wound rotor induction machine and its stability analysis.

5.1.2 Speed control with rotor circuit chopper (Three resistances)

Wound rotor induction generators of the Alaçatı wind farm are equipped with rotor circuit chopper with three phase resistances which is also shown in Figure 4.5 and Figure 5.2. Analyzing and developing the appropriate model of this rotor circuit design is therefore important for further simulations of the thesis.

The effective per-phase value of the resistance across the diode bridge is;

$$R_e^* = \frac{1}{2} \cdot (\delta \cdot R_{bs}) \quad (5.13)$$

where R_{bs} is an equivalent resistance to represent switching and conduction power losses of the diode bridge and the IGBT.

Turn-on and turn-off v-i characteristics are also given in Figure 5.4 by assuming linear with time, where, t_{on} is turn-on time, t_{off} is turn-off time, t_{con} is conduction time, P_{on} is turn-on power loss, P_{off} is turn-off power loss, P_{con} is conduction power loss. During each transition from on to off, and vice versa, the switch has simultaneously high current and voltage, as seen from the switching waveforms. As most of the losses are due to high frequency switching; when the switching frequency gets higher, the power losses also increase.

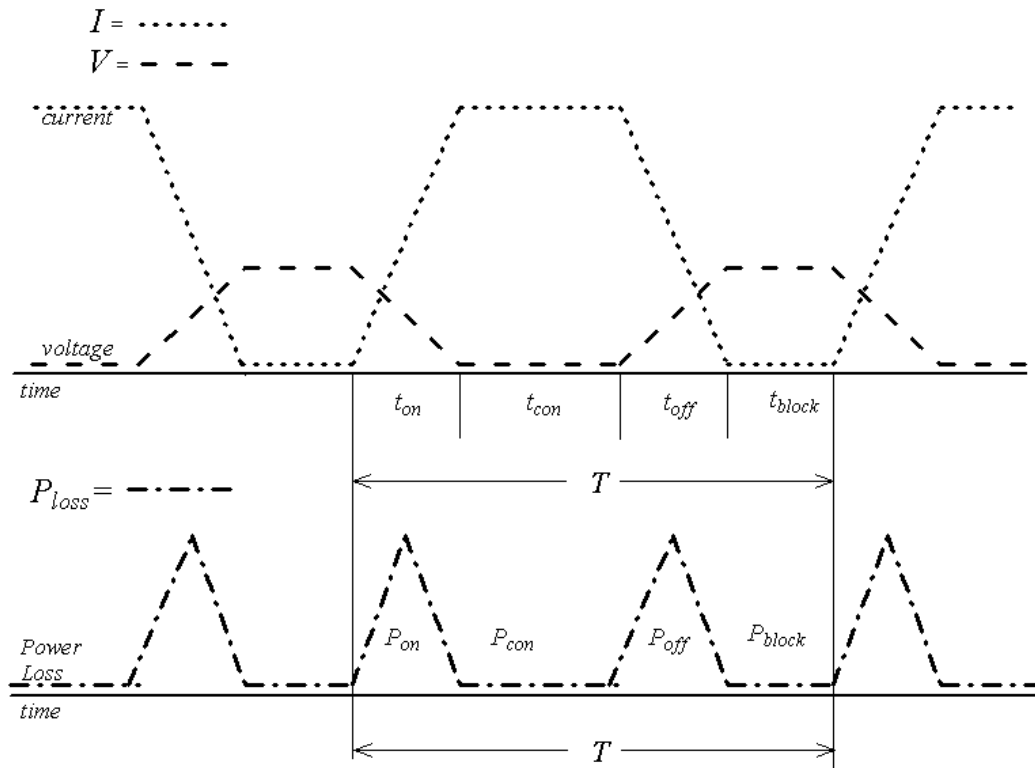


Figure 5.4 Turn-on and turn-off trajectories.

The instantaneous power loss in the switch is the product of current and voltage as plotted. The average value of the losses, P_{loss} is;

$$P_{loss} = P_{sw} + P_{con} = \frac{1}{2} V.I.(t_{on} + t_{off}).f_s + V_{ce}.I.\delta \quad (5.14)$$

and P_{sw} is independent from δ . When the controller changes δ , t_{con} (P_{con}) change for a given $T(f_s)$. Since P_{loss} is equal to P_{Rbs} ;

$$P_{sw} + P_{con} = P_{Rbs} \quad (5.15)$$

$$\frac{1}{2}V.I.(t_{on} + t_{off}).f_s + V_{ce}.I.\delta = I^2 R_{bs} \quad (5.16)$$

$$R_{bs} = \frac{1}{2} \frac{V}{I} (t_{on} + t_{off}).f_s + \frac{V_{ce}}{I}.\delta \quad (5.17)$$

where P_{Rbs} is the average value of the power dissipation at R_{bs} .

Total effective per-phase value of external circuit resistance becomes,

$$R_3^* = 0,5.(\delta.R_{bs}) + (1 - \delta)R_3 \quad (5.18)$$

Table.5.1 shows the results of effective resistance for two systems and different δ values.

Table 5.1. Results of the effective resistance for two different systems.

<i>System</i>	<i>Effective Resistance Formula</i>	δ	<i>Result</i>
One Resistance	$R_e^* = 0,5 \cdot [(1 - \delta)R]$	0	$R_e^* = 0,5 \cdot [R]$
One Resistance	$R_e^* = 0,5 \cdot [(1 - \delta)R]$	0.5	$R_e^* = 0,25 \cdot [R]$
One Resistance	$R_e^* = 0,5 \cdot [(1 - \delta)R]$	1	$R_e^* = 0$
Three Resistances	$R_3^* = 0,5 \cdot (\delta \cdot R_{bs}) + (1 - \delta)R_3$	0	$R_3^* = R_3$
Three Resistances	$R_3^* = 0,5 \cdot (\delta \cdot R_{bs}) + (1 - \delta)R_3$	0.5	$R_3^* = 0,25 \cdot [R_{bs}] + 0,5 \cdot [R_3]$
Three Resistances	$R_3^* = 0,5 \cdot (\delta \cdot R_{bs}) + (1 - \delta)R_3$	1	$R_3^* = 0,5 \cdot [R_{bs}]$

In the equivalent circuit of an induction machine, the power transferred across the air-gap (P_{ag}) is given by;

$$P_{ag} = 3EI_r' \cos\theta_r \quad (5.19)$$

where θ_r is the phase angle between phasors \bar{E} and \bar{I}_r' .

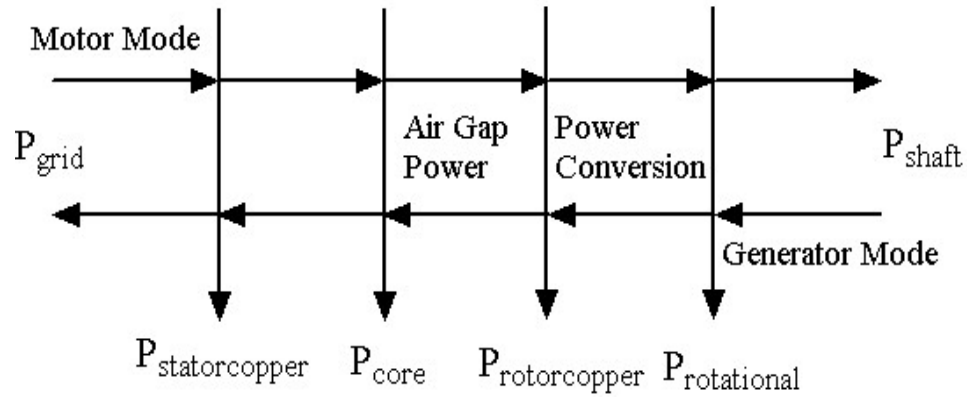


Figure 5.5 The power-flow diagram of an induction machine.

In the drive under consideration, the total power consumed in the rotor circuit (P_g') is;

$$P_g' = 3I_{rms}^2 (R_r + R_e^*) + P_m \quad (5.20)$$

Using (5.9) in (5.20);

$$P_g' = \frac{\pi^2}{3} I_r^2 (R_r + R_e^*) + P_m \quad (5.21)$$

The fundamental equivalent circuit of the drive must satisfy the condition $P_{ag} = P_g'$. Hence;

$$EI_r' \cos \theta_r = \frac{\pi^2}{9} I_r^2 (R_r + R_e^*) + \frac{P_m}{3} \quad (5.22)$$

P_m is the mechanical power developed by the fundamental rotor current.

$$P_m = P_{ag} - P_{rcl} = (1-s)P_{ag1} \quad (5.23)$$

$$P_m = 3I_r^2 (R_r + R_e^*) \frac{(1-s)}{s} \quad (5.24)$$

$$EI_r' \cos \theta_r = \left[\left(\frac{\pi^2}{9} - 1 \right) (R_r + R_e^*) + \frac{(R_r + R_e^*)}{s} \right] I_r'^2 \quad (5.25)$$

$$EI_r' \cos \theta_r = \left(R_h + \frac{R_f}{s} \right) I_r'^2 \quad (5.26)$$

where

$$R_h = \left(\frac{\pi^2}{9} - 1 \right) (R_r + R_e^*) \quad (5.27)$$

$$R_f = (R_r + R_e^*) \quad (5.28)$$

The per-phase fundamental equivalent circuit of the drive referred to the stator, shown in Figure 5.6, can be obtained from;

$$EI_r' \cos \theta_r = \left(R_h' + \frac{R_f'}{s} \right) I_r'^2 \quad (5.29)$$

where R_h' and R_f' are respectively the values of R_h and R_f referred to the stator side. Thus;

$$R_h' = a_{T1}^2 R_h \quad (5.30)$$

$$R_f' = a_{T1}^2 R_f \quad (5.31)$$

where a_{Tl} is the stator to rotor turns ratio. Resistance $\left(\frac{R_f}{s}\right)$ accounts for the developed mechanical power and the fundamental rotor copper loss. Resistance R_h' accounts for the rotor harmonic copper loss (Dubey, 1989).

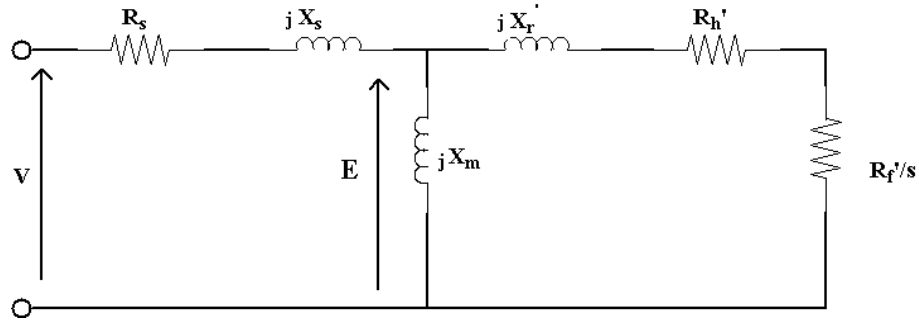


Figure 5.6 The per-phase fundamental equivalent circuit of the drive referred to the stator

By calculating the Thevenin equivalent circuit seen from the rotor circuit, the reduced equivalent circuit which is given in Figure 5.8, can be obtained where \bar{V}_{TH} and \bar{Z}_{TH} are the Thevenin's voltage and impedance, which are given by;

$$\bar{V}_{TH} = \bar{V} \left(\frac{Z_M}{Z_M + Z_S} \right) \quad (5.32)$$

$$Z_{TH} = R_{TH} + jX_{TH} = \frac{Z_M Z_S}{Z_M + Z_S} \quad (5.33)$$

where $Z_M = jX_M$ and $Z_S = R_S + jX_S$.

The resistance R_m that represents the core losses can be added in parallel to the magnetizing branch as shown in Figure 5.7. Its value depends slightly on slip frequency $\omega_s = s\omega$, as non-negligible core losses also occur in the rotor core for $s.f_1 > 5$ Hz (Boldea, 2005).

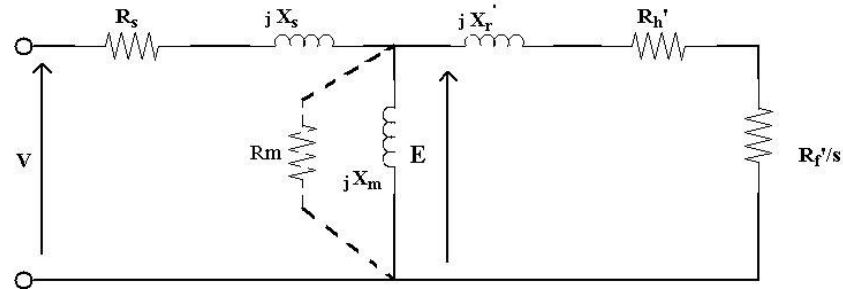


Figure 5.7 R_m in parallel to the magnetizing branch of equivalent circuit.

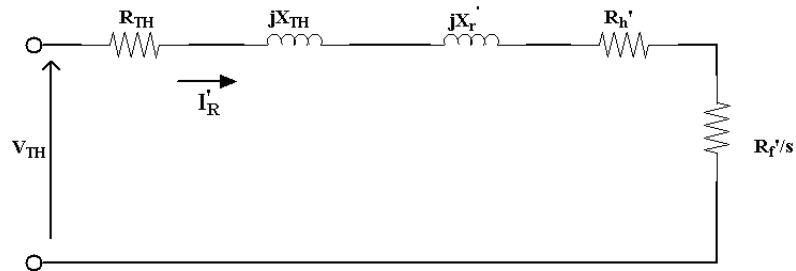


Figure 5.8 The per-phase reduced equivalent circuit of the drive referred to the stator

From the reduced equivalent circuit, the magnitude of the rotor current can be calculated by using;

$$|\bar{I}_R| = I_R' = \frac{V_{TH}}{\sqrt{(R_{TH} + R_h' + \frac{R_f'}{s})^2 + (X_{TH} + X_R')^2}} \quad (5.34)$$

$$T_E = \frac{R_f'}{s} I_R'^2 = \frac{R_f'}{s} \frac{V_{TH}^2}{(R_{TH} + R_h' + \frac{R_f'}{s})^2 + (X_{TH} + X_R')^2} \quad (5.35)$$

For given values of δ and s , the rotor current and torque can be calculated from the equations. The nature of torque-speed curves for different values of δ is shown in Figure 5.9. For $\delta=1$, R is fully bypassed by the semiconductor switch S . However, due to the conduction losses in chopper circuit; the torque-speed curve for $\delta=1$ lies below natural torque-speed curve. For a given torque, speed reduces with increased δ . The control region consists of the area enclosed in ABCD. Any operating point in this region can be obtained by controlling δ . This operation is not possible in the area

AD0. This control region is increased and AD0 is decreased when the value of the external R is increased. In case of three resistances, R_{bs} increases the interval between natural torque-speed curve and the torque-speed curve for $\delta=1$ due to switching and conduction power losses of the diode bridge and the IGBT.

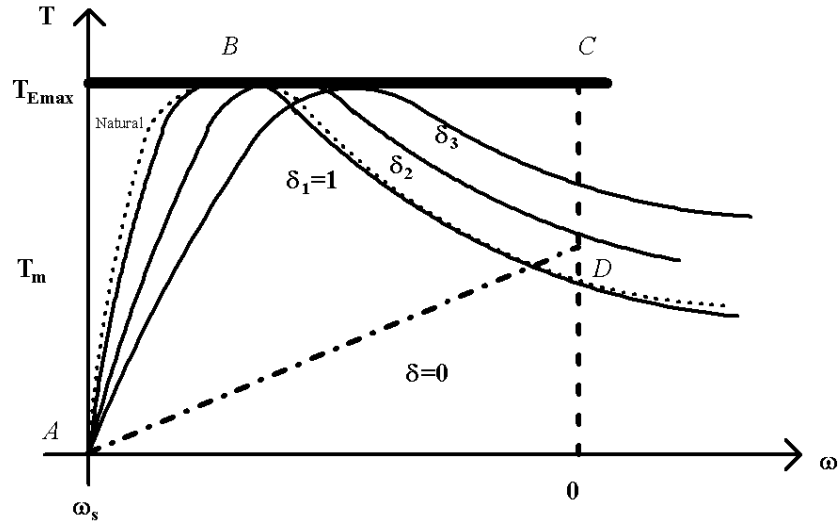


Figure 5.9 Torque-speed curves

Compared to mechanically varying the resistance, the static rotor resistance control has the disadvantage of requiring machine derating. Since only the fundamental rotor current is assumed to contribute to the torque, the same value of the fundamental rotor current is necessary to produce a given torque, whether the current is sinusoidal or nonsinusoidal. For the rated thermal loading, the rms current is fixed, irrespective of whether it is sinusoidal or nonsinusoidal, when the increase in machine resistance due to skin effect is neglected. Therefore, the maximum fundamental current rating of the machine will decrease by the factor $\left(\frac{I_r}{I_{rms}}\right)$. The machine power rating will also decrease by this factor (Dubey, 1989). This drive has;

$$\text{Machine Derating} = \left(\frac{I_r}{I_{rms}}\right) = \left(\frac{3}{\pi}\right) = 0,95$$

If the ripple in the I_d , commutation overlap in the diode bridge, skin effect, and the reduction in full load speed due to losses in diode bridge, inverter, transformer, and

semiconductor switch are considered, the derating of the machine will be much higher.

If the rotor of the wound rotor induction machine is driven faster than synchronous speed, the machine becomes a generator, converting mechanical power to electric power. While operating as a generator, the electrical and mechanical torques, and the generator active power are negative quantities. Nevertheless, in the figures of the thesis, they are presented as positive ones, in order to facilitate understanding.

When a mechanical torque is applied to the wound rotor induction machine with a constant δ , two equilibrium points are defined, which are given by the intersection between the T - ω curve and T_m line in Figure 5-10.

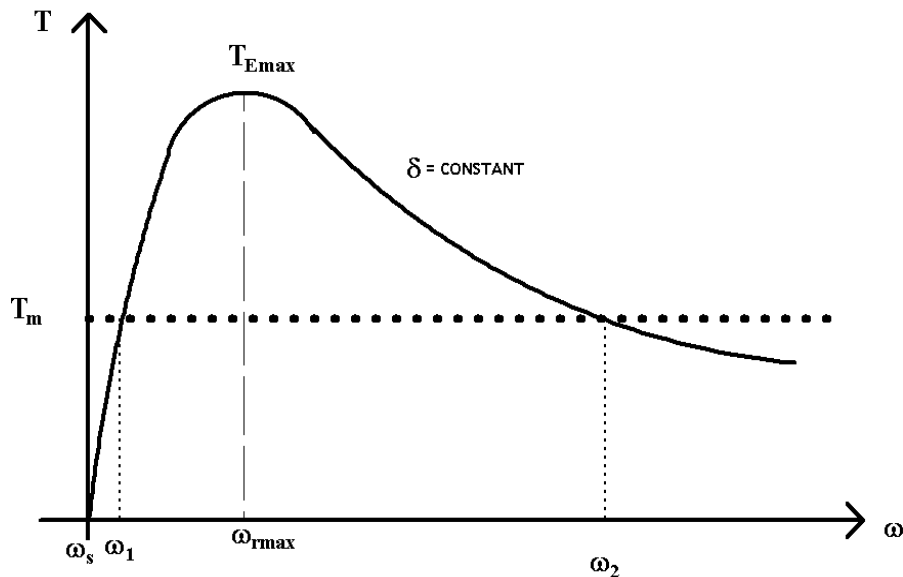


Figure5.10 Torque-speed curve with constant δ and T_m

This points correspond to the rotor speeds ω_1 and ω_2 as shown in Figure 5.10. The first one is the stable equilibrium point and the second one is the unstable equilibrium point. If the mechanical torque is continuously increased, there is a critical condition $\omega_1 = \omega_2 = \omega_{rmax}$ which corresponds to the critical or maximum

electrical torque T_{Emax} . When the mechanical torque is larger than T_{Emax} , the generator accelerates and loses the steady state stability.

Thus, the operating point $(\omega_{rmax}, T_{Emax})$ defines the generator steady-state stability limits for a constant δ , like squirrel cage induction generator. This point can be promptly calculated by solving $\frac{dT_E}{ds} = 0$, which results in the expressions for the steady state maximum slip (the slip of the rotor at maximum torque) and maximum torque.

$$s_{\max} = -\frac{R_f'}{\sqrt{(R_{TH} + R_h')^2 + (X_{TH} + X_R')^2}} \quad (5.36)$$

$$T_{E\max} = \frac{1}{2} \frac{V_{TH}^2}{(R_{TH} + R_h') - \sqrt{(R_{TH} + R_h')^2 + (X_{TH} + X_R')^2}} \quad (5.37)$$

$$\omega_{r\max} = (1 - s_{\max})\omega_s \quad (5.38)$$

If δ is reduced, T_{Emax} does not change as can be seen in Figure 5.9, but the steady state maximum slip increases. The operating points for each δ value can be calculated with the same method; like $\delta_1 (\omega_{rmax}, T_{Emax})$, $\delta_2 (\omega_{rmax}, T_{Emax})$.

At the steady-state stability limit, the machine delivers P_{TEmax} . The generator active power P_E can be calculated by;

$$P_E = R_s I_s^2 + (R_h' + \frac{R_f'}{s}) I_R'^2 \quad (5.39)$$

The magnitude of the stator current can be determined by;

$$|\bar{I}_s| = I_s = \left| \frac{\bar{V}}{Z} \right| = \left| \frac{\bar{V}}{Z_s + (Z_M \| Z_R')} \right| = \left| \bar{V} \cdot \left[\frac{Z_M + Z_R'}{Z_M Z_R' + Z_s (Z_M + Z_R')} \right] \right| \quad (5.40)$$

where $Z_R' = R_h' + \frac{R_f'}{s} + jX_R'$.

Note that both I_R' and I_s are dependent on the slip. At the steady-state stability limit condition, where $s = s_{max}$, these currents can be referred as steady-state maximum rotor current I_{Rmax} and steady-state maximum stator current I_{Smax} . Finally P_{TEmax} can be obtained by substituting s , I_R , and I_s by s_{max} , I_{Rmax} and I_{Smax} .

CHAPTER SIX
MODELLING AND SIMULATION OF WIND FARM FOR POWER
SYSTEM STUDY

Since the models of the grid and the wind farm, have to comply with common requirements of the simulation platforms; this chapter initially presents modeling concepts for grid integrated wind farms. After that presentation; Alaçatı wind farm PSCAD/EMTDC simulation models are given.

6.1 Simulations and Modelling

Computer simulation makes it possible to investigate a multitude of properties in design and application phase. The correctness of a computer simulation depends on the quality of the built-in models and of the applied data. In order to investigate the effects of wind energy conversion systems on power system and vice versa; it is necessary to develop accurate models of both systems.

Power system simulation packages are commonly used for power system operational studies by TSO. All power system components are modelled by reasonably accurate and low-capacity-demanding models. Simplifications are done for every component model used in the system to get convenient computation time and results. Models of the new types of generation units, like wind turbines, have to comply with this requirement. There are simulation packages, which in principle can describe a complete wind turbine with all units. However, the turbine description used in those programs can not be viable in grid simulations packages because of high computational burden and can not be used to represent wind farms containing hundred of wind turbines in grid simulations without proper simplifications.

The amount of electricity generated from wind is increasing day by day. Large wind farms are planned and connected to the high voltage transmission lines all over the world. The penetration of wind energy in power systems will increase and they may begin to influence overall power system behavior. This situation increases the

need for adequate models of wind energy conversion systems to use in grid investigation studies and simulations.

When the aim is to investigate grid integration of wind turbines, there are three main interests; steady-state voltage level influence, rapid voltage fluctuations(flicker), and response to grid disturbances.

6.1.1 Steady-State Voltage

The voltage difference between the infinite system and the PCC of the wind farm is given by (2.2) and (2.3). The voltage difference, ΔU , is related to the short circuit impedance, the real and reactive power output of the wind farm.

Infinite system (or busbar) represents interconnected grid, where voltage never changes from the designed value. So it is an important decision for us that at which feeder in the model voltage never changes. Power system components between the infinite system and the PCC of the wind farm; transmission lines/cables and transformers, have to be modelled exactly in the simulation. Otherwise the effect of system X/R ratio(ratio between grid reactance and grid resistance) on wind farm terminal voltage can not be modelled correctly.

154 kV busbar of Alaçatı Substation is directly connected to Turkish national interconnected grid. Transmission line, which is that busbar is connected to, has a constant voltage/frequency characteristic. The voltage/frequency of the connected line are monitored by TEİAŞ transmission line control centre and all probable deviations are diminished directly by the control centre commands. For this reason; 154 kV busbar of Alaçatı Substation was the best location to be chosen as infinite busbar in the PSCAD/EMTDC simulations.

The first term and real part of the voltage difference ΔU , which is given in (2.3), is ΔU_p :

$$\Delta U_p = \frac{R_k P_g + X_k Q_g}{U_g} \quad (6.1)$$

The effect of system X/R ratio on the voltage difference can be examined by monitoring the magnitudes of the two terms on the nominator of ΔU_p . No-load power factor correction, which means that the wind-farm reactive power consumption will be zero at no load, must be set for a clear examination. With a relatively low X/R value, the first term of ΔU_p predominates, and voltage rises over the loading range. When X/R value is relatively high, the second term of ΔU_p , which goes negative with increasing reactive consumption, predominates at higher active power generation.

The impact on the steady-state voltage level by the fixed speed wind turbine system with an induction generator directly connected to the grid is predestined and cannot be controlled during the operation. There is a capacitor bank connected at the turbine, which is typically designed to compensate for the induction machine no-load reactive power consumption like in wind farm. As the active power production increases, the reactive power consumption rises as well. These outcomes, in combination with the grid X/R value, determine if the voltage level in the PCC is increasing with increasing power production or not.

For variable-speed turbines, the reactive power is controllable and is usually kept close to zero in order to obtain a power factor of one. This means that the voltage level increases as the power production increases. However, if desired, the wind turbine converters can produce any reactive power, provided that the rating of the converter allows it (Petru & Thiringer, 2002).

6.1.2 Flicker

As previously mentioned; there are two types of flicker emissions associated with wind turbines. In order to predict the rapid power fluctuations from fixed-speed turbines, there is a need to represent the wind field arriving at the turbine, since the flicker emission during continuous operation is mainly caused by fluctuations in the

output power due to wind speed variations, the wind gradient and the tower shadow effect.

Switching operations like start, stop and switching between generators or generator windings, also produce flicker. When the limits of the flicker emission are given, the maximum allowable number of switching operations in a specified period can be examined by appropriate models in simulations. Model of a single wind energy conversion system must take into consideration soft starter, capacitor group, pitch control, and wind speed variations.

The wind farm at hand has the active-stall regulated system that produces similar rapid power fluctuations to fixed speed system since the pitching of the blades are done slowly. Each wind turbine control unit of the wind farm, which is shown in overall control system diagram in Figure 4.7, individually makes changes at the pitch angle of turbine blades. Additional data acquisition system which can acquire data of; pitch angle (β), wind speed(w), wind direction and yaw angle for every wind turbine in order to model pitch controller for any simulation. When modelling the complete wind farm in PSCAD/EMTDC simulations, it is not necessary to model the pitch control system since it has a rather slow impact(bigger time constant) on input torque, related to the individual wind speed.

6.1.3 Grid Disturbances

When the response to grid disturbances is of interest, it is mainly the generator description that affects the response of the turbine. For assessing the stability margin of the wind farm-grid integration, small-signal dynamic model of the system must be formed in simulation platforms.

Wind speed, pitch control and input torque to generator are usually assumed constant for transient analysis, since mechanical system time steps are too larger than time constant of electrical system. The worst case scenario must be defined, like maximum wind speed and minimum load conditions.

In case of a grid disturbance; the wind farm is allowed to disconnect from the grid for avoiding negative effects of the fault. The voltage level in the PCC decreases and oscillates afterwards the fault which can cause overspeed and instability of wound rotor induction generators at low voltage levels.

To simulate the response of variable-speed systems to grid disturbances, the details of the control and protection of the power electronic converters must be known and implemented in the simulation(Petru & Thiringer, 2002). For variable-speed wind turbines with a power electronic converter between the stator and the grid, the short-circuit current can be determined by the converter and will generally not exceed the nominal current of the converter. A DFIG is directly coupled to the grid but it has a relatively small scaled power electronic converter connected between the rotor windings and the grid. During a grid fault, a protection system, like crowbar, protects the converter from short circuits, otherwise high currents can cause thermal breakdown of the converter(Morren & de Haan, 2007).

6.2 Aggregated Modeling

Representing a wind farm, which consists of many relatively small power rated wind turbines, by one or few large power rated wind turbines by addition of power ratings of the small power rated wind turbines, can be stated as “aggregated modeling”. When the effect of a wind farm on power systems is studied, the behavior of the wind farm at the PCC to power system can be represented by an equivalent model derived from the aggregation of wind turbines into an equivalent wind turbine, instead of the complete model including the modelling of all the wind turbines . The structure of an aggregated wind farm model should be such, that maximum user friendliness is achieved while keeping the results as close to reality as possible(Slootweg & Kling, 2002).

After getting results for the complete model including the modelling of all wind turbines, simulations were done with the aggregated model of the wind farm. The

advantage of an aggregated model is that it eliminates the need to develop a detailed model of a wind farm with tens or hundreds of wind turbines and their interconnections, and to specify the wind speed at each individual wind turbine within the wind farm.

(Akhmatov, 2004) stated that, the wind farm could be represented by one-machine equivalent when no mutual interaction was indicated and the aim was to investigate voltage stability of the transmission system. It is found that there is neither risk of mutual interaction nor power oscillations between fixed-speed wind turbines of a large power rated wind farm(Akhmatov, Knudsen, Nielsen, Pedersen & Poulsen, 2003).

One machine equivalent model represents the collective response of the wind farm at PCC to grid assuming; no impedances within the wind farm, a uniform wind speed distribution in the wind farm(no difference in incoming wind), no park effect or shadowing between the rows of wind turbines and as a result same operating states for all wind turbines throughout the simulation. However, equivalent model is not valid if wind turbines receiving different incoming winds are aggregated, since the operation conditions of each wind turbine are different.

Groups of wind turbines with similar winds can be aggregated by an equivalent model which results representing a large power rated wind farm by a few large wind turbines. An example of such representation for a fictitious wind farm is shown in Figure 6.1. There are three sections with identical wind turbines facing similar wind speeds. Power ratings of representative wind turbines are according to the addition of the wind turbines inside the sections;1, 2, and, 3. The effective value of the wind is reduced per row of the wind turbines because of shadowing and generation of turbulence in the wind farm. Aggregating just the electrical system of variable speed wind turbines, including electrical controls and the electrical part of the generators and to model the mechanical system of each individual turbine and generator is another option for modelling. This model maintains the nonlinear characteristics, but

it reduces calculation speed considerable compared to a fully detailed, non-aggregated wind farm model(Pöller & Achilles, 2003).

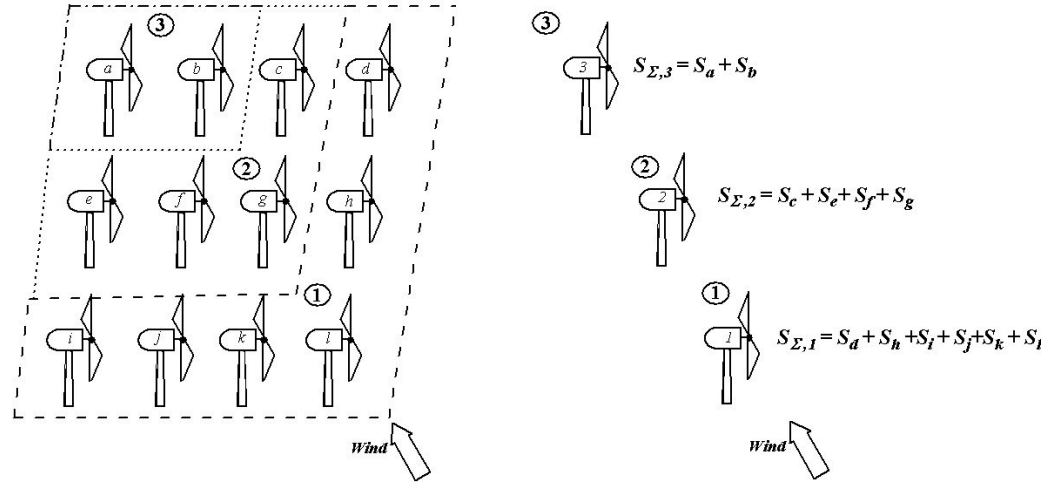


Figure 6.1 Aggregated modelling of a wind farm by a few large wind turbines.

(Conroy & Watson, 2009) investigated the behaviour of a wind farm containing full converter wind turbine generators subjected to a voltage dip, with a number of aggregate modelling options. It was shown that simplified aggregated models that represent the wind farm behaviour at the PCC can be used for large wind farms in stability investigations.

6.3 Validation Procedure of Wind Farm Models

Models of grid connected wind farms can be validated with field measurement results to represent correct prediction of wind farm behavior. The response of the aggregated and the detailed models have to show a high degree of similarity, both during normal operation as well as during disturbances for model validation, like in (Slootweg & Kling, 2002). Also results from the simulations can be validated against field measurement data as done by (Perdana, Uski, Carlson & Lemström, 2006) and (Martins, Perdana, Ledesma, Agneholm & Carlson, 2007). (Kazachkov, Feltes & Zavadil, 2003) used another way of model validation; the comparison of the response of PSS/E models to the response of more detailed, higher-bandwidth models created for use with PSCAD/EMTDC.

Field measurements for validation and data acquisition requires simultaneous electrical and wind speed measurements. The SCADA systems are usually used by wind farm operators to acquire data for operation conditions.

However substation-load conditions and different power system faults may not be observed by this way. External measurement system which is capable of acquiring reliable data with optimum equipment should be used for additional measurements. Additional measurement points also can cause synchronization and data storage problems for both wind farm operators and study groups.

The case study has given beneficial outputs about a grid connected wind farm. Field measurements were used for PSCAD/EMTDC complete model verification process of the wind farm. PCC of the wind farm is Alaçatı Substation 34.5 kV feeder which was chosen as the electrical measurement point. Grid and load conditions could not be controlled or measured during electrical measurements. Wind speed measurement results, related to the same period of the electrical measurements, were obtained from early installed wind speed anemometer in the wind farm. The control algorithm of wind turbine was not provided by the system operators for the wind farm considered.

6.4 Simulation Tool: PSCAD/EMTDC

The simulation model of the grid connected wind farm is developed in power system analysis tool, PSCAD/EMTDC. The grid and the electrical components of the wind farm are built with standard electrical component models from PSCAD/EMTDC library. The models of the wind, the aerodynamic and control components of the wind turbine are built with custom components developed in PSCAD/EMTDC. Simulations are performed to analyze the mutual effects of the wind farm with the grid.

To derivate the true model of the whole wind farm for the analysis at hand, recent studies have been examined attentively and beneficial experiences and conclusions of them have been noted. When the aim is to develop models for grid connected wind turbines, there are various headlines that have to be checked during model derivation. All the WECS concepts classified in the previous chapters had been analyzed due to the power system operational aspects by different researchers. Models have been developed and used for the studies. Different methods, simplifications and evaluations have been done for all models of distinct wind turbines and wind farms. The following are widely used keywords for simulation of grid connected WECS in the previous studies;

- Offshore Wind Farms / Onshore Wind Farms,
- Large Power Rated Wind Farms / Small Power Rated Wind Farms,
- Fixed Speed Turbine/ Variable Speed turbine,
- Analysis During Normal Operation / Analysis During Disturbances,
- Long Time Analysis / Transients Analysis,
- Strong Grids / Weak Grids,
- MV/HV AC Connections / HVDC Connections,
- Stiff Grid Codes / Loose Grid Codes, etc.

Modelling issues of WECS are related to these keywords with respect to classification. These keywords are exact definitions for classification in every study about grid connected WECS. While developing models for Alaçatı wind farm, these keywords are used for appropriate model development with the help of same class of modelling studies.

6.5 Models for the Wind Farm

6.5.1 Generator Modelling

The fifth order non-linear model of the induction machine is considered in this study. The models of lower order than the fifth-order model are usually used for

power system studies. The reduced order models of induction machines for power system studies with series of measurements are compared in (Thiringer & Luomi, 2001). The third order model is applicable if the stator voltage is sinusoidal and not disturbed. When the power quality problems under the distortion of bus voltage is considered, which is the case in wind turbines, the fifth order model is more accurate than the third order model. The saturation of magnetic circuit is neglected and data of the wound rotor induction machine is given in Table 4.1. All resistances(except external resistance) and inductances are referred to the stator side.

6.5.2 Control System Model

Control circuit is employed on the rotor current for effective power extraction. The three phase resistor connected to the rotor terminals takes over the rotor current due to the operation of chopper circuit at the rectifier output. The IGBT of the chopper is switched on and off with 3 kHz switching frequency at varying duty cycle for this purpose. This speed control technique is described in section “5.1.2 Speed control with rotor circuit chopper (Three resistances)” and it keeps the slip between approximately 0.6% and 10% by adjusting the duty cycle.

The validity of model is tested at two different switching frequencies. Experimental and simulation results are seen in Figure 6.2(a) and 6.2(b), respectively. It can be seen that the voltage and current waveforms from the simulation are similar to experimental ones for 0.5 kHz and 5 kHz switching frequencies. Detailed results are presented in (Balıkcı, Akpınar & Mutlu, 2008).

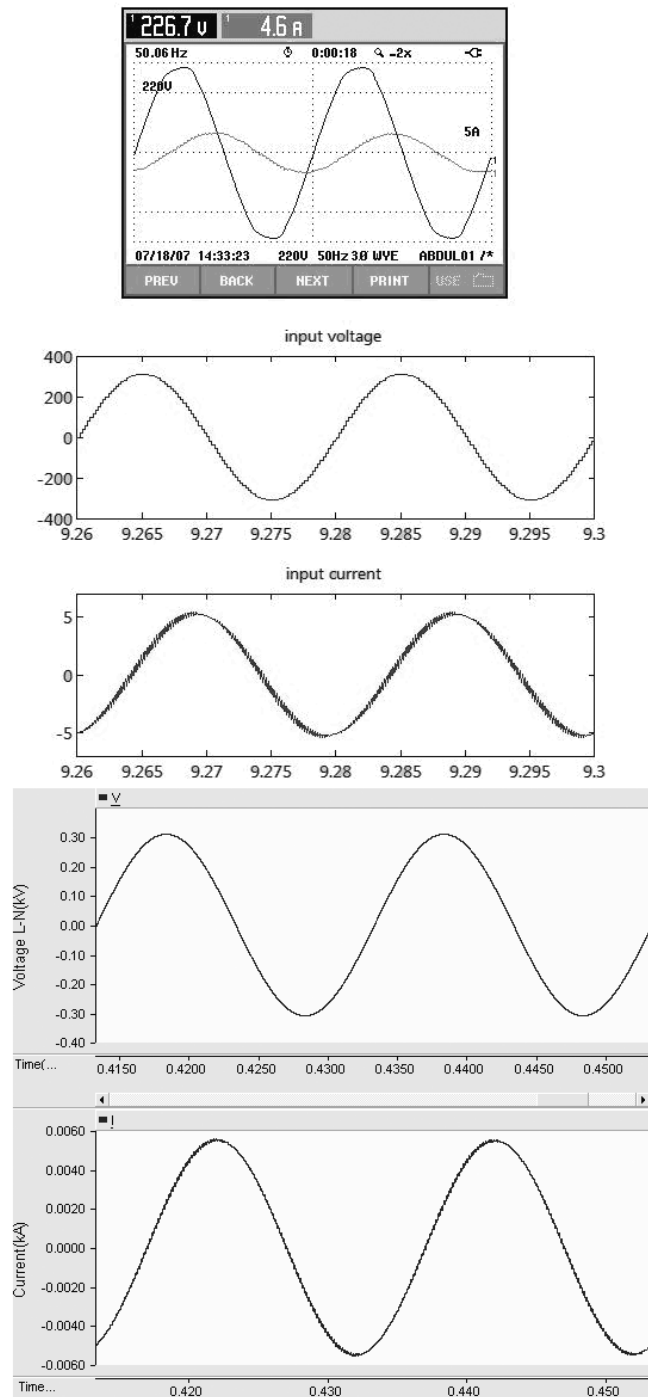


Figure 6.2(a) Input voltage and current signal results for phase “A” in laboratory and simulation studies for 5 KHz switching frequency.

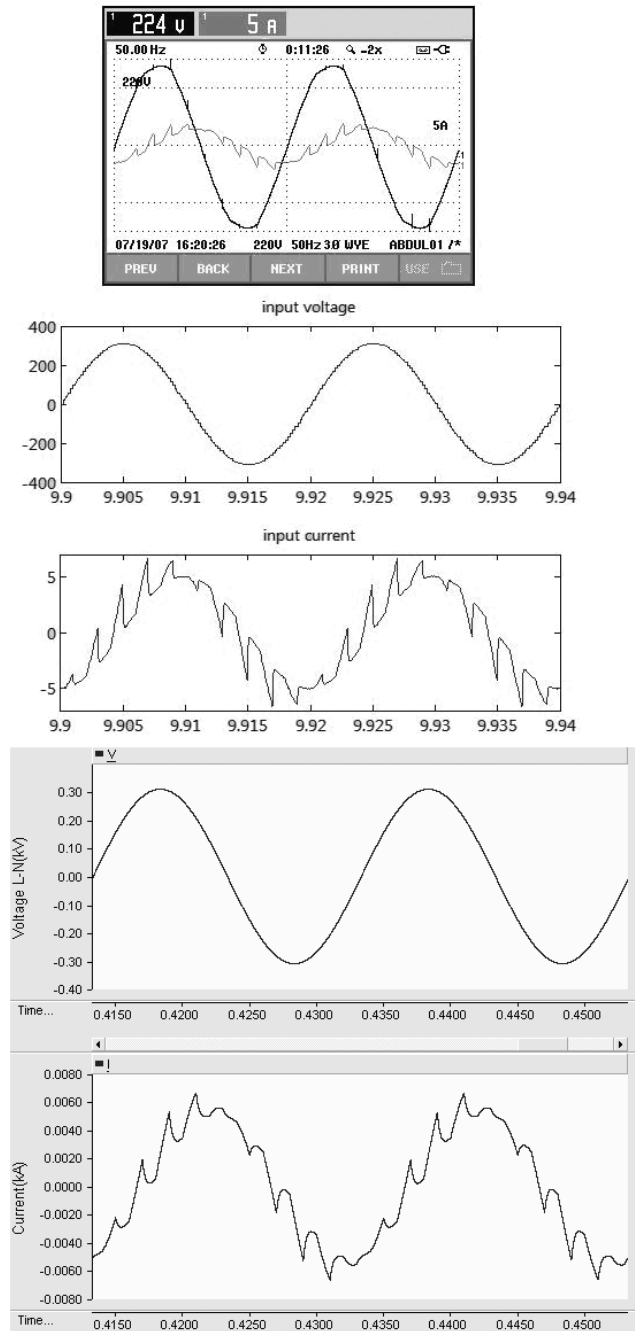


Figure 6.2(b) Input voltage and current signal results for phase “A” in laboratory and simulation studies for 0.5 KHz switching frequency.

Table 6.1 Wind Speed – Torque

Wind Speed (m/s)	Torque (p.u.)
1.53	0.00438
2.01	0.0046
2.53	0.00376
3.03	-0.00376
3.49	-0.01468
4.02	-0.03498
4.5	-0.05468
4.99	-0.07956
5.49	-0.10766
6.01	-0.149
6.45	-0.18862
7.02	-0.24492
7.50	-0.30444
7.99	-0.37652
8.52	-0.43314
8.98	-0.51018
9.49	-0.58742
10.01	-0.68474
10.52	-0.75856
11.01	-0.8472
11.50	-0.87584
12.01	-0.9263
12.52	-0.9584
13.02	-0.98328
13.50	-0.99224
13.69	-1.00054
14.45	-0.9987
15.02	-1.00576
15.39	-1.00354
15.95	-1.00398
16.46	-1.00366
16.97	-1.00106

6.5.3 Turbine Model

Figure 6.3 depicts the block diagram of wind turbine model used for PSCAD/EMTDC simulations.

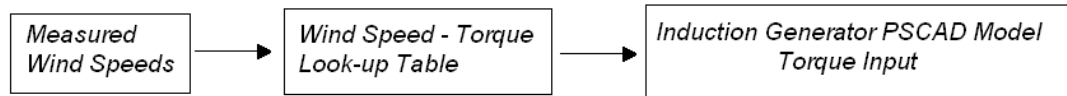


Figure 6.3 Structure of developed Model for Wind Speed – Torque

A torque subsystem generates shaft torque values for induction generator from the user defined look-up table, based on measured wind speeds and manufacturers' data given in Table 6.1.

6.5.4 Model of Wind

The wind model is essential to obtain the power fluctuations during continuous operation of the wind farms (Sørensen, Hansen, Janosi, Bech, & Bak-Jensen, 2001). The wind can be modeled as a four-component model and can be described as (Anderson & Bose, 1983):

$$V_{wind} = V_{base} + V_{gust} + V_{ramp} + V_{noise} \quad (6.2)$$

where V_{base} is the average value of the wind speed(m/s), V_{gust} is the gust wind component(m/s), V_{ramp} is the ramp wind component(m/s), and V_{noise} is the noise wind component(m/s), (Slootweg & Kling, 2002). Figure 6.4 shows the measured wind speed results by an anemometer that is located on the nacelle of the wind turbine. PSCAD/EMTDC wind model uses the equation given in (6.2) to specify the random fluctuations of the wind speed. This simulation package program reads the number of noise components, noise amplitude controlling parameter, surface drag coefficient and turbulence length scale that can be set according to the data collected for a wind farm. Gust and ramp components are neglected which require multiple wind measurements in the wind farm and geographical layout analysis of the wind farm. The average value of the wind speed and noise wind component are used for the simulations. Since the simulation of wind farm is carried out for 6 seconds, the average speed of wind is considered constant. During this short time of operation, the pitch angle is assumed constant. The wind speed results that had been measured in

the fourth day (between 72 and 96 hours in Figure 6.4) are used in simulation. The average value, V_{base} is taken as 8.9 m/s.

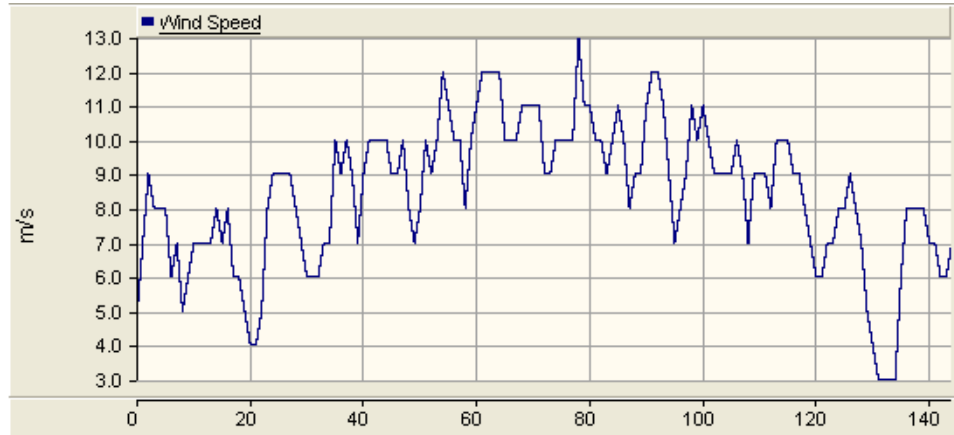


Figure 6.4 Measured wind speed in wind farm.

6.5.5 Alaçati Substation

Alaçati substation is represented by a 50 MVA three phase two winding transformer component of PSCAD/EMTDC. The substation also ensures that the electric power generated from wind is delivered to the transmission line at constant voltage level of 154 kV and 50 Hz.

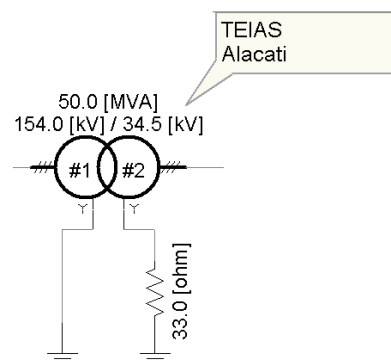


Figure 6.5 Three phase two winding transformer model that is used to model Alaçati Substation in PSCAD/EMTDC simulation.

6.5.6 Power System(Grid)

The equivalent circuit between the wind farm and the grid is shown in Figure 6.6. The equivalent impedance consists of: transmission line; 4 km. length [3*(1*95)mm²] XLPE cable, and transformer; 50 MVA, impedances. When the equivalent impedances is relatively high; the network that the wind farm is connected to, is called as a weak network. The short circuit capacity at the PCC is one of the important factors that affects the security and stability of the wind farms. With the increase of the output power of the wind farm, the amount of current through the equivalent impedance increases that cause larger voltage variations from the infinite bus voltage. To increase the short circuit capacity; the voltage level of PCC must be increased or the equivalent impedance must be reduced for the wind farm.

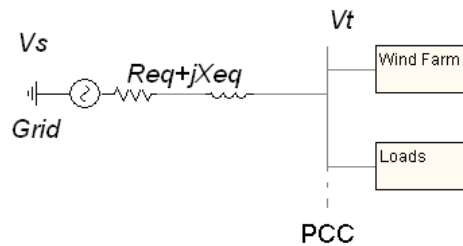


Figure 6.6 Equivalent circuit between the wind farm and the National Grid.

6.6 Wind Farm Simulation Results with PSCAD/EMTDC

The simulation is performed to analyze the power quality of the grid model including the wind turbines. Simulated and measured results of current on wind farm feeder while all wind turbines (12 wind turbines) were generating active power, are shown in Figure 6.7 and Figure 6.8, respectively. These 12 turbines are identical and assumed to be running under same shaft torque.

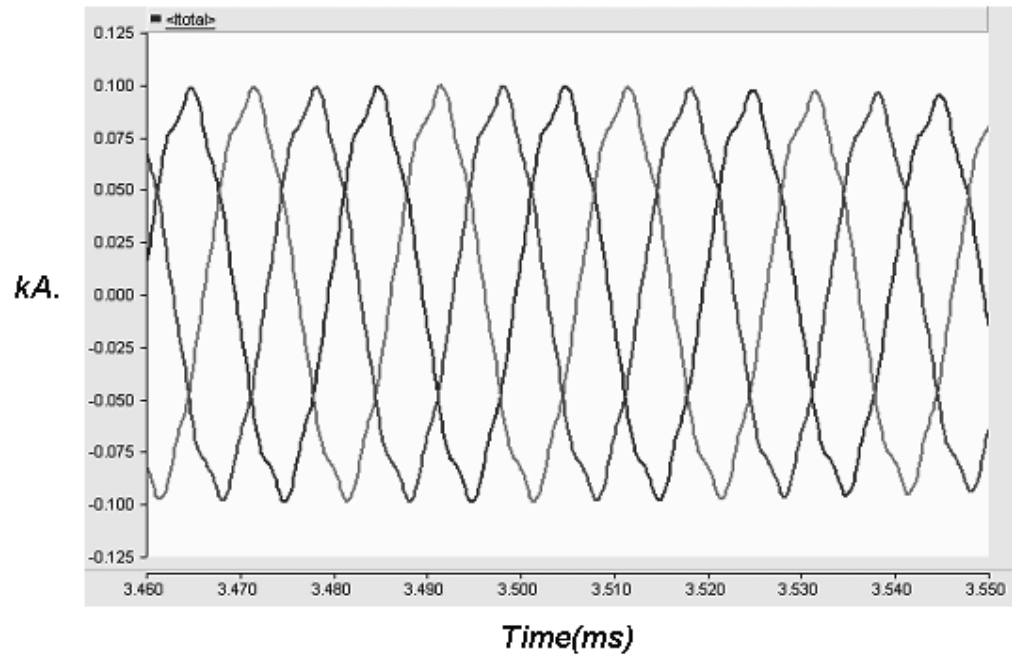


Figure 6.7 Simulated result of current on wind farm feeder.

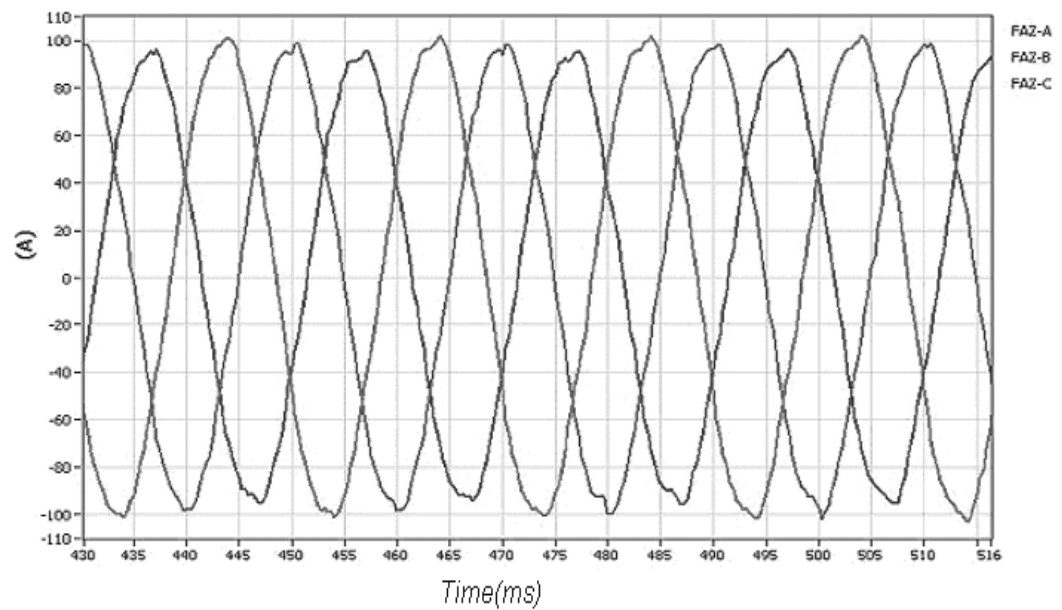


Figure 6.8 Measurement result of current on wind farm feeder.

Two fixed valued capacitor groups are installed in the simulation to set power factor correction for no-load operation. Simulated active and reactive power results

are shown in Figure 6.9. Base power for per unit system used in simulation is chosen as 9 MVA, the simulation result shows that the real power changes between 3.15 MW and 5 MW while the reactive power varies between 450 kVAR and 900 kVAR.

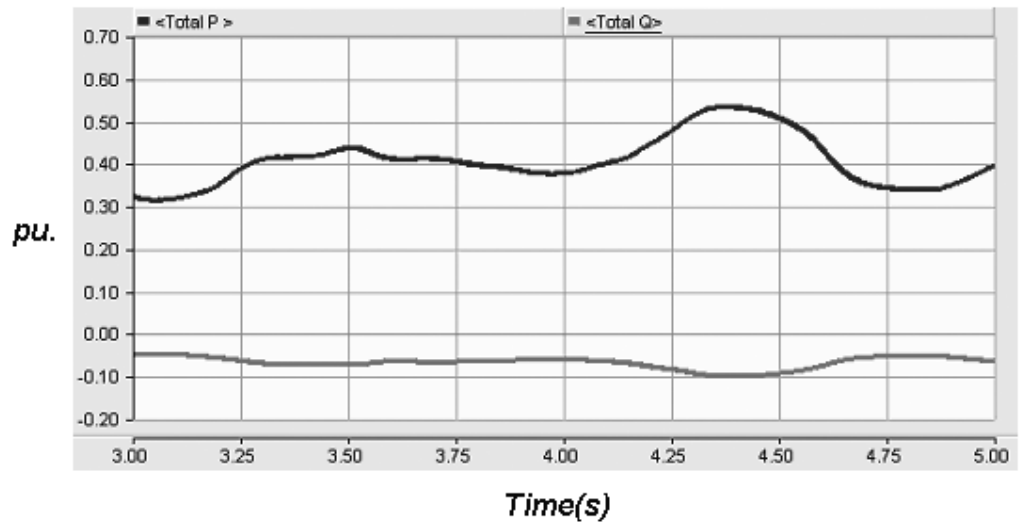


Figure 6.9 Simulation result of power on wind farm feeder.

Measured THD of current in wind farm feeder is shown in Figure 6.10. These measured values show that the THD is usually less than the limit of specified by IEEE Std. 519 for industrial harmonics loads. IEEE Std 519 establishes harmonic limits on voltage as 5% for total harmonic distortion and 3% of the fundamental voltage for any single harmonic.

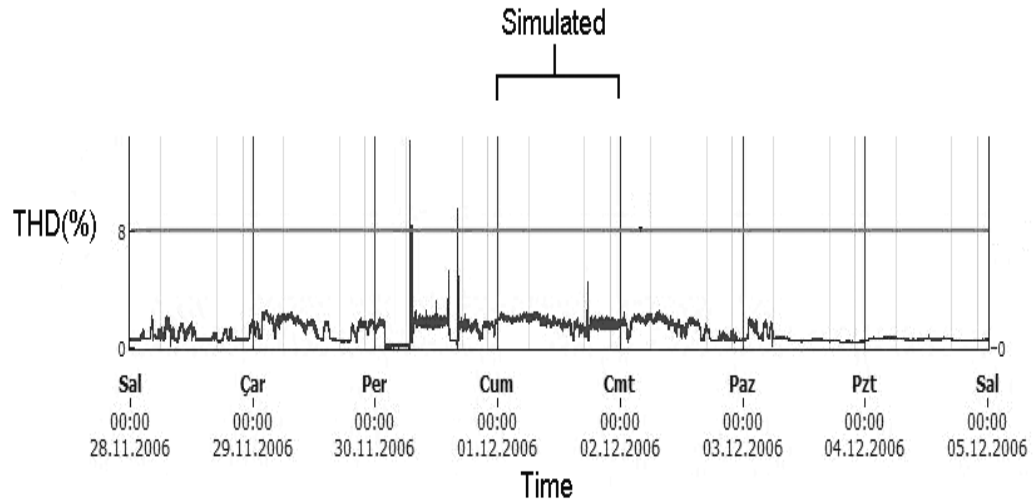


Figure 6.10 Measurement result of THD on wind farm feeder-34.5 kV.

Although measured wind speed values at site was used in the simulation, the wind speed is measured with one single anemometer located on the nacelle, whereas the rotor has a larger surface and wind speed is not constant on surface. The wind speed is disturbed by rotor wake. Therefore, it is not possible to observe the validation of simulation results given in Figure 6.11 with the measured ones. Simulation values show that the THD is also less than the limit of specified by IEEE Std. 519.

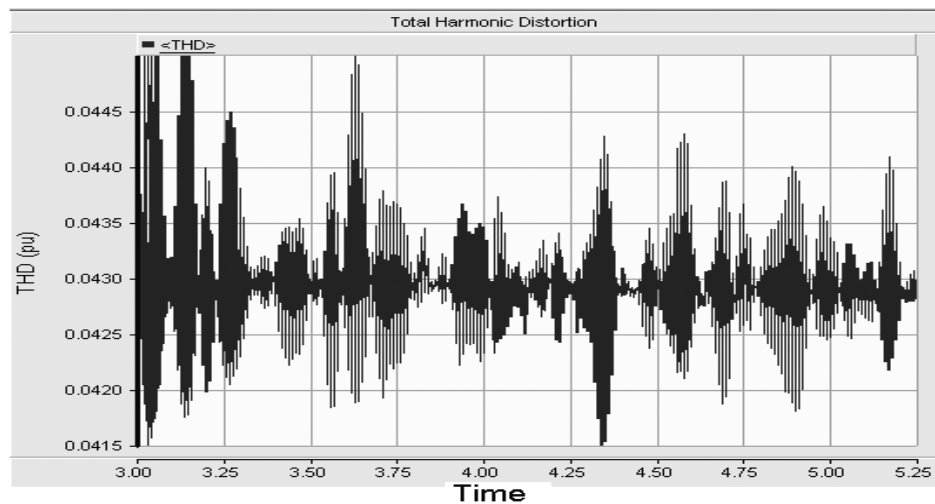


Figure 6.11 Simulation result of THD on wind farm feeder-34.5 kV.

6.7 Aggregated Model of the Wind Farm

Wind farm models may be built to various level of detail ranging from a one-to-one modelling approach to full aggregation. A wind farm one-line model, including N wind turbines equipped with wound rotor induction generators, is shown in Figure 6.12. Generators, capacitor banks, and transformers are assumed identical. Aggregated equivalent system can be obtained by aggregating the N sets of generators, capacitor banks, and transformers into one equivalent generator set composed by one of each component as shown in Figure 6.13. Turbine aggregation is mathematically exact only when all the involved wind turbines are similar and receive the same wind speed from the same direction.

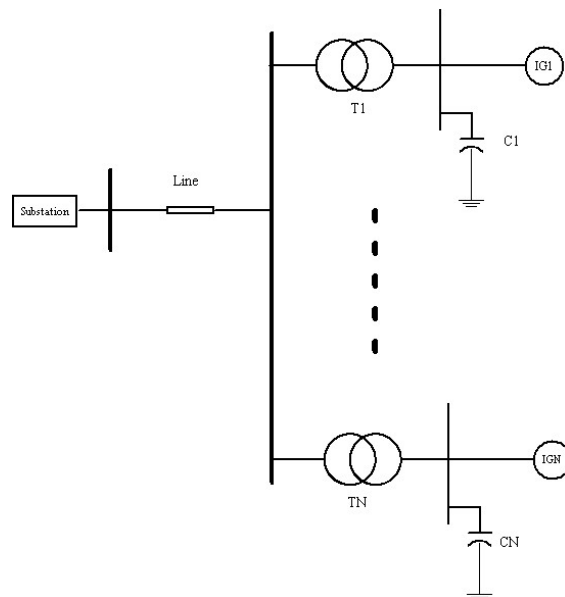


Figure 6.12 Wind-farm one line diagram

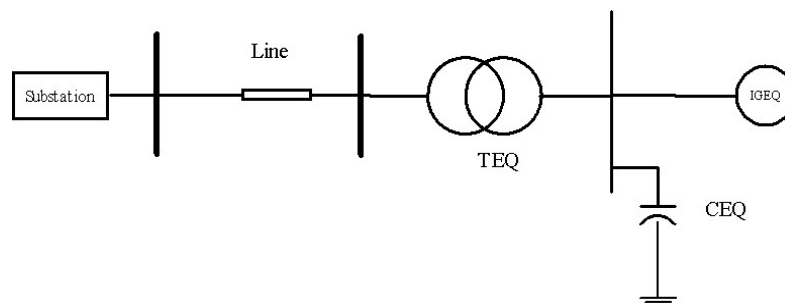


Figure 6.13 Wind-farm one line diagram with aggregated model

In the aggregated model, single component capabilities are multiplied by N and all the per-unit impedances are kept at original values while multiplying the MVA base of each component by N . Aggregated model can be represented by the equivalent circuit shown in Figure 6.14. In this figure, V_{sub} is the substation voltage, R_{sub} and X_{sub} represent the substation short-circuit level, R_L and X_L are the line resistance and reactance, X_{TR} is the transformer reactance and Z_C is the equivalent impedance of the local capacitor bank.

Aggregated model equivalent circuit can be reduced to equivalent circuit of Figure 6.15 by applying Thevenin's theorem to the circuit seen from the generator terminals(A-B).

$$Z'_{TH} = R'_{TH} + jX'_{TH} = Z_C \parallel Z_{Sub} + Z_L + Z_{TR} = \frac{Z_C \cdot (Z_{Sub} + Z_L + Z_{TR})}{Z_C + Z_{Sub} + Z_L + Z_{TR}} \quad (6.3)$$

$$V'_{TH} = \frac{Z_C}{Z_{Sub} + Z_L + Z_{TR} + Z_C} V_{Sub} \quad (6.4)$$

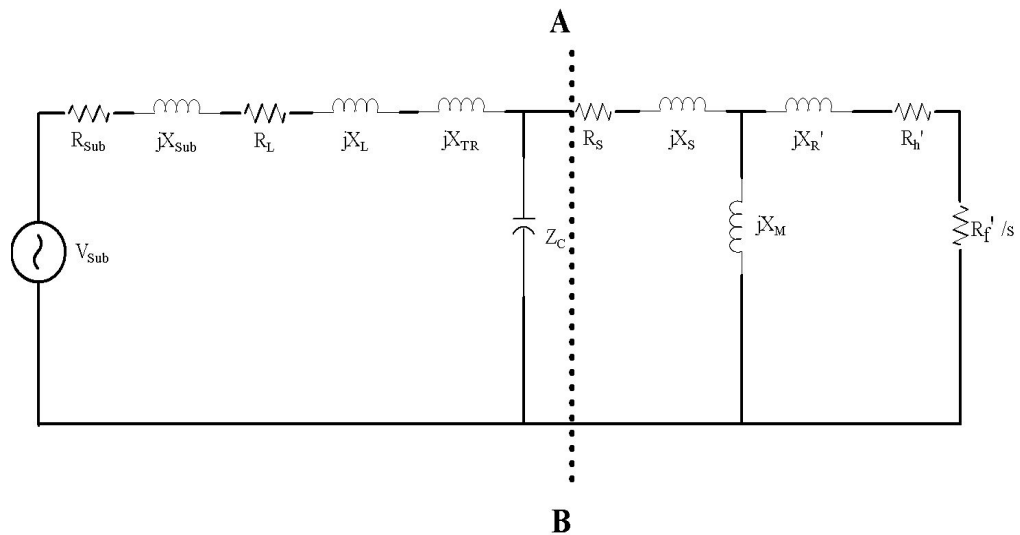


Figure 6.14 Equivalent circuit of aggregated model

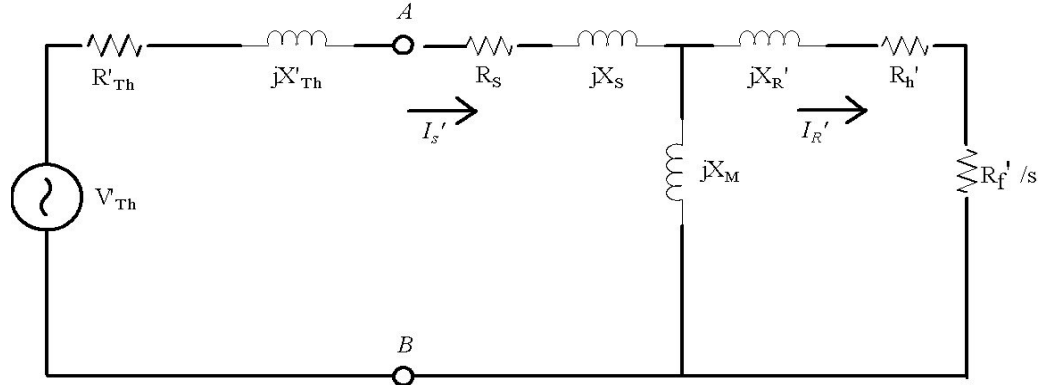


Figure 6.15 Reduced equivalent circuit of aggregated model

The circuit of Figure 6.15 can be reduced to the circuit of Figure 5.8 by substituting Z_S by $Z'_{Th} + Z_S$ in (5.32) and (5.33) and V by V'_{TH} in (5.32).

$$\bar{V}_{TH} = \bar{V}'_{TH} \left(\frac{Z_M}{Z_M + Z'_{TH} + Z_S} \right) \quad (6.5)$$

$$Z_{TH} = \frac{Z_M (Z'_{TH} + Z_S)}{Z_M + Z'_{TH} + Z_S} \quad (6.6)$$

By this way; power system parameters are applied to the aggregated model of wind farm. Adding power system components to the equivalent circuit of wind farm effects the steady-state stability margin of the model as can be seen from (5.37). System components cause a reduction in the maximum mechanical torque that can be applied to the machine. This fact reduces the steady-state stability margin and the maximum generator active power. The expression for the equivalent generator terminal voltage V_G considering the complete system can be obtained as;

$$|V_G| = |I'_S \cdot [Z_S + (Z_M || Z'_R)]| \quad (6.7)$$

$$|V_G| = \left| I'_S \cdot \frac{Z_S (Z_M + Z'_R) + Z_M Z'_R}{Z_M + Z'_R} \right| \quad (6.8)$$

6.7.1 Aggregated Model PSCAD/EMTDC Simulation Results

In this subsection, the effect of main parameters on steady-state stability margin is evaluated and discussed by the help of aggregated wind farm model results. The results help to understand the steady-state stability phenomena in wind farms equipped with wound rotor induction generators. The studied parameters are; power system components, rotor resistance control and substation voltage level. The developed aggregated model of the wind farm is used for simulation studies in PSCAD/EMTDC.

Aggregated mechanical torque that is applied to the wound rotor induction machine, is increased step by step to determine the maximum mechanical torque that can be applied to the machine. Wound rotor induction machine loses its stability if mechanical torque input gets bigger than the determined maximum value, T_{EMAX} . Scalar addition of the swing equation as an aggregation technique for N turbines of a wind farm, is given in (6.9) in per-unit by (Shafiu, Anaya-Lara, Bathurst, & Jenkins, 2006). H is the inertia constant, P_{in} and P_{out} are power input and output of wind turbine where $H^{agg} = \sum_{i=1}^N H_i$, $P_{in}^{agg} = \sum_{i=1}^N P_{ini}$, $P_{out}^{agg} = \sum_{i=1}^N P_{outi}$.

$$2H^{agg} \frac{d\omega}{dt} = P_{in}^{agg} - P_{out}^{agg} \quad (6.9)$$

6.7.2 Effect of Power System Components

Figure 6.16 presents aggregated model PSCAD/EMTDC simulation results of two different situations by the $T-\omega$ curves; first, wound rotor induction machine equipped wind turbine is connected directly to source: without power system components (strong grid); transformer, overhead line or underground cable (T_{EMAX1} , ω_{EMAX1}) and latter, wind turbine is connected to distribution system (weak-resistive grid): with power system components (T_{EMAX2} , ω_{EMAX2}). δ is equal to 0.95 in both situations.

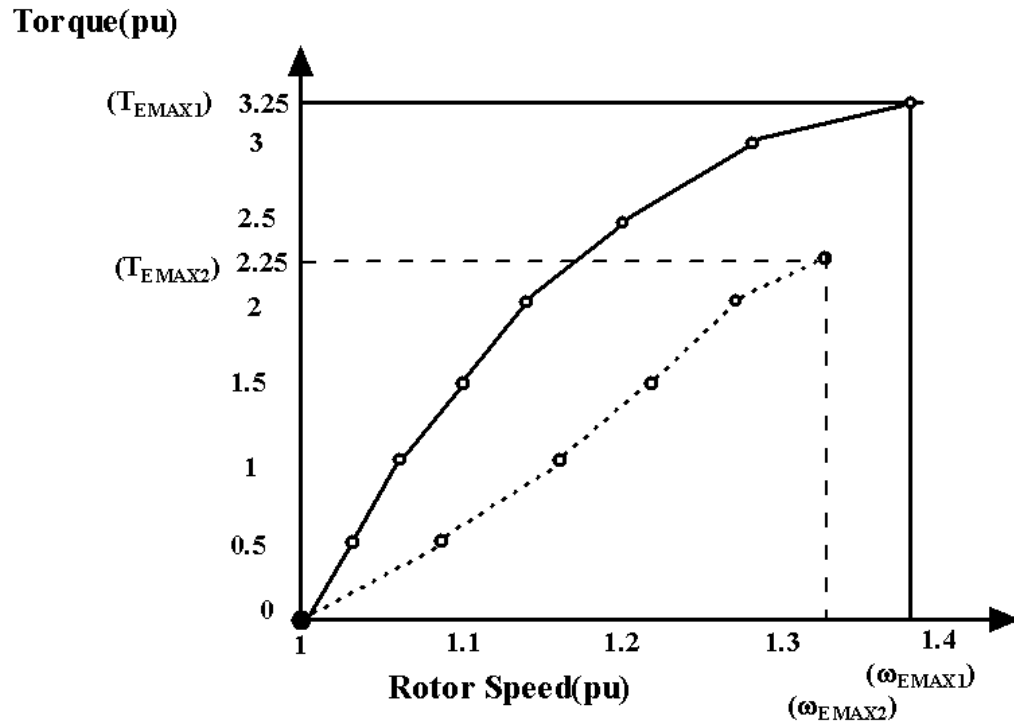


Figure 6.16 Torque-speed curve for two different situations

These aggregated model simulation results show that impedances of power system components, which connect the wind farm to grid, cause reduction in the maximum mechanical torque that can be applied to the generator. As given in (2.4), R_{sc} ; measure of the strength decreases as the impedance Z_k increases. Strong grids with minimal connection impedances are the best options for wind farm-grid connections.

6.7.3 Effect of Rotor Resistance Control

Figure 6.17 presents aggregated model PSCAD/EMTDC simulation results of three different situations to analyze the impact of the external resistance control of wound rotor induction machine.

First; $\delta_1=0.9$, $R_3^* = 0.45[R_{bs}] + 0.1 [R_3] \Omega$,

second; $\delta_1=0.85$, $R_3^* = 0.425[R_{bs}] + 0.15[R_3] \Omega$,

and third; $\delta_1=0.8$, $R_3^* = 0.4[R_{bs}] + 0.2 [R_3] \Omega$; $\delta_1 > \delta_2 > \delta_3$.

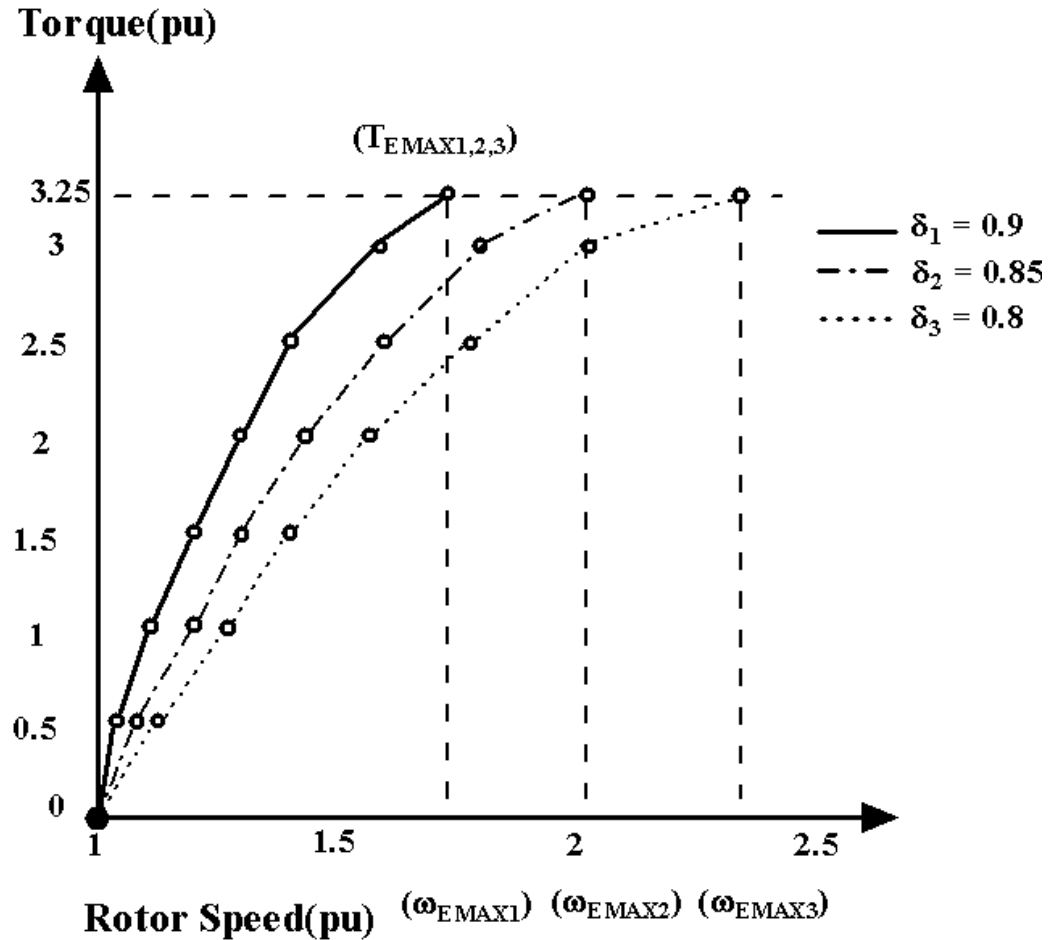


Figure 6.17 Torque-speed curve for three different situations

These aggregated model simulation results show that maximum electrical torque values are independent of rotor equivalent resistance as given (5-37), but the critical slips at which maximum electrical torque values occur are proportional to it, as given (5-36).

Effect of the rotor external resistance control to rotor speed can be seen from the difference of ω_{EMAX} ; $\omega_{EMAX1} < \omega_{EMAX2} < \omega_{EMAX3}$. When δ is decreased by controller, R_f and R_h are increased. These increments in R_f and R_h cause an increment in s_{max} , since R_f has a dominant affect than R_h over s_{max} ; as a result, the higher resistance of the rotor, the higher the slip is. Maximum electrical torques are equal for all situations as expected; $T_{EMAX1} = T_{EMAX2} = T_{EMAX3}$.

6.7.4 Effect of Substation Voltage Level

Figure 6.18 presents aggregated model PSCAD/EMTDC simulation results of two different situations to analyze the impact of the PCC voltage difference; first system with substation voltage %100 (T_{EMAX1} , ω_{EMAX1}) and second system with substation voltage %80 (T_{EMAX2} , ω_{EMAX2}).

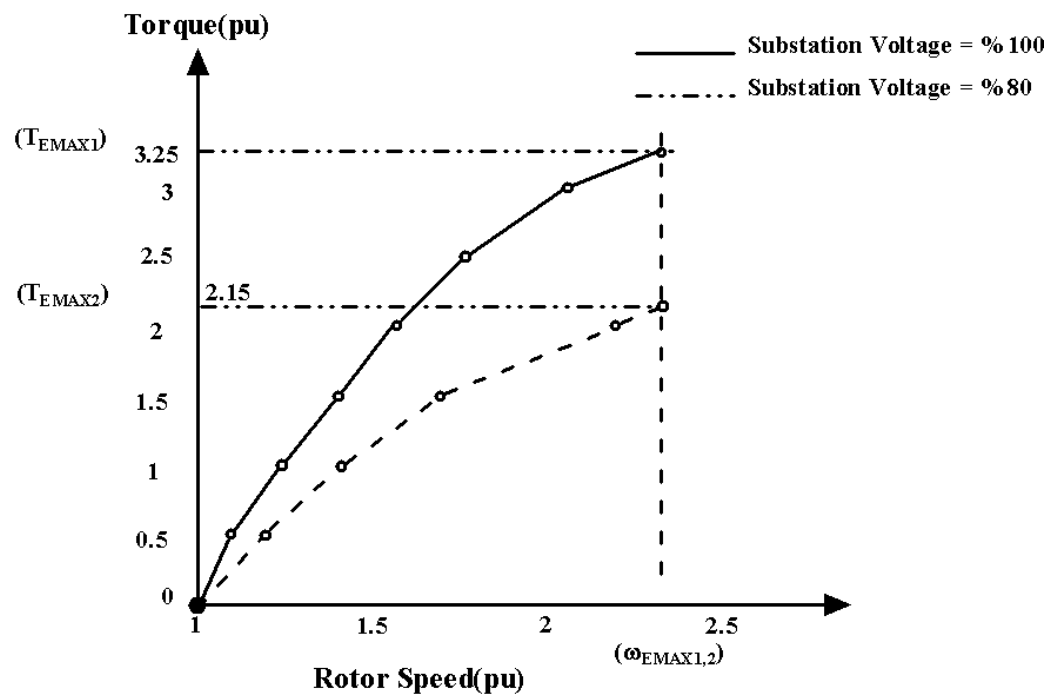


Figure 6.18 Torque-speed curve for two different situations

These aggregated model simulation results show that the PCC voltage reduction cause reduction in the maximum mechanical torque that can be applied to the generator. This means that the voltage reduction at the PCC in case of high wind speeds (full power output of the wind farm) can result as losing rotor speed stability and cut out of the wind turbine as a consequence.

6.8 Comparison of Aggregated Model PSCAD/EMTDC Simulation Results with Complete Model PSCAD/EMTDC Simulation Results

PSCAD/EMTDC simulation results of the developed aggregated wind farm model are compared with the PSCAD/EMTDC simulation results of complete wind farm model for verification. The effectiveness of the aggregated model to represent the collective response of the wind farm is demonstrated by comparing the simulation results of aggregated and complete models both during standart operation and grid disturbance.

Figure 6.19 and 6.20 show the real and reactive power output results of; complete wind farm model and aggregated model, respectively. In complete model simulation, the slope of the power output lines are smaller than aggregated model simulation, since wound rotor induction machines of wind turbines start to operate as a generator one by one, after $t = 1.5$. In aggregated model simulation; slope is rather high with respect to the complete model.

In case of standart operation: balanced source voltage, fault free operation, no noise component in wind speed and constant incoming wind speed for all wind turbines; resulting values for real and reactive power are the same as seen in the graphs. The results demonstrate the effectiveness of the aggregated model to approximate the collective response of the wind farm for steady-state power systems studies.

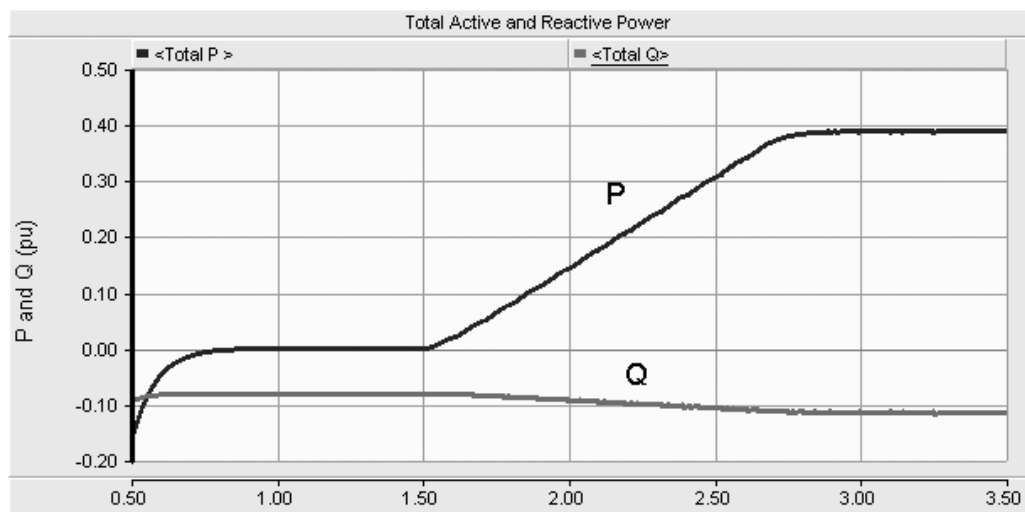


Figure 6.19 Complete model real and reactive output of the wind farm

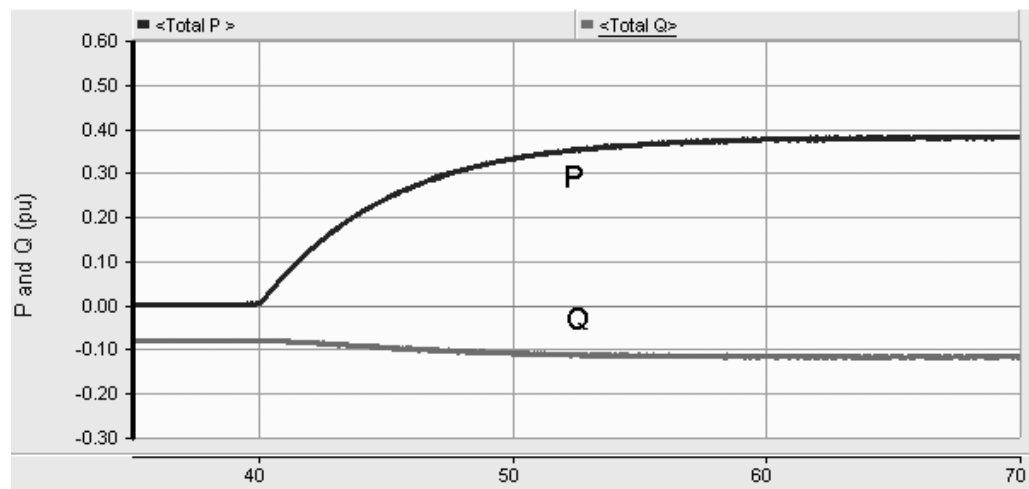


Figure 6.20 Aggregated model real and reactive output of the wind farm

Figure 6.21 and 6.22 show the current waveform results of; complete wind farm model and aggregated model in case of steady-state operation, respectively. There are harmonic contents because of rotor circuit resistance control. But in complete model current waveform, these harmonic contents are reduced due to mutual interactions of individual machines. Although twelve wound rotor induction

machines are modeled separately in complete model; aggregated machine model can not eliminate harmonic contents in current waveform.

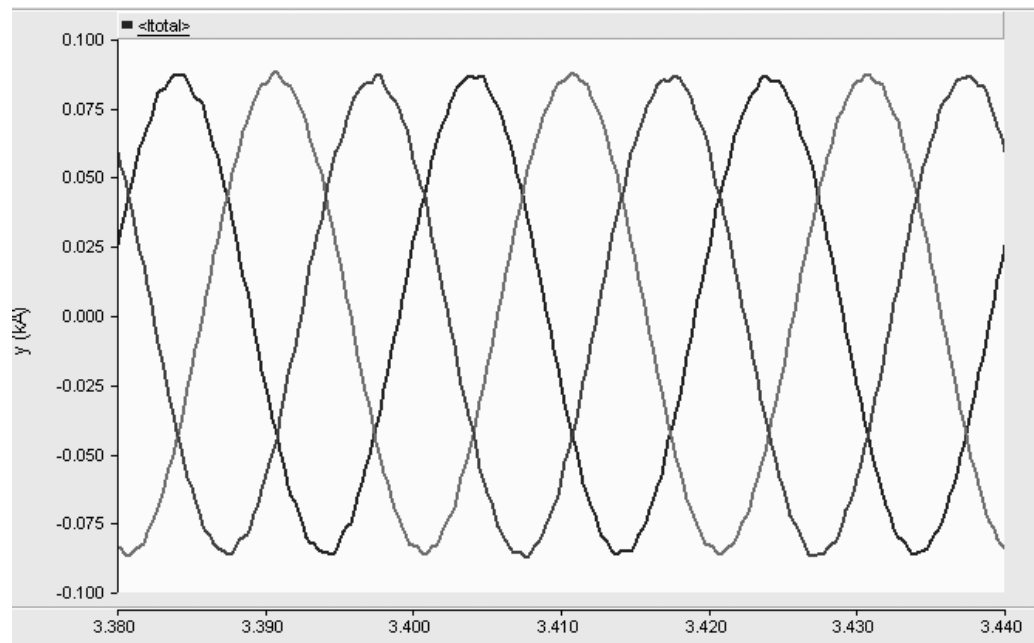


Figure 6.21 Complete model current output of the wind farm

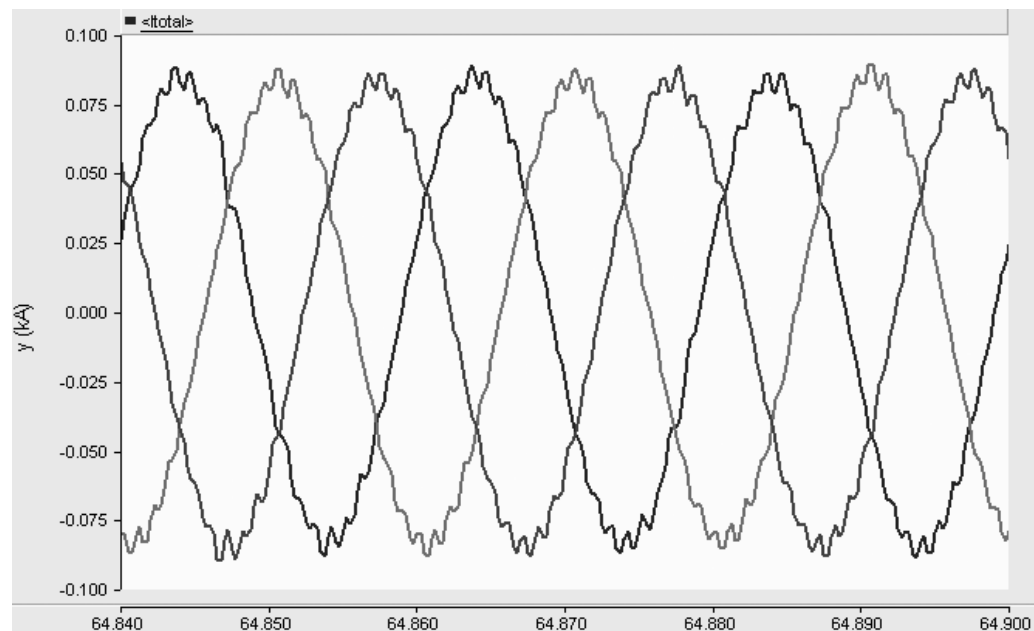


Figure 6.22 Aggregated model current output of the wind farm

Figure 6.23 and 6.24 show the real and reactive power output results of complete wind farm model and aggregated model in case of three phase-ground short-circuit fault for 150 milliseconds at the transmission line which connects the wind farm to grid. Standart operation is valid except the fault situation.

As seen from the graphs at post fault time interval, real and reactive power changes show different characteristics. Although transient time interval results are not the same in both models, aggregated model real and reactive power results are valid for steady-state operation.

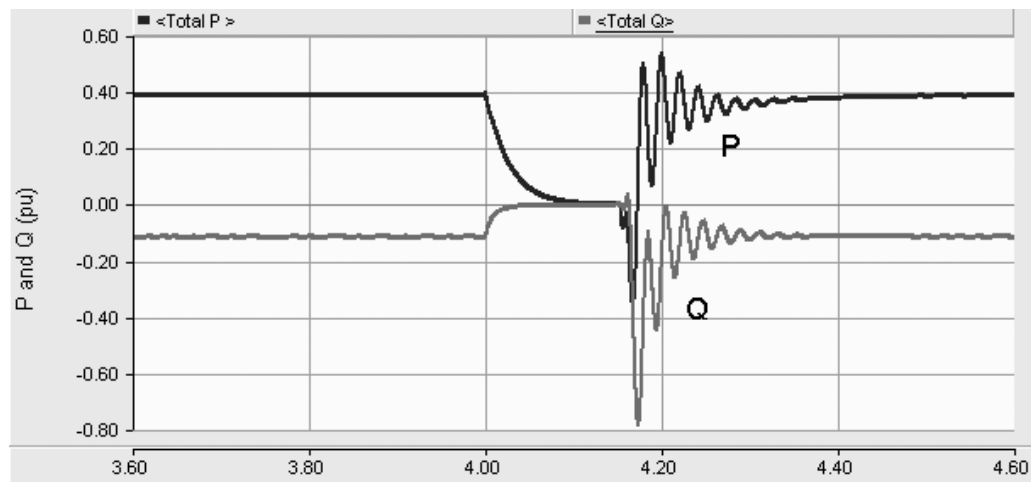


Figure 6.23 Complete model real and reactive power output of the wind farm in case of 150 ms grid fault.

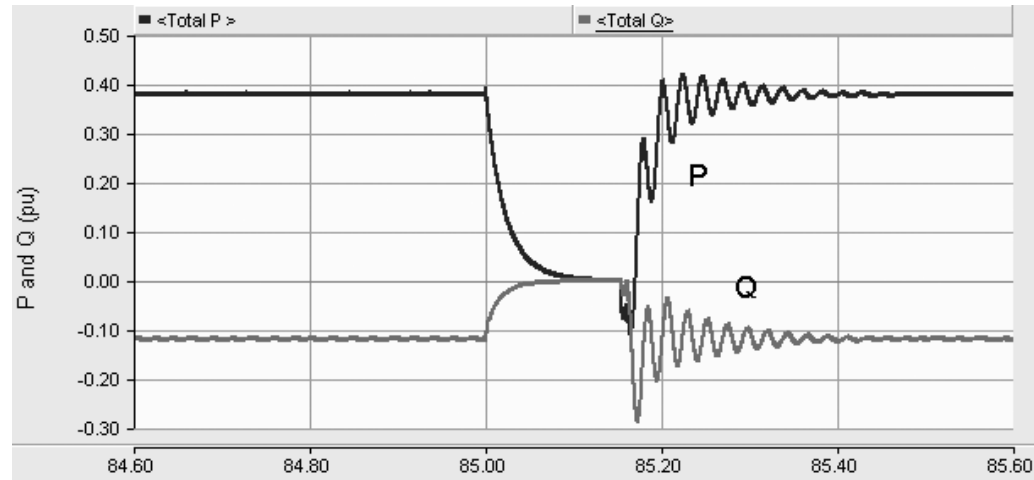


Figure 6.24 Aggregated model real and reactive power output of the wind farm in case of 150 ms grid fault.

6.9 Power Quality Project

Mobile Power Quality Measurements had been carried out in many substations in all around Turkey. The main goal of Mobile Power Quality Measurements is to identify the problems of of power system in terms of power quality indices.

Measurements at each point had been performed continuously for at least seven days according to IEC 61000-4-30 Std. and in this way; the data concerning weekday/weekend, day/night, and peak times were collected. This measurement system were used for obtaining changes of the electrical power quality magnitude such as active and reactive power flows, voltage and current magnitudes, and harmonics. In the case that an event occurred during the seven-day period of the measurement, even this process was recorded in a detailed way.

The measurements in the wind farm of Alaçatı had been carried out in the substation during 7 days in a week by power quality monitoring set-up shown in Figure 6.25. It collected the raw data in accordance with IEC 61000-4-30/Class B, and carried out on-line data processing according to IEC 61000-4-7/Class B, IEC 61000-4-15/Class B and IEEE Std. 519. Locations of measurements are shown on one-line diagram of the substation given in Figure 6.26.

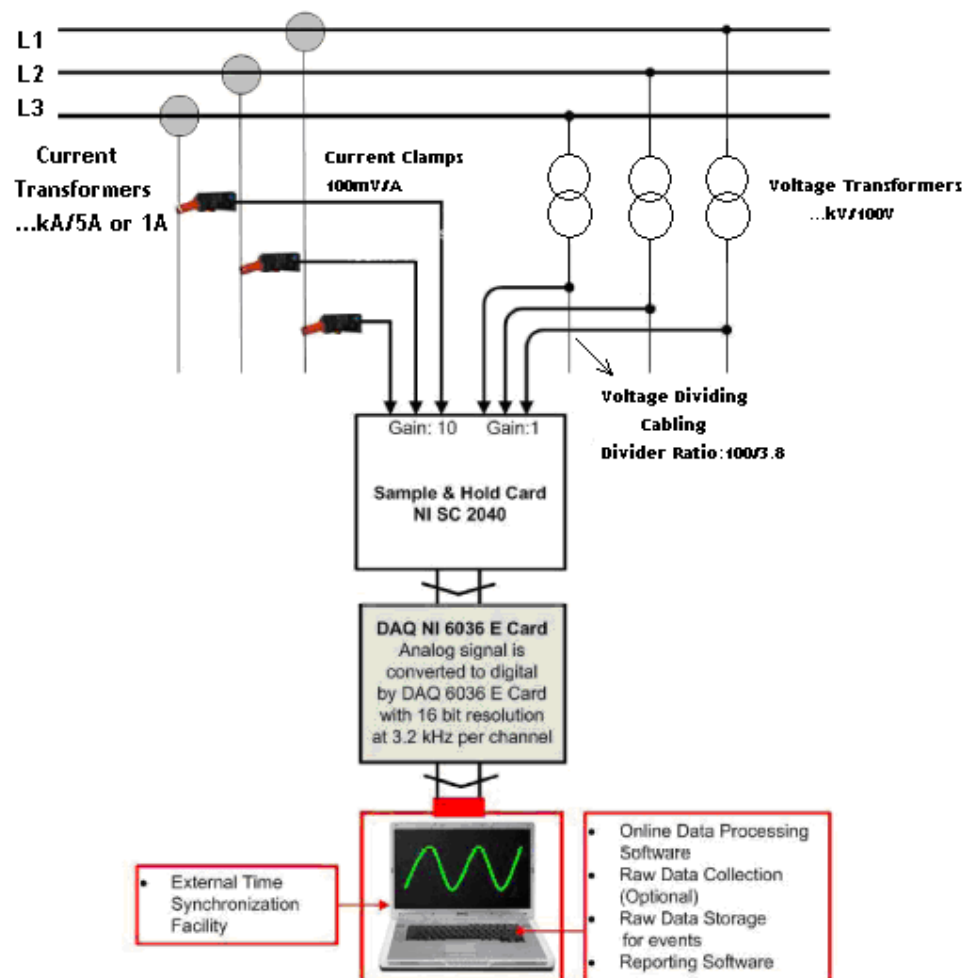


Figure 6.25 Block Diagram of Power Quality Monitoring Set-up

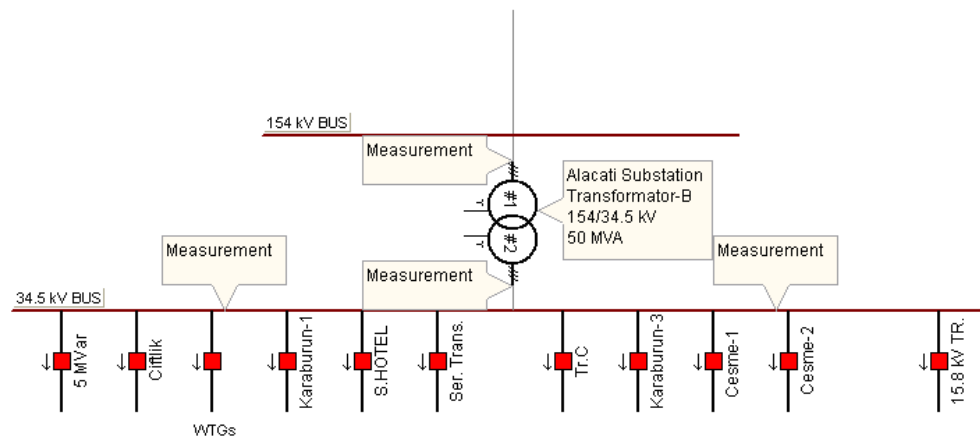


Figure 6.26. Location of measurements in Alaçatı Substation

6.9.1 Results of Power Quality

The active, reactive, apparent powers and power factor were measured and recorded at every ten minutes on wind farm feeder and the results are shown in Figure 6.27 and Figure 6.28.

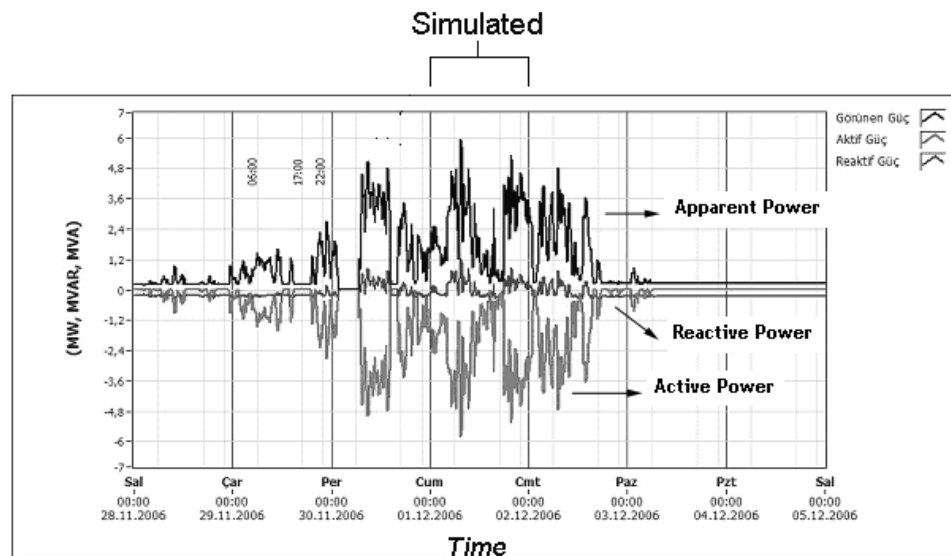


Figure 6.27 Measured Real, Reactive and Apparent Power results in wind farm feeder for 7 days

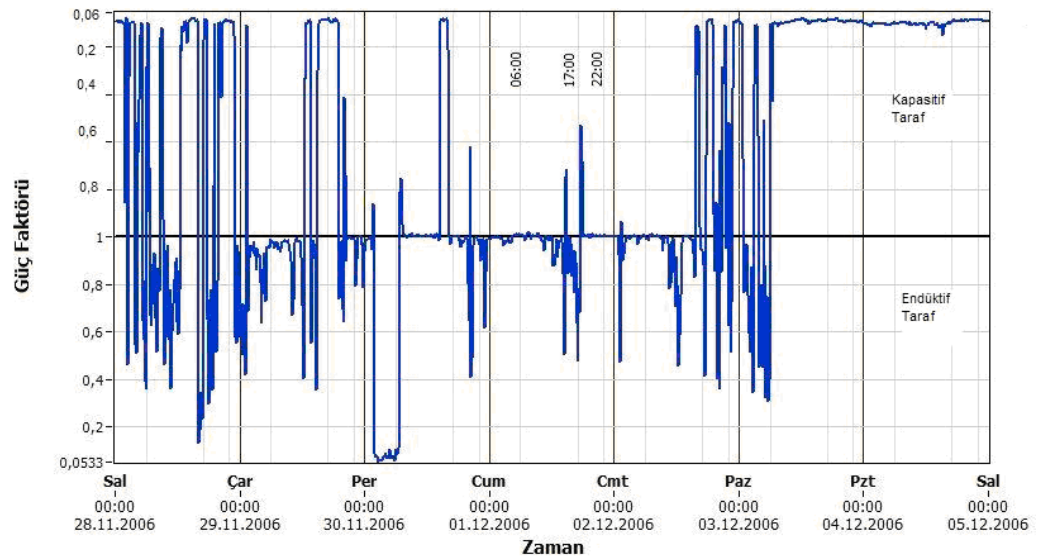


Figure 6.28 Measured power factor results in wind farm feeder for 7 days

The voltage and current magnitudes are measured at the bus of wind farm and at the output of wind generators. Recorded data is analyzed according to the definitions of IEC 61000-4-30; and 63 events observed for the seven days; 33 voltage sags, 4 voltage swells, 4 voltage shortages, 22 voltage unbalances on the substation voltages.

Examples of voltage sag, voltage swell, voltage shortage and voltage unbalance waveforms with synchronous current waveforms are given in Figure 6.29-6.36, respectively.

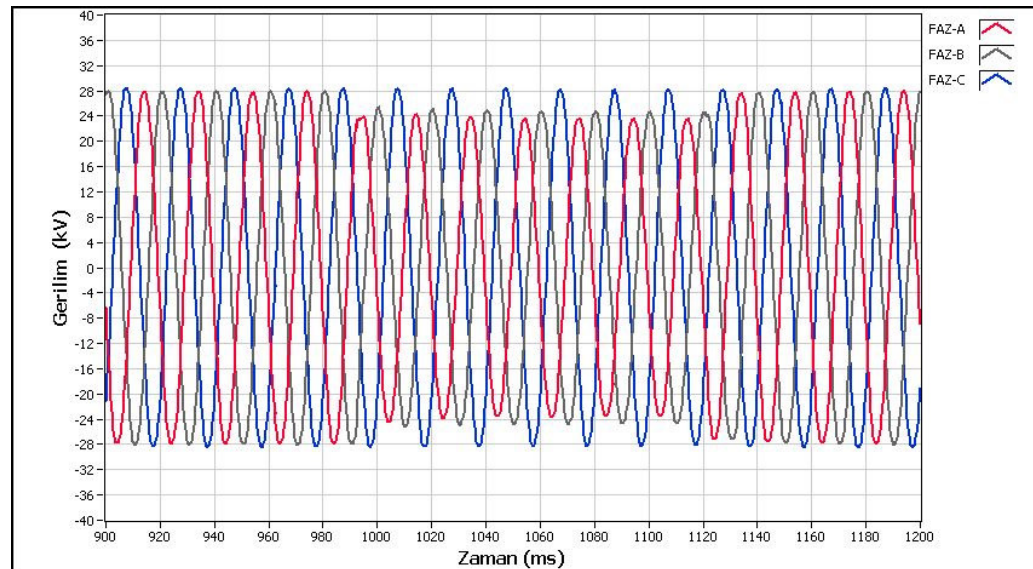


Figure 6.29 Voltage sag.

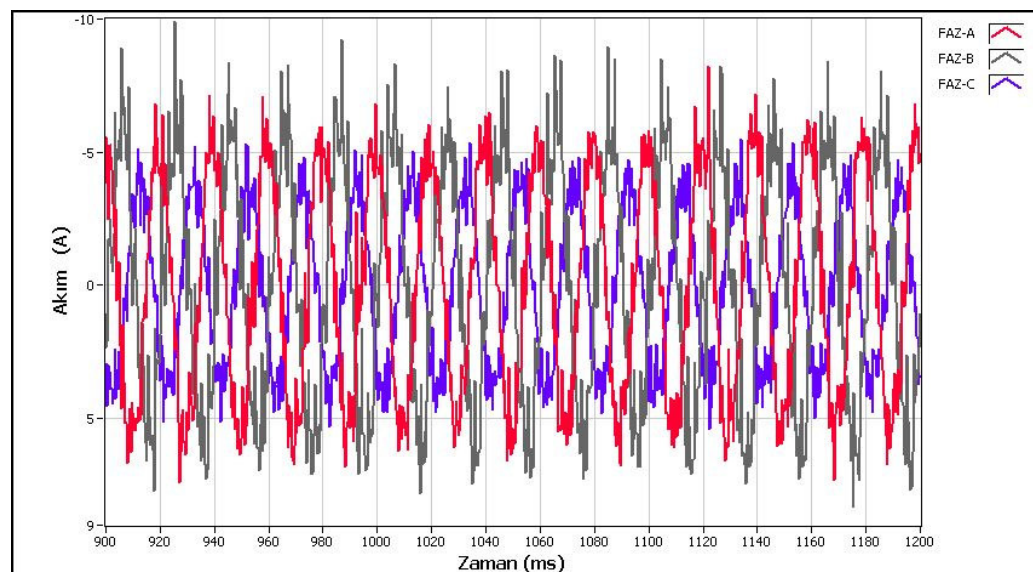


Figure 6.30 Current waveforms during the voltage sag.

Figure 6.29 and 6.30 show the voltage sag and phase current measured at the same time. The recorded data for phase current contains only noise component. This implies that; the wind farm is not able to supply current to the grid at the moment because of a preceding factor.

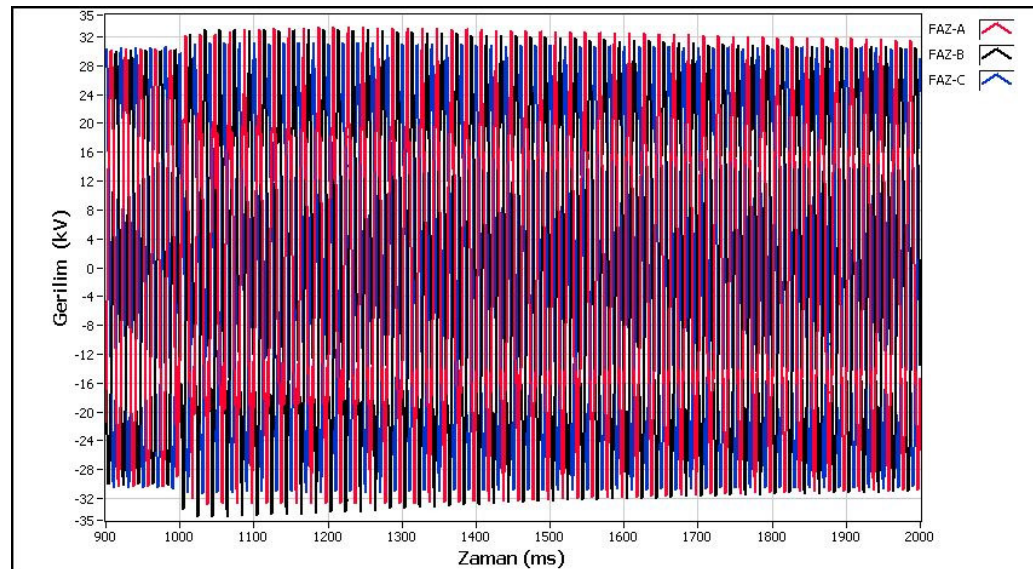


Figure 6.31 Voltage swell.

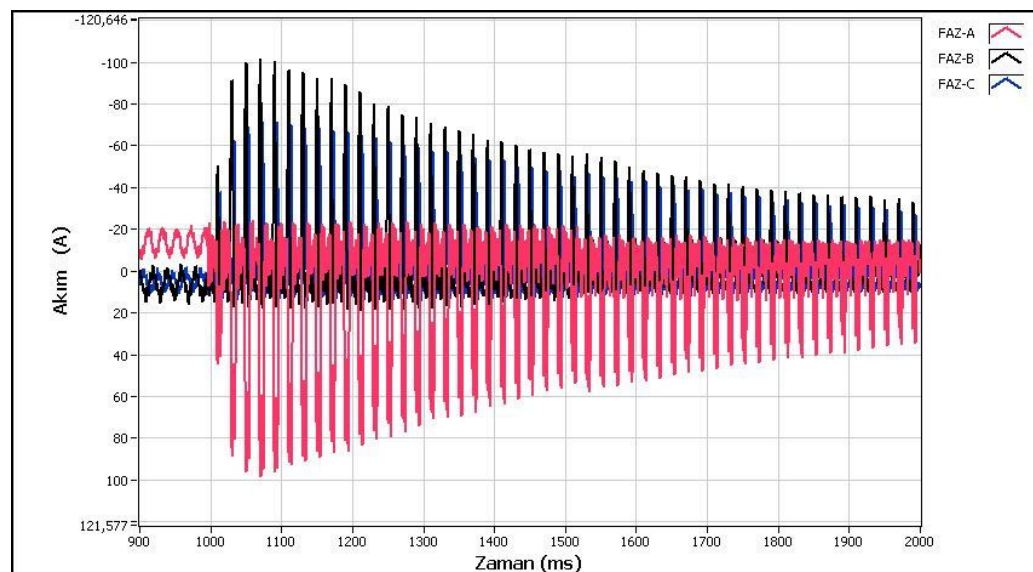


Figure 6.32 Current waveforms during the voltage swell.

Figure 6.31 and 6.32 show the voltage swell and phase current measured at the same time. Voltage swells is occurred because of a start-up in wind farm. As given in Chapter-2, output power of the wind farm and the short circuit impedance determines the voltage difference at the PCC.

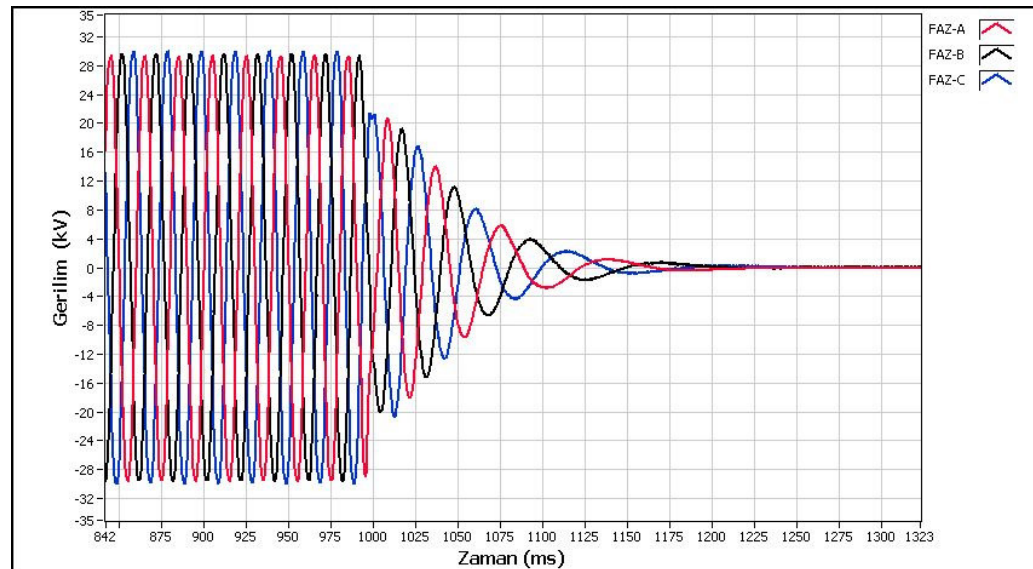


Figure 6.33 Voltage shortage.

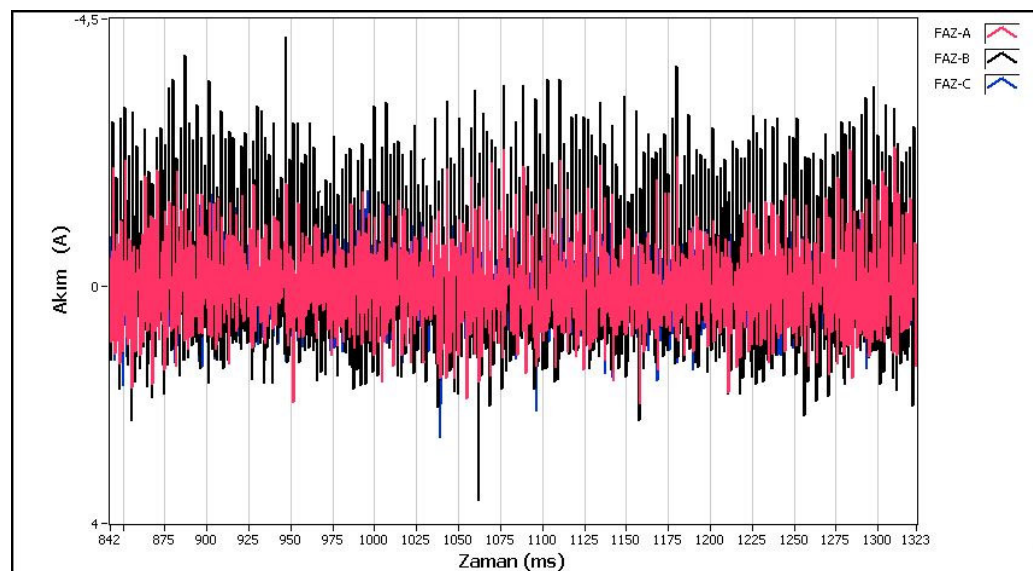


Figure 6.34 Current waveforms during the voltage shortage.

Figure 6.33 and 6.34 show the voltage shortage and phase current measured at the same time. The recorded data for phase current contains only noise component like in Figure 6.30. In case of a grid fault(event) series, wind turbine control system disconnects the wind turbine from the grid. Wind farm generators continues to operate in “motor” mode until the next control order.

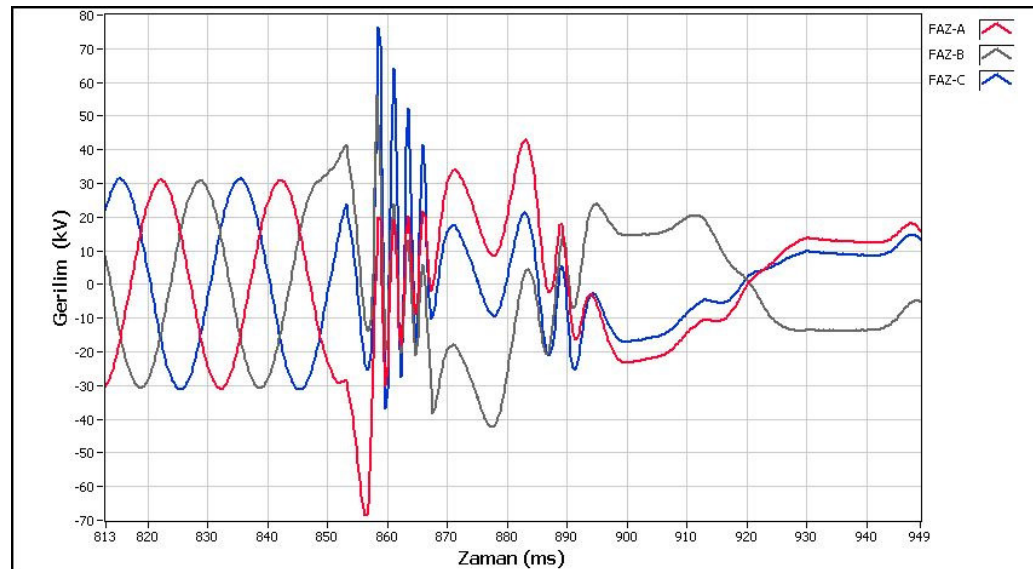


Figure 6.35 Voltage unbalance.

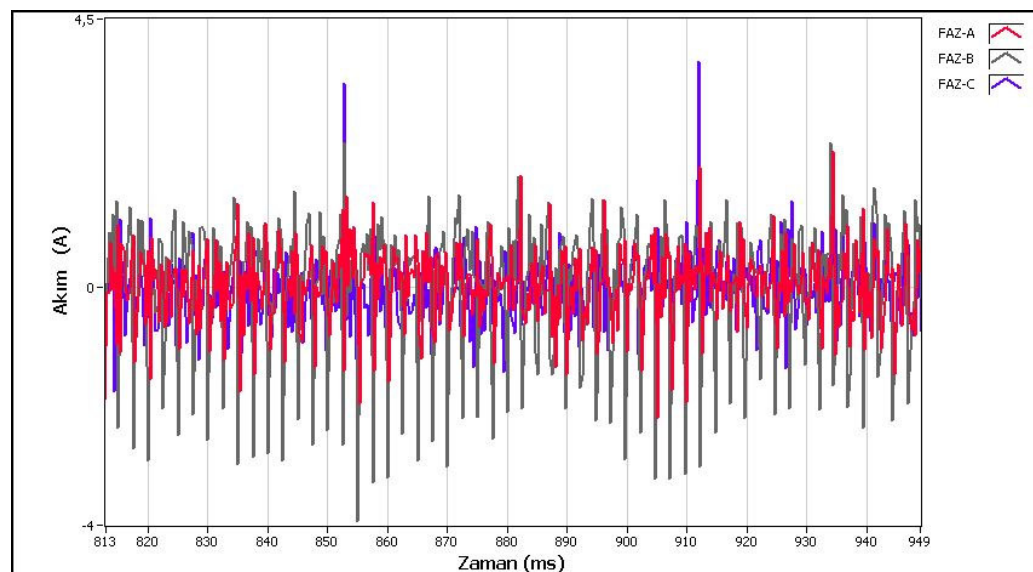


Figure 6.36 Current waveforms during the voltage unbalance.

Figure 6.35 and 6.36 show the voltage unbalance and phase current measured at the same time. Voltage waveform has a particular characteristic, which provides information about how phase voltage can be changed in case of a grid event.

The simulations are based on real measurement and a realistic model of the system. However it is necessary to make the following statements, which affect the accuracy of the simulation results:

Although measured wind speed values at site was used in the simulation, the wind speed is measured with one single anemometer located on the nacelle, whereas the rotor has a larger surface and wind speed is not constant on surface. The wind speed is disturbed by rotor wake. Therefore, it is not possible to observe the validation of simulation results with the measured ones.

Individual control system of wind turbines works independently for the incoming wind speed and wind direction. There is no a record of each wind turbine status during the measurement period. Although the wind speed is measured, gust and ramp components are neglected which require multiple wind measurements in the wind farm and geographical layout analysis of the wind farm.

There are various types of loads; mostly residential and commercial, fed from 34.5 kV common bus of Alaçatı Substation which wind farm is connected. Since electrical measurement procedure is set to record data only before and after the disturbances and synchronization of measurements at different buses are not guaranteed; the load feeders; including power factor correction feeder, can not be controlled or measured during the measurement period. A very high capacity data acquisition system, which is neither present in Alaçatı substation nor has been used by mobile measurement system, is required to obtain synchronous data for multiple measurements

Despite these statements, the case study has given beneficial outputs about a real system. The combination of measurements and simulation model makes it possible to estimate power quality and stability margin of the system that would otherwise be difficult to predict and to measure.

CHAPTER SEVEN

CONCLUSIONS

The share of wind energy in Turkish electrical power system is getting higher each year. The wind farms have different impacts and functions on the performance of power system than conventional power plants, because of variation of wind speed in time. Power system operators have to be sure about the reliability of the system after wind energy integrations. As a result; accurate models of wind farms and power system are needed for accurate analysis.

In this thesis, a case study has been performed about grid-connected wind farms and related power quality issues. The model of the drive circuit with slip ring induction machine is verified by the experimental results then model is implemented to the wind farm having 12 turbines. The field measurements have been carried out according to standarts. The line current, real power, reactive power and THD are predicted from simulation program and compared to measured results.

The ratio between short circuit current and installed capacity of WECS is around 41, therefore, the distortion of bus voltage is not significant. If the pitch angle control is also included into the model, then the power disturbances due to the wind speed variation can also be accurately predicted. This control algorithm is not provided by the system operators for the wind farm considered here.

Finally an accurate aggregated model for wound rotor induction machine was newly developed and results were compared with the complete model. Aggregated model of the wind farm in PSCAD/EMTDC was used to evaluate the effects of main parameters on steady-state stability margin. Also the effectiveness of the equivalent model to represent the collective response of the wind farm is demonstrated by comparing the simulation results of aggregated and complete models both during standart operation and grid disturbances.

Like in other countries, which have particular wind energy conversion system integrated into overall power system, in Turkey TEİAŞ needed grid codes for wind energy conversion systems. The case study has given beneficial outputs about the grid connected wind farm and contribution have been done during thesis for developing grid code for wind energy conversion systems of TEİAŞ by the help of the case study results obtained.

According to the developed new grid code for wind farms; wind farm investors have to provide evidence of the fulfilment of grid code capabilities like; LVRT capability, power quality affect and any other, by simulations which include steady state as well as dynamic studies before wind farm installations.

It has been more than ten years since Alaçatı wind farm started to operate. According to the site measurement results, Alaçatı wind farm has problems about compliance with power quality standarts. In addition, all regulations and grid codes will be more demanding and more restrictive with revisions. Although TEİAŞ can not demand compliance with the new grid code for Alaçatı wind farm operator, limited improvements may be discussed by both sides. LVRT capability and control of frequency can not be provided with present wound rotor induction generators. A new dynamic reactive power control system like a STATCOM can be established instead of present capacitor banks. Thus; fast and smooth reactive power control, PCC voltage level control, flicker mitigation and as a result; power quality improvement can be provided for the wind farm and the grid.

REFERENCES

- Akhmatov, V., Knudsen, H., Nielsen, A. H., Pedersen, J. K., & Poulsen, N. K. (2003). Modelling and Transient Stability of Large Wind Farms. *Electrical Power & Energy Systems*, 25(2), 123 – 144.
- Akhmatov, V. (2004). An Aggregated Model of a Large Wind Farm with Variable-speed Wind Turbines Equipped with Doubly-fed Induction Generators. *Wind Engineering*. 28(4), 479 – 488.
- Akhmatov, V. (2006). System stability of large wind power networks: A Danish study case. *Electrical Power and Energy Systems*, (28), 48 – 57.
- Akpınar, E. & Pillay, P.(1990) Modeling and Performance of Slip Energy Recovery Induction Motor Drive. *IEEE Transactions on Energy Conversion*, Vol.5, No:1, pp 203-210.
- Anderson, P.M. & Bose A. (1983). Stability simulation of wind turbine systems. *IEEE Transactions on Power Apparatus and Systems*. 102(12), 3791 – 3795.
- Balıkcı, A. (2008). *Comparing two different slip energy drives in WECS based on fuzzy logic controller. M.Sc Thesis*, DEU.
- Balıkcı, A., Akpınar, E.& Mutlu, Ö.S. (2008). Harmonic Analysis of Slip Ring Induction Machine Drives Used in WECS. Submitted to *Renewable Energy*.
- Boldea, I. (2005). *Variable Speed Generators*. U.S.A. CRC Press.
- Bose, B. K. (2002). *Modern Power Electronics and Ac Drives*. U.S.A. Prentice Hall PTR.

- Chen, Z., Blaabjerg, F., & Sun, T. (2004). Voltage Quality of Grid Connected Wind Turbines. *Proc. of the Workshop of Techniques And Equipments For Quality And Reliability Of Electrical Power*, Bucharest, Romania. (11-16).
- Chen, Z. (2005a). Issues of Connecting Wind Farms into Power Systems. *Proc. of IEEE/PES Transmission and Distribution Conference & Exhibition 2005 : Asia and Pacific-China*.
- Chen, Z. (2005b). Characteristics of induction generators and power system stability. *Proceedings of the Eight International Conference on Electrical Machines and Systems*, ICEMS 2005, Volume 2, 919-24.
- Chowdhury, B. H., & Chellapilla, S. (2006). Double-fed Induction Generator Control for Variable Speed Wind Power Generation. *Electric Power Systems Research*, 76, 786–800.
- Conroy, J., & Watson, R. (2009). Aggregate modelling of wind farms containing full-converter wind turbine generators with permanent magnet synchronous machines: Transient stability studies. *IET Renew. Power Gener.*, 2009, Vol. 3, No. 1, pp. 39–52
- Dinic N, Fox B, Flynn D, Xu L, & Kennedy A. (2006). Increasing wind farm capacity. *IEE Proc-Gener. Transm. Distrib.* 153(4): 493-98.
- Divya, K. C., & Rao, P. S. N. (2006). Models for wind turbine generating systems and their application in load flow studies. *Electric Power Systems Research*, 76, 844–856.
- Dubey, G. K. (1989). *Power Semiconductor Controlled Drives*. USA. Prentice Hall International.
- El-Hawary, M. E. (2000). *Electrical Energy Systems*. U.S.A. : CRC Press.

- Erlich, I., Winter, W., & Dittrich, A. (2006). Advanced Grid Requirements for the Integration of Wind Turbines into the German Transmission System. *IEEE Power Engineering Society General Meeting* 2006.
- Estanqueiro, A. I., Tande, J. O., & Peças Lopes, J. A. (2007). Assessment of Power Quality Characteristics of Wind Farms. *IEEE Power Engineering Society General Meeting* 2007 (1 – 4).
- European Transmission System Operators-ETSO. (2007) European Wind Integration Study (EWIS) Towards a Successful Integration of Wind Power into European Electricity Grids. Retrieved April 25, 2008, from <http://www.windaction.org/documents/7995>.
- EWEA-European Wind Energy Association. (2005). Large scale integration of wind energy in the European Power Supply. Retrieved November 25, 2006, from http://www.ewea.org/fileadmin/ewea_documents/documents/publications/grid/05_1215_Grid_report.pdf.
- Fagan, E., Grimes, S., McArdle, J., Smith, P., & Stronge, M. (2005). Grid Code Provisions for Wind Generators in Ireland. *IEEE Power Engineering Society General Meeting* 2005, (2),1241 – 1247.
- Karady, G. G. (2001). Concept of Energy Transmission and Distribution. In L. L. Grigsby,(Ed.). *The Electric Power Engineering Handbook* (368-379). U.S.A. : CRC Press.
- Gönen, T. (2004). Power Distribution. In W. Chen, (Ed.). *The Electrical Engineering Handbook* (749-759). U.S.A. : Elsevier Academic Press.

- Hansen, A. D. (2005). Generators and Power Electronics for Wind Turbines. In T. Ackermann, (Ed.). *Wind Power in Power Systems*, (53- 95). Great Britain : J.Wiley & Sons Ltd.
- Hansen A.D., Sorensen P., Janosi L. & Bech J.(2001) Wind Farm Modelling for Power Quality. *The 27th Annual Conference of the IEEE Industrial Electronics Society*. Denver, CO, USA. Volume 3, p.1959-64.
- Hase, Y. (2007). *Handbook of Power Systems Engineering*. Great Britain: John Wiley & Sons Ltd.
- Helle, L. & Blaabjerg, F. (2002). Wind Turbine Systems. In Marian P. Kazmierkowski and Frede Blaabjerg (Ed.). *Control in Power Electronics: Selected Problems*, (483-511). U.S.A. : Elsevier Academic Press.
- Holttinen,H., Meibom, P., Orths, A., Hulle F.V.,Ensslin C., Hofmann L., McCann J., Pierik J., Tande J.O., Estanqueiro A., Söder L., Strbac G., Parsons B., Smith J.C., Lemström B.(2006). Design and Operation of Power Systems with Large Amounts of Wind Power, First Results of IEA Collaboration. *Global Wind Power Conference*, Adelaide, Australia.
- International Electrotechnical Commission Standart No : 61000-4-15. (1997). *Testing and measurement techniques : Flickermeter - Functional and design specifications*.
- International Electrotechnical Commission Standart No : 61400-21.(2001). *Wind Turbine Generator Systems - Part 21: Measurement and Assessment of Power Quality Characteristics of Grid Connected Wind Turbines*.
- Iov, F., Hansen, A. D., Sørensen, P., & Cutululis, N. A. (2007). *Mapping of Grid Faults and Grid Codes*. Risø-R-Report 1617(EN). Retrieved August 10, 2007,

from http://www.risoe.dtu.dk/Risoe_dk/Home/Knowledge_base/publications/VEA.aspx.

Kazachkov, Y.A., Feltes, J.W. & Zavadil, R. (2003) Modeling Wind Farms for Power System Stability Studies. *Proceedings of PES General Meeting 2003*. 1526-1533.

Kenisarin, M., Karšli, V.M., Çağlar, M.(2006). Wind power engineering in the world and perspectives of its development in Turkey. *Renewable and Sustainable Energy Reviews*, 10, 341–369.

Kundur, P., Paserba, J., Ajarapu, V., Andersson, G., Bose, A., Canizares, C. et.al. (2004). Definition and Classification of Power System Stability. *IEEE Transactions On Power Systems*, 19(2), 1387-1401.

Larsson, A. (2002). Flicker Emission of Wind Turbines During Continuous Operation. *IEEE Transactions On Energy Conversion*, 17(1), 114-118.

Ledesma P., Usaola J., & Rodríguez J.L. (2003). Transient Stability of a Fixed Speed Wind Farm. *Renewable Energy*. 28 (9): 1341-55.

Lubosny, Z. (2003). *Wind Turbine Operation in Electric Power Systems*. Berlin : Springer-Verlag.

Manwell, J. F., McGovan, J. G. , & Rogers A.L. (2002). *Wind Energy Explained: Theory, Design and Application*. Great Britain : J.Wiley & Sons Ltd.

Matevosyan, J., Ackermann T., & Bolik, S. M. (2005). Technical Regulations for the Interconnection of Wind Farms. In T. Ackermann, (Ed.). *Wind Power in Power Systems* (115-142). Great Britain : J.Wiley & Sons Ltd.

- Martins, M., Perdana, A., Ledesma, P., Agneholm, E., & Carlson O. (2007). Validation of Fixed Speed Wind Turbine Dynamic Models With Measured Data. *Renewable Energy* 32. 1301–1316.
- Mäki, K., Repo, S., & Järventausta, P. (2006). Network Protection Impacts of Distributed Generation –A Case Study on Wind Power Integration. *Proc. Nordic Wind Power Conference 2006*, Espoo, Finland.
- Morren, J. & de Haan, S.W.H. (2007) Short-Circuit Current of Wind Turbines With Doubly Fed Induction Generator. *IEEE Transactions on Energy Conversion*, Vol. 22, No. 1, 174-180.
- Mutlu, Ö.S., Akpınar, E. & Balıkcı, A. (2009). Power Quality Analysis of Wind Farm Connected to Alaçatı Substation in Turkey. *Renewable Energy* 34(5). Pages 1312-1318
- Mutlu, Ö.S. & Akpınar, E. (2005). *Şebeke Kesintilerinin Asenkron Jeneratörlü Rüzgar Enerjisi Dönüşüm Sistemi Üzerinde Etkisi. (The Effect of Power Disturbances on the Wind Energy Conversion System with Induction Generator)*, III. Yenilenebilir Enerji Kaynakları Sempozyumu, Mersin-Turkey.157-163.
- Perdana, A., Uski, S., Carlson, O., & Lemström, B. (2006) Validation of Aggregate Model of Wind Farm with Fixed-speed Wind Turbines against Measurement. *Proc. Nordic Wind Power Conference 2006*, Espoo, Finland.
- Petru, T., & Thiringer T. (2002). Modeling of Wind Turbines for Power System Studies. *IEEE Transactions On Power Systems*, 17(4), 1132-1139.
- Pöller, M., & Achilles, S. (2003) Aggregated wind park models for analyzing power system dynamics. *4th International workshop on large-scale integration of wind power and transmission network for off-shore wind-farms*, Billund, Denmark.

- Samuelsson, O., & Lindahl, S. (2005). On Speed Stability. *IEEE Transactions On Power Systems*, 20(2), 1179-1180.
- Shafiu, A., Anaya-Lara, O., Bathurst, G., & Jenkins, N. (2006). Aggregated Wind Turbine Models for Power System Dynamic Studies, *Wind Engineering*, Volume 30(3). 171-186.
- Slootweg, J. G. & Kling, W. L. (2002). Modeling of Large Wind-farms in Power System Simulations, *Proc. IEEE Power Engineering Society Summer Meeting*. 503-508
- Sun, T., Chen, Z., & Blaabjerg, F. (2005). Flicker Study on Variable Speed Wind Turbines With Doubly Fed Induction Generators. *IEEE Transactions On Energy Conversion*, 20(4), 896-905.
- Sürgevil, T. (2004). *Modeling and Simulation of Wind Energy Conversion System Using PWM Converters. Ph.D Thesis*, DEU.
- Sørensen, P., Hansen, A., Janosi, L., Bech, J., & Bak-Jensen, B. (2001). *Simulation of Interaction Between Wind Farm and Power System*. Technical Report Risø-R-1281(EN), Risø National Laboratory. Retrieved May 10, 2005, from http://www.risoe.dtu.dk/Risoe_dk/Home/Knowledge_base/publications/VEA.aspx.
- Tande, J. O. (2005). Power Quality Standarts for Wind Turbines. In T. Ackermann, (Ed.). *Wind Power in Power Systems*, (79- 96). Great Britin : J.Wiley & Sons Ltd.
- TEİAŞ - Türkiye Elektrik İletim Anonim Şirketi. (2008). *Grid Codes for Wind Farm Grid Connections.- Rüzgar Enerjisine Dayalı Üretim Tesislerinin Şebeke Bağlantı Kriterleri*.

- Thiringer, T., & Luomi, J. (2001). Comparison of Reduced-Order Dynamic Models of Induction Machines. *IEEE Transactions On Power Systems*, 16(1), 119-126.
- Thiringer, T., Petru, T., & Lundberg, S. (2004). Flicker Contribution From Wind Turbine Installations. *IEEE Transactions On Energy Conversion*, 19,(1), 157-163.
- Venkatasubramanian, M., & Tomsovic, K. (2004). Power System Analysis. In W. Chen, (Ed.). *The Electrical Engineering Handbook* (761-768). U.S.A. : Elsevier Academic Press.

APPENDICES

LIST OF TABLES

- Table 2.1 Factors and characteristics with impact on the power quality of wind farms
- Table 2.2 Short-term and Long-term flicker disturbance factor limits for Turkish National Transmission System
- Table 3.1 Components of Grid Connected WECS
- Table 4.1 Wind farm generator parameters
- Table 5.1 Results of the effective resistance for two different systems.
- Table 6.1 Wind Speed – Torque

LIST OF FIGURES

- Figure 1.1 Impacts of wind power on power systems, divided in different time scales and width of area relevant for the studies.
- Figure 2.1 The main parts of typical AC 3 phase power system
- Figure 2.2 (a) One line diagram of wind farm connection to a grid, (b) Phasor diagram
- Figure 2.3 Different wind farm connections to a grid.
- Figure 2.4 Classification of power system stability.
- Figure 2.5 LVRT capability limits for wind turbines connected before 01.01.2009 to transmission system of Turkey.
- Figure 2.6 LVRT capability limits for wind turbines connected after 01.01.2009 to transmission system of Turkey
- Figure 2.7 Reactive power requirements for wind farms in Turkey.

- Figure 2.8 Voltage support characteristic of wind farms in Turkey.
- Figure 2.9 Frequency range for wind farms in Turkey.
- Figure 2.10 Power-frequency control curves: (a) Without underfrequency control, (b) With underfrequency control
- Figure 3.1 Wind Farm Configuration
- Figure 3.2 Major components of a wind turbine.
- Figure 3.3 Type A configuration.
- Figure 3.4 Type B configuration.
- Figure 3.5 Type C configuration.
- Figure 3.6 Type D configuration.
- Figure 3.7 Power versus wind speed characteristics of a wind turbine.
- Figure 4.1 Wind farm.
- Figure 4.2 Wind turbine 0.69/34.5 kV star-delta connected transformer in wind farm
- Figure 4.3 Wind farm one line diagram.
- Figure 4.4 TEİAŞ-Alaçati Substation one line diagram.
- Figure 4.5 WRIG with rotor circuit
- Figure 4.6 A photo of rotor circuit.
- Figure 4.7 Wind Turbine Control System.
- Figure 4.8 Overview of MATLAB/Simulink simulation circuit.
- Figure 4.9 IGBT current waveform for MATLAB/Simulink simulation.
- Figure 5.1 Speed control with rotor circuit chopper (One resistance)
- Figure 5.2 Speed control with rotor circuit chopper (Three resistances)
- Figure 5.3 Rotor phase voltage and phase current

- Figure 5.4 Turn-on and turn-off trajectories.
- Figure 5.5 The power-flow diagram of an induction machine.
- Figure 5.6 The per-phase fundamental equivalent circuit of the drive referred to the stator
- Figure 5.7 R_m in parallel to the magnetizing branch of equivalent circuit.
- Figure 5.8 The per-phase reduced equivalent circuit of the drive referred to the stator
- Figure 5.9 Torque-speed curves
- Figure 5.10 Torque-speed curve with constant δ and T_m
- Figure 6.1 Aggregated modelling of a wind farm by a few large wind turbines.
- Figure 6.2(a) Input voltage and current signal results for phase “A” in laboratory and simulation studies for 5 KHz switching frequency.
- Figure 6.2(b) Input voltage and current signal results for phase “A” in laboratory and simulation studies for 0.5 KHz switching frequency
- Figure 6.3 Structure of developed Model for Wind Speed – Torque
- Figure 6.4 Measured wind speed in wind farm.
- Figure 6.5 Three phase two winding transformer model that is used to model Alaçatı Substation in PSCAD/EMTDC simulation.
- Figure 6.6 Equivalent circuit between the wind farm and the National Grid.
- Figure 6.7 Simulated result of current on wind farm feeder.
- Figure 6.8 Measurement result of current on wind farm feeder.
- Figure 6.9 Simulation result of power on wind farm feeder.
- Figure 6.10 Measurement result of THD on wind farm feeder – 34.5 kV.
- Figure 6.11 Simulation result of THD on wind farm feeder – 34.5 kV.

- Figure 6.12 Wind-farm one line diagram
- Figure 6.13 Wind-farm one line diagram with aggregated model
- Figure 6.14 Equivalent circuit of aggregated model
- Figure 6.15 Reduced equivalent circuit of aggregated model
- Figure 6.16 Torque-speed curve for two different situations
- Figure 6.17 Torque-speed curve for three different situations
- Figure 6.18 Torque-speed curve for two different situations
- Figure 6.19 Complete model real and reactive output of the wind farm
- Figure 6.20 Aggregated model real and reactive output of the wind farm
- Figure 6.21 Complete model current output of the wind farm
- Figure 6.22 Aggregated model current output of the wind farm
- Figure 6.23 Complete model real and reactive output of the wind farm in case of 150 ms fault.
- Figure 6.24 Aggregated model real and reactive output of the wind farm in case of 150 ms fault.
- Figure 6.25 Block Diagram of Power Quality Monitoring Set-up
- Figure 6.26 Location of measurements in Alaçatı Substation
- Figure 6.27 Measured Real, Reactive and Apparent Power results in wind farm feeder for 7 days
- Figure 6.28 Measured power factor results in wind farm feeder for 7 days
- Figure 6.29 Voltage sag.
- Figure 6.30 Current waveforms during the voltage sag
- Figure 6.31 Voltage swell
- Figure 6.32 Current waveforms during the voltage swell.

- Figure 6.33 Voltage shortage
- Figure 6.34 Current waveforms during the voltage shortage
- Figure 6.35 Voltage unbalance
- Figure 6.36 Current waveforms during the voltage unbalance

LIST OF ABBREVIATIONS

- A : *intercepting area(the area of the wind turbine rotor)*
- a_{T1} : *stator to rotor turns ratio*
- $c_f(\psi_k, v_a)$: *flicker coefficient of the wind turbine*
- $C_p(\beta, \lambda)$: *power coefficient of the rotor*
- C_{pmax} : *the Betz limit*
- $C_T(\beta, \lambda)$: *torque coefficient of the turbine*
- DFIG* : *doubly fed induction generator*
- f : *frequency*
- HVDC* : *high voltage direct current*
- H : *inertia constant*
- I_d : *current of diode*
- I_g : *current of the wind farm*
- I_r : *fundamental rotor current*
- I_{rms} : *rms value of rotor phase current*
- IEC* : *International Electrotechnical Commission*
- J : *combined moment of inertia of the rotating system*
- $k_f(\psi_k)$: *flicker step factor of the wind turbine*

$LVRT$:	<i>low voltage ride through</i>
N_{wt}	:	<i>number of wind turbines in the wind farm(connected to the PCC)</i>
$N_{10,i}$:	<i>number of switching operations of the individual wind turbine within 10 minute period</i>
P	:	<i>given electrical wind power capacity</i>
P_{ag}	:	<i>power transferred across the air-gap</i>
P_{agl}	:	<i>fundamental air-gap power</i>
P_g	:	<i>real output power of the wind farm</i>
P_g'	:	<i>total power consumed in the rotor circuit</i>
P_{mc}	:	<i>ten minutes average data(maximum permitted power)</i>
P_{60}	:	<i>maximum measured power (60 second average value)</i>
$P_{0.2}$:	<i>maximum measured power (0.2 second average value)</i>
$P_{n,i}$:	<i>rated real power of the individual wind turbine</i>
$P_{0.2i}$:	<i>highest valid 0.2 second average real power data of the individual wind turbine recorded during the measurement period</i>
P_{st}	:	<i>short term flicker disturbance factor</i>
P_{lt}	:	<i>long term flicker disturbance factor</i>
P_{on}	:	<i>turn-on power loss of the power electronic switch</i>
P_{off}	:	<i>turn-off power loss of the power electronic switch</i>
P_{con}	:	<i>conduction power loss of the power electronic switch</i>
P_{sw}	:	<i>average value of the switching losses of the power electronic switch</i>
P_r	:	<i>average power absorbed by resistance R during a period</i>
P_e	:	<i>per-phase power consumed by resistance R_e</i>
P_m	:	<i>mechanical power developed by the fundamental rotor current</i>

P_{rcl}	:	<i>rotor copper loss</i>
P_{out}	:	<i>power output of a wind farm/ turbine</i>
P_{in}	:	<i>power input of a wind farm/turbine</i>
P_{rated}	:	<i>rated power of wind farm</i>
P_t	:	<i>mechanical power of wind turbine</i>
PCC	:	<i>point of common coupling</i>
Q_g	:	<i>reactive power of the wind farm</i>
Q_{mc}	:	<i>reactive power at P_{mc}</i>
Q_{60}	:	<i>reactive power(60 second average value) at P_{60}</i>
$Q_{0.2}$:	<i>reactive power(0.2 second average value) at $P_{0.2}$</i>
$Q_{n,i}$:	<i>rated reactive power of the individual wind turbine</i>
$Q_{0.2i}$:	<i>0.2 average reactive power data at $P_{0.2i}$ of the individual wind turbine</i>
R_{SC}	:	<i>measure of the strength</i>
R	:	<i>turbine radius</i>
R^*	:	<i>effective value of resistance R</i>
R_e^*	:	<i>effective value per-phase value of R_e</i>
R_3^*	:	<i>effective per-phase value of R_3</i>
R_r	:	<i>rotor resistance</i>
R_m	:	<i>resistance that represents the core losses</i>
R_{sub}, X_{sub}	:	<i>resistance and reactance to represent the substation short-circuit level</i>
R_L	:	<i>line resistance</i>
S_{sc}	:	<i>short circuit power</i>

$S_{n,i}$:	<i>rated apparent power of the individual wind turbine</i>
s	:	<i>slip</i>
T_a	:	<i>accelerating torque</i>
T_w	:	<i>torque available from the wind turbine</i>
T_e	:	<i>torque developed by the induction generator</i>
T	:	<i>period</i>
t_{on}	:	<i>on time period of the power electronic switch</i>
t_{off}	:	<i>off time period of the power electronic switch</i>
t_{con}	:	<i>conduction time period of the power electronic switch</i>
TSO	:	<i>transmission system operator</i>
U_g	:	<i>voltage at the PCC</i>
U_s	:	<i>network voltage at the assumed infinite busbar</i>
ΔU	:	<i>voltage difference between the infinite system and the PCC</i>
X_L	:	<i>line reactance</i>
X_{TR}	:	<i>transformer reactance</i>
X_{TH}	:	<i>thevenin's impedance</i>
v_a	:	<i>given annual average wind speed at hub-height of the wind turbine</i>
v_n	:	<i>rated wind speed</i>
v_{cut-in}	:	<i>cut-in wind speed</i>
$v_{cut-out}$:	<i>cut-out wind speed</i>
V_{base}	:	<i>average value of the wind speed</i>
V_{gust}	:	<i>gust wind component</i>
V_{ramp}	:	<i>ramp wind component</i>
V_{noise}	:	<i>noise wind component</i>

V_{sub}	:	<i>substation voltage</i>
V_{TH}	:	<i>thevenin's voltage</i>
$W(Annual)$:	<i>sum of the energy produced by the wind farm for a year</i>
W_R	:	<i>energy absorbed by resistance R during T</i>
Z_k	:	<i>equivalent short circuit impedance of the network</i>
Z_C	:	<i>equivalent impedance of the local capacitor bank</i>
ψ_k	:	<i>network impedance phase angle at the PCC</i>
β	:	<i>pitch angle</i>
ρ	:	<i>air density</i>
λ	:	<i>tip speed ratio</i>
ω_t	:	<i>rotational speed of the turbine</i>
$\eta_{overall}$:	<i>overall turbine efficiency</i>
ω	:	<i>angular velocity</i>
δ	:	<i>switch duty ratio</i>
θ_r	:	<i>phase angle between phasors</i>

On-line power quality analysis software is as illustrated:

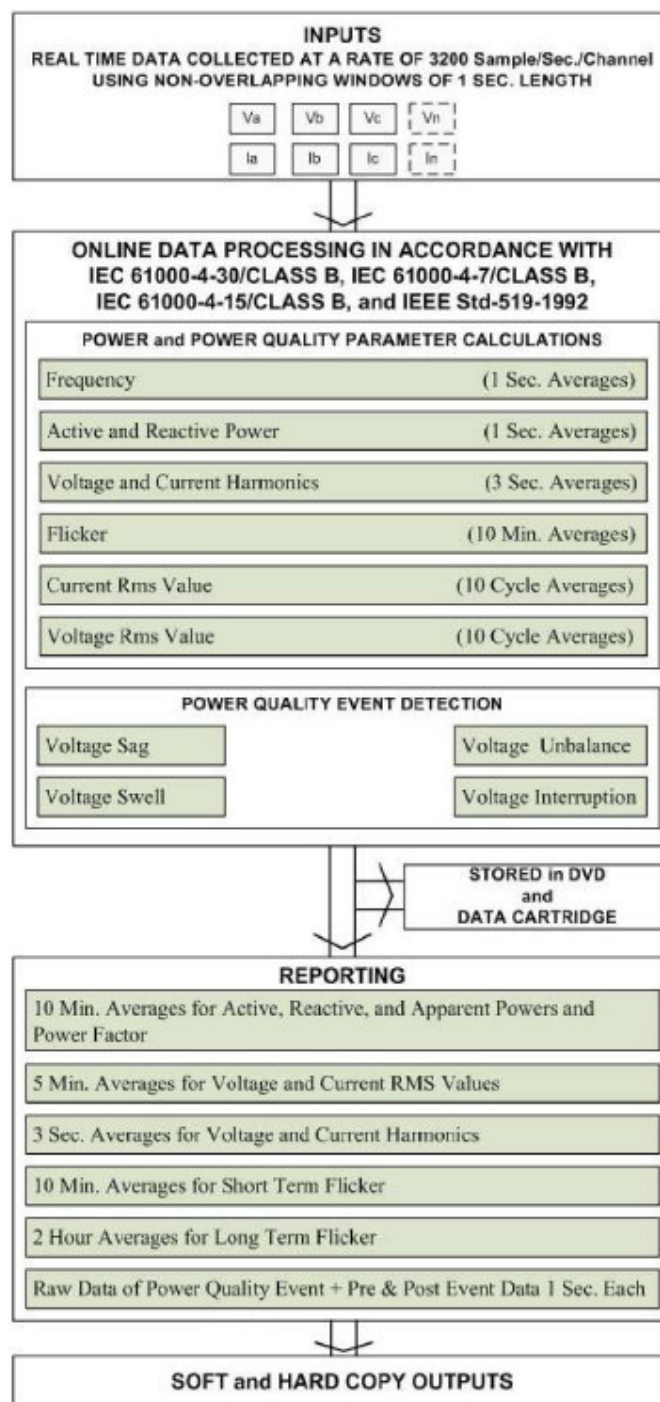


Figure A.1 An illustration of on-line power quality analysis software.



Figure A.2 A photo from on-line power quality analysis.



Figure A.3 A photo from on-line power quality analysis in Alaçatı Substation.

IEC 61400-21 Sample Report Format

Sample report format

This sample report format gives a suggested format for reporting the results of measurements for characterizing the power quality parameters of a wind turbine.

REPORT ON RESULTS OF WIND TURBINE POWER QUALITY TESTS

The reported characteristics are valid for the specific configuration of the assessed wind turbine only. Other configurations, including altered control parameters, that cause the wind turbine to behave differently with respect to power quality, require separate assessment.

Name of test organization	
Report number	
Wind turbine type designation	
Wind turbine manufacturer	
Serial number of wind turbine tested	

The wind turbine identified above has been tested in accordance with IEC 61400-21.

This test report is accompanied by the documents specified below.

Type of information	Document name and date
Description of the tested wind turbine, including settings of control parameters	
Description of test site and grid connection	
Description of test equipment	
Description of test conditions	
Note of exceptions to IEC 61400-21	

Author	
Checked	
Approved	
Date of issue	

Characteristic parameters that are determined otherwise than outlined in IEC 61400-21 are marked. This includes parameters that are calculated instead of measured. The document(s) with exceptions to IEC 61400-21 describes the alternative procedure(s) that has been applied.

The resulting characteristic parameters are stated below.

A.1 General data

Wind turbine type (horizontal/vertical axis)	
Number of blades	
Rotor diameter (m)	
Hub height (m)	
Blade control (pitch/stall)	
Speed control (fixed/two-speed/variable)	
Generator type and rating(s) (kW)	
Frequency converter type and rating (kW)	
Identification of wind turbine terminals	

A.2 Rated data

Rated power, P_n (kW)	
Rated wind speed, v_n (m/s)	
Rated apparent power, S_n (kVA)	
Rated reactive power, Q_n (kvar)	
Rated current, I_n (A)	
Rated voltage, U_n (V)	

A.3 Maximum permitted power

Assessed value, P_{mc} (kW)	
Normalized value, $p_{mc} = P_{mc} / P_n$	

A.4 Maximum measured power

A.4.1 60 s average value

Measured value, P_{60} (kW)	
Normalized value, $p_{60} = P_{60} / P_n$	

A.4.2 0,2 s average value

Measured value, $P_{0,2}$ (kW)	
Normalized value, $p_{0,2} = P_{0,2} / P_n$	

A.5 Reactive power

Output power (% of P_n)	Output power (kW)	Reactive power (kvar)
0		
10		
20		
30		
40		
50		
60		
70		
80		
90		
100		

Assessed reactive power at P_{mc} (kvar)	
Assessed reactive power at P_{60} (kvar)	
Assessed reactive power at $P_{0,2}$ (kvar)	

A.6 Voltage fluctuations

A.6.1 Continuous operation

Network impedance phase angle, ψ_k (deg.)	30	50	70	85
Annual average wind speed, v_a (m/s)	Flicker coefficient, $c(\psi_k, v_a)$			
6,0				
7,5				
8,5				
10,0				

A.6.2 Switching operations

Case of switching operation	Start-up at cut-in wind speed			
Maximum number of switching operations, N_{10}				
Maximum number of switching operations, N_{120}				
Network impedance phase angle, Ψ_k (deg.)	30	50	70	85
Flicker step factor, $k_f(\Psi_k)$				
Voltage change factor, $k_U(\Psi_k)$				

Case of switching operation	Start-up at rated wind speed			
Maximum number of switching operations, N_{10}				
Maximum number of switching operations, N_{120}				
Network impedance phase angle, Ψ_k (deg.)	30	50	70	85
Flicker step factor, $k_f(\Psi_k)$				
Voltage change factor, $k_U(\Psi_k)$				

Case of switching operation	Worst case switching between generators			
Maximum number of switching operations, N_{10}				
Maximum number of switching operations, N_{120}				
Network impedance phase angle, Ψ_k (deg.)	30	50	70	85
Flicker step factor, $k_f(\Psi_k)$				
Voltage change factor, $k_U(\Psi_k)$				

A.7 Harmonics

This clause is only relevant for wind turbines with a power electronic converter.

Order	Output power (kW)	Harmonic current (% of I_n)	Order	Output power (kW)	Harmonic current (% of I_n)
2			3		
4			5		
6			7		
8			9		
10			11		
12			13		
14			15		
16			17		
18			19		
20			21		
22			23		
24			25		
26			27		
28			29		
30			31		
32			33		
34			35		
36			37		
38			39		
40			41		
42			43		
44			45		
46			47		
48			49		
50					

Maximum total harmonic current distortion (% of I_n)	
Output power at maximum total harmonic current distortion (kW)	

Data Sheet for Wind Turbine Test(Enercon-Windguard)

Referenzertrag		Leistungskurve			
PP04077		v_{Wst} in m/s	P_{Wst} in kW	c_p	Werte- Anzahl
Auftraggeber:	ENERCON GmbH	1.53	-2.19	-0.78	7
WEA-Typ:	ENERCON E-40/5.40 schalloptimiert	2.01	-2.30	-0.36	16
Hersteller:	ENERCON GmbH	2.53	-1.88	-0.15	72
Nennleistung:	500 kW	3.03	1.88	0.09	87
Rotordurchmesser:	40.3 m	3.49	7.34	0.22	87
Abschaltwindgeschwindigkeit:	25 m/s	4.02	17.49	0.34	112
Messbericht:	DEWI 047PV0003-06	4.50	27.34	0.38	128
Messinstitut:	Deutsches Windenergie-Institut GmbH	4.99	39.78	0.41	122
Messort:	Dornum	5.49	53.83	0.42	82
Berichtsdatum:	01.09.2000	6.01	74.50	0.44	87
Richtlinie:	MEASNET 2000	6.45	94.31	0.45	71
EEG-konform:	Ja	7.02	122.46	0.45	67
Korrekturen:	Keine	7.50	152.22	0.46	64
		7.99	188.26	0.47	73
		8.52	216.57	0.45	51
		8.98	255.09	0.45	46
		9.49	293.71	0.44	39
		10.01	342.37	0.44	38
		10.52	379.28	0.42	24
		11.01	423.60	0.41	20
		11.50	437.92	0.37	15
		12.01	463.15	0.34	19
		12.52	479.20	0.31	18
		13.02	491.64	0.29	12
		13.50	496.12	0.26	12
		13.96	500.27	0.24	7
		14.45	499.35	0.21	8
		15.02	502.88	0.19	9
		15.39	501.77	0.18	2
		15.95	501.99	0.16	10
		16.46	501.83	0.14	5
		16.97	500.53	0.13	5

Berechneter Referenzertrag	
Nabenhöhe in m	Referenzertrag in kWh
44	4987475

Anmerkungen bzgl. der Eignung für das EEG
(Zutreffendes ist angekreuzt)

Die verwendete Leistungskurve wurde entsprechend FGW- oder MEASNET- Richtlinie unter Berücksichtigung der Ergänzungen dieser Richtlinie vermessen. Die ausgewiesenen Referenzerträge sind uneingeschränkt für Anlagen gleichen Typs nutzbar.

Die verwendete Leistungskurve wurde nach einem „vergleichbaren“ Verfahren vor dem 01.01.2000 ermittelt. Die ausgewiesenen Referenzerträge sind nur zu verwenden, wenn mit der Errichtung von Anlagen des Typs nach dem 31.12.2001 im Geltungsbereich des EEG nicht mehr begonnen wurde.


Die verwendete Leistungskurve wurde aus den Konstruktionsunterlagen des Anlagentyps ermittelt. Die ausgewiesenen Referenzerträge sind nur zu verwenden, wenn Anlagen des Typs nach dem 01.04.2000 im Geltungsbereich des EEG nicht mehr in Betrieb genommen worden sind.


Die hier angegebenen Referenzenergieerträge erfüllen nicht alle Bedingungen des Erneuerbaren-Energien-Gesetzes und sind daher als Grundlage für die Ermittlung der Laufzeit der erhöhten Vergütung nicht geeignet.

DEUTSCHE WINDGUARD

Deutsche WindGuard Consulting GmbH
Windfläe 15
D-26316 Varel
Tel.: 04451/9515-0 · Fax 9515-29
Email: info@windguard.de

Varel, 22.03.2004


 Unterschrift
 (Dipl.-Phys. A. Albers)


 Unterschrift
 (Dipl.-Phys. J. Mander)

Calculation of Switching Loss

SKM 800GA176D is an IGBT module, manufactured by SEMIKRON, that is used in wind power applications. Its characteristics given at the manufacturers' sheet can be used for equations (Semikron, 2009): Turn-on time t_{on} , is consist of; turn-on delay time $t_{d(on)}$ and rise time t_r , and is given as totally 320 ns. The turn-off time t_{off} , is defined as the sum of turn-off delay time $t_{d(off)}$ and fall time t_f , and is given as totally 1190 ns. The given values are for $V_{cc} = 1200$ Volts and $I_c = 600$ Amps.

Energy dissipation during turn-on E_{on} ; energy dissipation during turn-off E_{off} per cycle are 335 mj and 245 mj according to the data sheet, respectively. Power loss during switching may be calculated by multiplication of the switching frequency f with E_{on} and E_{off} :

$$P_{sw} = f.(E_{on} + E_{off}) = 3000.(335 + 245) = 1740000 \text{ mW} = 1740 \text{ W}$$

By using turn-on and turn-off times;

$$P_{sw} = \frac{1}{2} V.I.(t_{on} + t_{off}).f_s = \frac{1200.600}{2} .(320 + 1190).10^{-9}.3000 = 1630.8 \text{ W}$$

Both results are not far away from each other.

For a duty ratio $\delta = 0.9$ of the switch, $V_{ce} = 1.5$ Volts, R_{bs} becomes;

$$R_{bs} = \frac{1}{2} \frac{V}{I} (t_{on} + t_{off}).f_s + \frac{V_{ce}}{I} .\delta = \frac{1}{2} \frac{1200}{150} (320 + 1190).10^{-9}.3000 + \frac{1.5}{150} .0.9$$

where rated rotor current of the wind turbine generator is given as 150 A.

$$R_{bs} = 0.01812 + 0.009 = 0.02712$$

Total effective per-phase value of external circuit resistance becomes,

$$R_3^* = 0,5 \cdot (\delta \cdot R_{bs}) + (1 - \delta) R_3 = 0,5x(0,9x0,02712) + (1 - 0,9) \cdot 1 = 0,112204$$

$$R_h = \left(\frac{\pi^2}{9} - 1\right)(R_r + R_e^*) = \left(\frac{\pi^2}{9} - 1\right)(0,067375 + 0,112204) = 0,01751$$

$$R_f = (R_r + R_e^*) = (0,067375 + 0,112204) = 0,179579$$

$$R_h' = a_{T1}^2 R_h = 0,081225 \times 0,01751 = 0,001422$$

$$R_f' = a_{T1}^2 R_f = 0,081225 \times 0,179579 = 0,014586$$

$$\bar{V}_{TH} = \bar{V} \left(\frac{Z_M}{Z_M + Z_S} \right) = 690 \left(\frac{j2,39}{j2,39 + 0,00357 + j0,055} \right) = \frac{j1649,1}{j2,445 + 0,00357} = 674,47$$

$$Z_{TH} = R_{TH} + jX_{TH} = \frac{Z_M Z_S}{Z_M + Z_S} = \frac{j2,39(j0,055 + 0,00357)}{j2,39 + j0,055 + 0,00357} = \frac{-0,13145 + j0,00853}{0,00357 + j2,445}$$

$$Z_{TH} = 0,00341 + j0,05376$$

$$\begin{aligned} |\bar{I}_R| = I_R' &= \frac{V_{TH}}{\sqrt{(R_{TH} + R_h' + \frac{R_f'}{s})^2 + (X_{TH} + X_R')^2}} \\ &= \frac{674,47}{\sqrt{(0,00341 + 0,001422 + \frac{0,014586}{s})^2 + (0,05376 + 0,0662)^2}} \end{aligned}$$

$$\begin{aligned} T_E = \frac{R_f'}{s} I_R'^2 &= \frac{R_f'}{s} \frac{V_{TH}^2}{(R_{TH} + R_h' + \frac{R_f'}{s})^2 + (X_{TH} + X_R')^2} \\ &= \frac{0,014586}{s} \frac{(674,47)^2}{(0,00341 + 0,001422 + \frac{0,014586}{s})^2 + (0,05376 + 0,0662)^2} \end{aligned}$$

The control unit calculates the necessary effective resistance using the current reference and measured rotor current for any given slip. When the duty ratio δ is changed by the controller unit, the torque and reactive power characteristics of the machine are changed.

for s = %2;

$$|\bar{I}_R| = I_R' = \frac{674.47}{\sqrt{(0.00341 + 0.001422 + \frac{0.014586}{0.02})^2 + (0.05376 + 0.0662)^2}}$$

$$I_R' = 906.7$$

$$I_R = \frac{906.7}{12.31} = 73.65 \text{ A.}$$

$$T_E = \frac{0.014586}{0.02} \frac{(674.47)^2}{(0.00341 + 0.001422 + \frac{0.014586}{0.02})^2 + (0.05376 + 0.0662)^2}$$

$$T_E = 599569$$

for s = %1;

$$|\bar{I}_R| = I_R' = \frac{674.47}{\sqrt{(0.00341 + 0.001422 + \frac{0.014586}{0.01})^2 + (0.05376 + 0.0662)^2}}$$

$$I_R' = 459.34$$

$$I_R = \frac{459.34}{12.31} = 37.31 \text{ A.}$$

$$T_E = \frac{0.014586}{0.01} \frac{(674.47)^2}{(0.00341 + 0.001422 + \frac{0.014586}{0.01})^2 + (0.05376 + 0.0662)^2}$$

$$T_E = 307757$$